

UC San Diego

UC San Diego Electronic Theses and Dissertations

Title

Neuropeptide Y in early kidney development

Permalink

<https://escholarship.org/uc/item/7cd2j28d>

Author

Choi, Yohan

Publication Date

2009

Peer reviewed|Thesis/dissertation

UNIVERSITY OF CALIFORNIA, SAN DIEGO

Neuropeptide Y in Early Kidney Development

A dissertation submitted in partial satisfaction of the requirements for the degree Doctor of
Philosophy

in

Biomedical Sciences

by

Yohan Choi

Committee in charge:

Professor Sanjay K. Nigam, Chair
Professor Jeffrey D. Esko
Professor Sylvia M. Evans
Professor Robert L. Sah
Professor Scott C. Thomson

2009

© Yohan Choi, 2009

All rights reserved.

The Dissertation of Yohan Choi is approved, and it is acceptable in quality and form for publication on microfilm and electronically:

Chair

University of California, San Diego

2009

DEDICATION

This dissertation is dedicated to my many furry friends who forfeited their lives to bring us this information. RIP

EPIGRAPH

ॐ नमो भगवते वासुदेवाय

아리랑, 아리랑, 아라리요...
아리랑 고개로 넘어간다.
나를 버리고 가시는 님은
십리도 못가서 발병난다.

TABLE OF CONTENTS

Signature Page	iii
Dedication	iv
Epigraph.....	v
Table of Contents	vi
List of Abbreviations	x
List of Figures	xi
List of Tables	xiv
Acknowledgements.....	xv
Vita.....	xvi
Abstract of the Dissertation	xvii
CHAPTER 1: Introduction	1
1.1 Kidney function and structure.....	1
1.1.1 Renal agenesis.....	2
1.1.2 Adult kidney disorders	3
1.1.3 Tissue Engineering & Wolffian duct formation	4
1.2 Kidney development.....	4
1.2.1 Wolffian duct formation and budding.....	5
1.2.2 Ureteric bud branching	6
1.2.3 Metanephric mesenchyme induction	7
1.2.4 Similarities between budding and branching	9
1.3 Molecular control of Wolffian duct budding	9
1.3.1 GDNF.....	9
1.3.2 Balance of growth factors and inhibitors	10
1.3.3 Receptor tyrosine kinase signaling (Ret & FGFR)	12
1.3.4 GDNF-independent budding.....	13
1.4 Microarrays in the study of renal development	13
1.4.1 Microarray analysis of kidney development.....	14
1.5 NPY	15
1.5.1 NPY structure and localization	15

1.5.2 NPY receptors and signal transduction.....	16
1.5.3 NPY in the kidney.....	17
1.5.4 NPY in development.....	18
1.6 Scope of the Dissertation	19
1.7 Figures	21
Chapter 2: WD Budding In Vitro.....	29
Abstract.....	29
2.1 Introduction.....	29
2.1.1. Whole WD culture	31
2.1.2 WD(+Intermediate Mesoderm) culture.....	31
2.1.3 Isolated WD (iWD) culture.....	31
2.2 Signaling pathway studies.....	32
2.2.1 Inhibitor studies	33
2.3 Microarray analysis.....	34
2.3.1 Affymetrix microarrays	35
2.3.2 Microarray samples.....	36
2.3.3 NMF.....	37
2.3.4 Fold-change analysis.....	37
2.3.5 ANOVA + Pattern Matching	38
2.3.6 NPY from microarray data.....	39
2.4 Discussion.....	39
2.5 Methods	42
2.5.1 Reagents.....	42
2.5.2 WD isolation and culture	42
2.5.3 Immunohistochemistry	43
2.5.4 Microarray preparation and analysis.....	43
2.6 Figures	45
Chapter 3: Neuropeptide Y Functions as a Facilitator of GDNF-induced Budding	58
Abstract.....	58
3.1 Introduction.....	59
3.2 Results.....	62

3.2.1 A microarray-based approach identifies genes potentially involved in UB formation from the WD	62
3.2.2 Expression and localization of NPY and its receptors	64
3.2.3 In vitro budding with GDNF	64
3.2.4 Role of NPY in GDNF-dependent budding	65
3.2.5 NPY augments GDNF-induced budding but not GDNF-independent budding	66
3.2.6 Rescue of BMP4 inhibition of budding by NPY and Restoration of Akt Phosphorylation	67
3.2.7 NPY transcriptional program	68
3.3 Discussion	70
3.4 Methods	74
3.4.1 Reagents	74
3.4.2 Isolation and culture of the Wolffian duct	75
3.4.3 NPY knockout animal	75
3.4.4 siRNA	76
3.4.5 Immunohistochemistry	76
3.4.6 Western blot	77
3.4.7 RT-PCR	77
3.4.8 Real-time PCR	78
3.4.9 Microarray analysis	79
3.5 Figures	81
Chapter 4: Differential Signaling between GDNF-independent and GDNF-dependent Ureteric Bud Formation Occurs with Overlapping Genetic Networks	102
Abstract	102
4.1 Introduction	103
4.2 Results	106
4.2.1 Ret mutant and wild-type kidneys	106
4.2.3 Microarray analysis of kidneys with and without Ret	106
4.2.4 Cross-species comparison of GDNF-dependent and independent budding	108
4.2.5 In vitro culture	109
4.2.6 GFR α 1 localization	109
4.2.7 Inhibitor Studies	109
4.2.8 Common budding genes	110

4.3 Discussion.....	111
4.4 Methods	114
4.4.1 Reagents.....	114
4.4.2 Isolation and culture of Wolffian ducts.....	115
4.4.3 Ret mutant kidneys	115
4.4.4 Microarray.....	115
4.4.5 Immunohistochemistry	116
4.5 Figures	118
Chapter 5: Conclusion.....	128
5.1 Supplemental data.....	128
5.1.1 NPY in isolated WD cultures.....	128
5.1.2 NPY added to isolated UB culture.....	129
5.1.3 Genetic mouse knockouts	129
5.1.4 Ret knockout mice	130
5.1.5 NPY knockout mice.....	131
5.1.6 Engrailed K/O	131
5.2 Summary of findings.....	132
5.3 Future directions	133
5.4 Figures	136
Supplemental Figures.....	141
References.....	146

LIST OF ABBREVIATIONS

BMP – bone morphogenetic protein	mTOR – mammalian target of rapamycin
cAMP – cyclic adenosine monophosphate	NMF – nonnegative matrix factorization
CLF-1 – cytokine-like factor 1	PKA – protein kinase A
CTX – cholera toxin	PP – pancreatic polypeptide
DB – <i>Dolichos biflorus</i>	PTX – pertussis toxin
E11, E13 – embryonic day 11, 13, etc.	PYY – peptide YY
ERK – extracellular signal-regulated kinase	RSV – Rous sarcoma virus
FGF – Fibroblast growth factor	siRNA – small interfering RNA
GDNF – glial cell-line-derived neurotrophic factor	SOM – self-organizing map
GFP – green fluorescent protein	UB – ureteric bud
GFR α 1 – GDNF family receptor α 1	WD – Wolffian duct
GPCR – G protein coupled receptor	WD(+IM) – Wolffian duct with intermediate mesoderm
HRG – heregulin-alpha (Neuregulin-1)	ZO-1 – tight junction protein 1 (zona occludens 1)
IKK – I κ B kinase	
IM – intermediate mesoderm	
iUB – isolated ureteric bud	
iWD – isolated Wolffian duct	
JNK – c-Jun N-terminal kinase	
MAPK – Mitogen-activated protein kinase	
MEK – MAPK/ERK kinase	
MET – mesenchymal to epithelial transformation	
MM – metanephric mesenchyme	

LIST OF FIGURES

Figure 1.1: Structure of the kidney	21
Figure 1.2: Nephron structure	22
Figure 1.3: Early kidney development.....	23
Figure 1.4: Mutual induction of UB and MM during kidney morphogenesis in mouse gestation days.....	23
Figure 1.5: GDNF produced in the MM	24
Figure 1.6: GDNF-centric transcriptional network model.....	24
Figure 1.7: Ret signaling.....	25
Figure 1.8: NPY structure from Protein Data Bank using QuickPDB viewer.....	26
Figure 1.9: Comparison of amino acid sequences of porcine NPY, PYY, and PP.....	26
Figure 2.1: Removal of WD & kidneys from embryo.	45
Figure 2.2: Separation of WD(+IM)	46
Figure 2.3: WD(+IM) culture system.	47
Figure 2.4: Isolated WD (iWD) culture system.	48
Figure 2.5: GDNF signaling in budding or inhibition of budding.....	49
Figure 2.6: WD budding.....	50
Figure 2.7: Summary of pathway inhibitors added to WDs cultured with 125 ng/ml GDNF and 125 ng/ml FGF1.....	51
Figure 2.8: Microarray conditions of Wolffian ducts.	52
Figure 2.9: Microarray Analysis	53
Figure 2.10: ANOVA and pattern matching.....	54
Figure 2.11: NPY and GDNF expression patterns in developing kidneys.	55
Figure 2.12: WD branching on filter.....	56
Figure 3.1: WD budding	81

Figure 3.2: Microarray analysis	82
Figure 3.3: Ingenuity Pathway Analysis (IPA) of microarray data generated several genetic networks.....	83
Figure 3.4: ANOVA and pattern matching.....	84
Figure 3.5: NPY expression.....	85
Figure 3.6: NPY augments bud formation in vitro.	86
Figure 3.7: siRNA.....	88
Figure 3.8: Budding in GDNF dependent (A) and independent (B) pathways.....	89
Figure 3.9: NPY rescue of BMP4 inhibition.....	90
Figure 3.10: NPY transcriptional network.....	91
Figure 3.11: Comparison of FGF1 and NPY vs. BMP4 and activin A.....	92
Figure 3.12: Budding signaling diagram.....	94
Figure 4.1: Mouse Ret(-/-) and WT kidneys.....	118
Figure 4.2: Kidney cultures.....	119
Figure 4.3: Scatter plots.	120
Figure 4.4: Ingenuity Pathway Analysis (IPA) networks.	120
Figure 4.5: Cross-species comparison of GDNF-dependent and independent microarrays	121
Figure 4.6: Budding with and without GDNF	121
Figure 4.7: GDNF-dependent and independent budding.....	122
Figure 4.8: Budding network	123
Figure 5.1: RT-PCR of NPY and its receptors.....	136
Figure 5.2: Isolated WD (iWD) cultured with 125 ng/ml GDNF and 1 μ M NPY	137
Figure 5.3: NPY budding model.....	138
Figure 5.4: NPY increases UB branching.....	139
Figure 5.5: Ret KO.....	140
Figure 5.6: Engrailed QPCR.....	140

Figure 6.1: Expanded schematic of Fig. 3.11 B-E	141
Figure 6.2: Schematic for generation of Fig 3.12	142
Figure 6.3: GDNF-dependent and independent budding networks	143
Figure 6.4: Schematic for generating IPA networks.....	144
Figure 6.5: Generation of the “Common budding network”.....	145

LIST OF TABLES

Table 1.1: Knockout mouse strains with budding defect phenotypes. Genes expressed in the metanephric mesenchyme are listed first.....	27
Table 1.2: Early branching genes.....	28
Table 2.1: Genes increased in budded conditions.....	57
Table 2.2: ANOVA and pattern matching genes with $P < 0.001$	57
Table 3.1: IPA networks	95
Table 3.2: ANOVA & pattern matching selected genes enriched in the isolated ureteric bud.....	96
Table 3.3: NPY Transcriptional Program (selected genes enriched in budded WDs).....	97
Table 4.1: Genes upregulated in Ret(-/-) kidneys	124
Table 4.2: Genes upregulated in wild-type kidneys compared to Ret(-/-).....	125
Table 4.3: Transcriptional regulators and signaling ligands upregulated in mouse Ret(-/-) kidneys compared to mouse and rat wild-type kidneys.....	126

ACKNOWLEDGEMENTS

I would like to thank Professor Sanjay Nigam for his support as the chair of my committee. Through multiple drafts his guidance has proved to be invaluable. I would like to acknowledge and thank the Nephrology Training Grant for providing financial support for 4.5 years.

I would also like to acknowledge all the present and past members of the lab who helped me in innumerable ways. I would like to especially thank Dr. Derina Sweeney and Dr. Kevin T. Bush for helping me with revising this manuscript.

Chapter 3, in full, is currently being prepared for submission for publication. Choi, Yohan; Tee, James B.; Gallegos, Thomas F.; Shah, Mita M.; Oishi, Hideto; Sakurai, Hiroyuki; Kitamura, Shinji; Nigam, Sanjay K. The dissertation author was the primary investigator and author of this paper.

Chapter 4, in part, is currently being prepared for submission for publication. Choi, Yohan; DeCambre, Marvalyn; Ito, Chiharu; Nigam, Sanjay K. The dissertation author was the primary investigator and author of this paper.

VITA

Bachelor of Science, Yale University

Research Assistant, University of California, San Diego

Master of Science, Chemical Engineering, University of California, San Diego

Development Engineer, IBM

Systems Consultant, Superior Consultant

Programmer, Symitar Systems

Research Assistant, University of California, San Diego

Doctor of Philosophy, University of California, San Diego

ABSTRACT OF THE DISSERTATION

Neuropeptide Y in Early Kidney Development

by

Yohan Choi

Doctor of Philosophy in Biomedical Sciences

University of California, San Diego, 2009

Professor Sanjay K. Nigam, Chair

The initiating step in metanephric kidney development is outgrowth of the ureteric bud (UB) from the Wolffian duct (WD) in response to signals arising from the metanephric mesenchyme. Defects in this critical morphogenetic process have been linked to some of the most common birth defects in humans. Despite its obvious importance in kidney development, much remains to be elucidated about the molecular regulation of the process. In order to address this problem, an in vitro model system was utilized which allows for direct assaying of the effects of positive and negative regulators of budding. Study of this regulation can lead to better understanding of the budding process, which in turn can lead to improved treatment or to refined tissue engineering approaches. Although a wealth of literature exists to implicate the glial cell-

line derived neurotrophic factor (GDNF) Ret pathway in UB budding, the precise signaling pathways activated by Ret have not been thoroughly studied. Of the various pathways examined, the PI3-kinase/Akt signaling pathway was found to be essential for budding while other Ret stimulated pathways appeared to be dispensable for UB budding. In addition, microarray analysis of numerous budded and unbudded conditions revealed a cluster of genes related to GDNF-Ret signaling involved in budding. Among the identified genes, neuropeptide Y (NPY) was the highest scoring gene product and correlated most significantly to the budded condition out of over 28,000 genes present on the cDNA microarray chip. Although NPY has not been previously implicated in kidney development, it has been shown to be involved in the GDNF-dependent development of enteric neurons, thus it is an ideal candidate for modulation of GDNF-dependent budding from the Wolffian duct. When NPY was added to the cultured Wolffian duct with GDNF impressive budding was observed; conversely, inhibition of the NPY receptors inhibited budding, confirming that NPY facilitates this process. Addition of BMP4 decreased budding through either downregulation of Ret and GFR α 1 or by blocking the PI3-kinase/Akt signaling pathway. This may explain how endogenous BMP4 inhibits ectopic budding. Addition of NPY to these BMP4-treated WDs rescued budding with a corresponding increase in phosphorylated Akt as well as Ret and GFR α 1 expression. This suggests that NPY may act through this pathway. This represents a novel mechanism for NPY in the development of the kidney. The formation of the ureteric bud may be a result from a combination of upregulation of the GDNF receptors along with genes that support GDNF signaling in a feed-forward loop. Experiments performed with WDs lacking the attached intermediate mesodermal cells suggest that there is an element produced by these mesenchymal cells that augments the budding processes.

CHAPTER 1:

Introduction

1.1 Kidney function and structure

The kidney is a marvelously complicated organ which performs many functions critical to the organism. In addition to filtering metabolic waste products (e.g. urea and uric acid) from the blood and excreting them as urine, the kidney maintains homeostasis for the body by regulating blood pH, maintaining blood pressure, and controlling plasma volume. The kidney also functions as an endocrine organ secreting various hormones, such as erythropoietin. In order to accomplish these diverse tasks, the kidney has a unique and complex 3D architecture (Figure 1.1) integrating afferent and efferent blood vessels, nephrons (the functional unit of the kidney) and a collecting system. There are approximately 1 million nephrons in humans and about 30,000 in rats (Figure 1.2). Each individual nephron is composed of a tuft of glomerular capillaries contained within Bowman's capsule, which is continuous with the proximal convoluted tubule, loop of Henle and distal convoluted tubule. Afferent and efferent blood vessels are intertwined with the nephron providing the basis of the osmolarity gradient critical to filtration and reabsorption.

Filtration occurs at the glomerulus of the nephron. High pressure within the afferent arteriole forces the liquid component of blood along with smaller molecules to pass through the fenestrated membranes of the glomerular capillaries and across the specialized basement membrane from the blood where it collects in the lumen of Bowman's capsule. Larger components such as red and white blood cells and most proteins remain in the blood stream. The

ultrafiltrate is essentially the liquid component of the blood and is largely composed of water, glucose, salts and urea. The ultrafiltrate then travels down the nephron where water and solutes (such as Na^+ , K^+ and Ca^{++}) are reabsorbed or secreted (depending on the body's need) to produce concentrated urine. This urine then flows out of the kidney via the collecting ducts and ureter to accumulate in the bladder.

The kidneys also regulate acid-base balance by adjusting proton levels and water composition. Blood pressure is increased by the kidneys through the release of renin or via reabsorption of sodium and water. Plasma volume and osmolality are regulated by water reabsorption.

As an endocrine organ, the kidney secretes erythropoietin, a hormone that controls red blood cell formation in bone marrow cells. The kidney also produces calcitriol, the active form of vitamin D, which increases the absorption of calcium.

1.1.1 Renal agenesis

Renal agenesis is one of the most frequent congenital defects in humans, with one in 2,000 live births suffering from unilateral agenesis (Pohl, Bhatnagar et al. 2002). Bilateral agenesis, which is fatal, is present in 1 in 5,000 to 10,000 infants. Renal agenesis may arise from mutations of genes known to affect glial cell-derived neurotrophic factor (GDNF) expression or signaling: SALL1 – Townes-Brock syndrome (Nishinakamura, Matsumoto et al. 2001), PAX2 – Renal-coloboma syndrome (Torres, Gomez-Pardo et al. 1995), and EYA1 – Branchio-Oto-Renal syndrome (Xu, Adams et al. 1999). Since renal malformations are often associated with dysgenesis during development, it is critical to understand the processes of renal embryology so we have a clearer picture of what occurs when misregulation in these processes occur.

1.1.2 Adult kidney disorders

Besides defects in kidney formation during gestation, a number of late onset problems can also arise which require treatment in the form of dialysis or kidney transplantation. Some acquired disorders are diabetic nephropathy (cause by angiopathy of capillaries in the glomeruli from diabetes), glomerulonephritis (inflammation of the glomeruli), hydronephrosis (enlargement of one or both kidneys due to obstructed urine flow), interstitial nephritis (caused by infection or reaction to medication), tumors and lupus nephritis (inflammation of the kidney from autoimmune reaction). Renal failure can be classified into acute or chronic. Acute renal failure can be caused by ischemia or by toxic overload. Kidneys can recover lost function after acute renal failure but that is not the case in chronic kidney disease. Two of the most common causes of chronic kidney disease are diabetes and hypertension. Polycystic kidney disease as well as some genetic disorders can also lead to chronic kidney disease.

26 million American adults have chronic kidney disease with millions of others at risk. Dialysis replaces some kidney functions, such as waste and fluid removal, but does not correct endocrine functions. The five-year survival probability for patients undergoing dialysis was 39% in the US and 54% in Japan during 1982 to 1987 (Held, Brunner et al. 1990). Chronic kidney disease begins without symptoms but can be detected by protein in the urine or increases in serum creatinine. As kidney function diminishes, blood pressure rises due to fluid overload and hormonal imbalance. Urea, potassium and other metabolites builds up in the blood, leading to various symptoms from lethargy and discomfort to cardiac arrhythmias. The kidneys produce less erythropoietin, which can lead to anemia.

Survival of patients with kidney transplants are approximately 7 years longer than those on dialysis; however, the waiting period to receive a kidney can be up to 3-5 years due to chronic shortages of donor kidneys. Transplanted kidneys come from either living or deceased donors. The kidney graft half-life varies from 10 to 26 years (Cecka 2005). Patient survivability is

shorter for recipients of cadaveric donor kidneys compared to living donors and is greatest for HLA identical donors. Survival also depends on donor age, cause of end-stage renal disease, and whether it is a first transplant or re-transplant. After transplantation patients must take immunosuppressive drugs for the remainder of their lives to prevent graft rejection. Some side effects of these drugs include increased infections, hypertension, hyperglycemia and, ironically, kidney injury.

1.1.3 Tissue Engineering & Wolffian duct formation

The goal of kidney tissue engineering is to create a fully implantable kidney from progenitor cells or tissue. This would solve the chronic problem of shortages of available kidneys for implantation. If the progenitor cells came from the patient's own cells it would also obviate the need for immunosuppressive drugs. One tissue engineering approach aims to produce a functional kidney by modeling the production process on the *in vivo* developmental programs of the kidney using stem cells as the starting material (Rosines, Sampogna et al. 2007). Formation of the WD or MM from progenitor cells has not yet been accomplished; however, growing UBs from the WD and getting it to branch in a 3D matrix has been accomplished *in vitro*. This work is related to one aspect of tissue engineering a kidney, namely the formation of the UB.

1.2 Kidney development

Three phases of kidney development are present in mammals: the pronephros, mesonephros and metanephros (Figure 1.3). At approximately day 22 in human embryos an epithelial tube called the nephric duct (later called the Wolffian duct) forms from intermediate mesoderm. The pronephros, a nonfunctional epithelial structure in humans, forms at

approximately the same time also from intermediate mesoderm. Fish and amphibians have functional pronephroi during gestation. Aquatic larvae perish due to excess fluid if their pronephros does not function. In the second phase of kidney development, the Wolffian duct induces intermediate mesoderm to form the mesonephric tubules in a linear sequence from cranial to caudal along the Wolffian duct. The mesonephros is the final kidney in fish and amphibians; however, in mammals the mesonephros later develops into parts of the male reproductive system or degenerates in females. The metanephric kidney, which is the permanent kidney in mammals, birds and reptiles, begins its development with the out-pouching of the Wolffian duct to form a single ureteric bud (UB) during the 5th week of gestation in humans and day 13 in rats (Shah, Sampogna et al. 2004). The UB interacts with metanephric mesenchyme to form the metanephros. Rather than the linear arrangement of tubules as found in the earlier mesonephros, metanephroi have a three-dimensional branched structure with a complex network of nephrons required to filter blood and concentrate urine.

1.2.1 Wolffian duct formation and budding

As the early embryo develops, intermediate mesoderm gives rise to parts of the urogenital system, namely the kidneys and gonads. The nephric/Wolffian duct (WD), a hollow epithelial tube, forms from the intermediate mesoderm on day 22 in humans, day 10.5 in rats and day 8.5 in mice. The WD is a paired structure that runs rostral to caudal along the body wall of the embryo and drains into the cloaca. There are three stages to WD morphogenesis. The first step is the specification of duct progenitors. The formation of the WD is dependent on the transcription factor *Lim1*, whose deletion results in agenesis of the WD (Shawlot and Behringer 1995). The transcription factors *Pax2* and *c-Sim1* are expressed in the mesenchymal progenitor cells after *Lim1* expression. Loss of *Pax2* does not affect this initial step; however, terminal differentiation

of the duct is impaired (Torres, Gomez-Pardo et al. 1995). The second stage is elongation of the progenitor cells in a caudal direction until it reaches the cloaca. Posterior extension of the pre-WD cells is dependent on the Pax2/8-regulated Gata3 expression (Grote, Souabni et al. 2006). The final stage in WD morphogenesis is the conversion of mesenchymal progenitor cells into tubular epithelial cells. This is one of the first mesenchymal-to-epithelial transitions to occur in the embryo. The tubulogenesis process is thought to be regulated by BMP4 (Obara-Ishihara, Kuhlman et al. 1999).

The metanephric mesenchyme (MM), also derived from intermediate mesoderm, is visible at day 12.5 in rats (10.5 in mice and E30 in humans, Figure 1.3). Signals from the MM cause the WD to outpouch into the ureteric bud (UB). A principle signal from the MM is GDNF, which binds to and activates its receptors c-Ret and GFR α 1 located on the WD. The UB then invades the MM, beginning the formation of the metanephric kidney. Defects in GDNF expression or in genes that regulate GDNF lead to failure of UB formation, which is discussed in more detail below. Table 1.1 summarizes some genes whose removal leads to loss of GDNF expression.

1.2.2 Ureteric bud branching

The single epithelial ureteric bud (UB) will eventually form the entire collecting system of the kidney: from the insertion site of the ureter into the bladder to the collecting tubules. It begins as a simple outpouching of the WD and eventually develops into a tree-like network. After its initial outgrowth from the WD, the UB invades the MM and then undergoes the initial branching event to form “T”-shaped structure. It then undergoes multiple iterations of growth and branching in response to signals received from the MM to form the tree-like renal collecting system. At the same time, some cells of the MM condense around the tips of the UB and are

induced to undergo a series of morphogenetic events ultimately forming the tubular nephron (Figure 1.4). This mutual induction gives rise to the complex patterning and 3D architecture of the metanephric kidney which is necessary for its many functions.

Branching morphogenesis is a phenomenon common to a variety of epithelial tissues such as lung, salivary gland, prostate gland, breast, and kidney (O'Brien, Zegers et al. 2002; Shah, Sampogna et al. 2004). UB branching is thought to be a key determinant in final nephron number, with the number of UB branch tips correlating to the number of nephrons. Iterative branching of the UB repeats approximately 15 times in human development to form the collecting system of the kidney, leading to 300,000 to 1,000,000 nephrons per kidney (Nyengaard and Bendtsen 1992). Various soluble factors from the MM (such as GDNF, which is discussed below) and pleiotrophin (Sakurai, Bush et al. 2001) play a crucial role in inducing the UB branching program. The early branching segments of the UB later dilate and grow to form the renal calyces and renal pelvis which continues on to the ureter. Defects or reductions in branching lead to fewer UB tips and thus fewer nephrons. A reduction in nephron number has been suggested to play a key role in the adult onset of hypertension (Keller, Zimmer et al. 2003). Table 1.2 summarizes mutations that affect branching.

1.2.3 Metanephric mesenchyme induction

The branching tips of the UB cause the MM to transform from a loose aggregate of undifferentiated cells into epithelial tubes, a process termed mesenchymal to epithelial transformation (MET). One recently discovered growth factor secreted by the UB that was identified by its ability to induce MM is cytokine-like factor 1 (CLF-1) (Schmidt-Ott, Yang et al. 2005). The pre-tubular MM cells first condense to approximately four or five cell layers around the tips of the UB (E11.5-E12 in mice, ~E13.5 in rats) (Klein, Langegger et al. 1988). The

epithelial aggregates extend to form comma-shaped and later S-shaped bodies. Eventually, the newly epithelialized portion of the nephron fuses to the collecting duct epithelium to form a continuous lumen in a process mediated by Cadherin-6 (Mah, Saueressig et al. 2000). The MM-derived portion of the kidney forms the glomerulus to the distal tubule of the nephron (Saxén 1987).

The MM can also form other parts of the kidney, such as the renal stroma, which comprises most of the MM that does not condense into nephrons. The renal stroma expresses neuronal cell markers rather than typical mesenchymal markers such as vimentin so some researchers believe that it is derived from neural crest instead of from the MM (Sainio, Nonclercq et al. 1994). Stroma cells can regulate branching morphogenesis. Vitamin A from an external source regulates Ret expression on the UB via RAR receptors found in the stromal cells (Batourina, Gim et al. 2001). Another type of cell in the kidney is the endothelial cell. The lineage of the kidney's endothelial cells may be derived from invading cells (angiogenesis) or from the MM itself (vasculogenesis). Both processes may contribute to renal blood vessel formation (Risau 1998). The source for vascular smooth muscle cells may also come from either the MM or invading blood vessels.

The growth of the kidney is rapid, with measurement of mouse kidneys showing a quadrupling in volume each day between E12 and E16 (Davies and Bard 1998). New nephrons continue to form until 2 weeks after birth in mice, but stop about 6 weeks before birth in humans; indicating the loss of blastemal cells (Bard, Gordon et al. 2001). Mutations in Bmp7, Fgf7, Fgf10, the IGFs, and PDGF lead to defects in kidney size (Bard 2002; Shah, Sampogna et al. 2004).

1.2.4 Similarities between budding and branching

Each iterative branching process could be a recapitulation of the initial UB budding event (Meyer, Schwesinger et al. 2004). Most known defects in kidney development result in complete agenesis, while relatively fewer affect the number of branching generations. During the branching process, the lumen remains patent while cells proliferate to form the new branch. Since this process occurs within the developing embryo it is difficult to study *in vivo*; however, various *in vitro* culture systems exist to study WD budding, UB branching or MM MET. The WD *in vitro* budding system will be discussed further in chapter 2 while the UB branching system will be briefly mentioned in chapter 5.

1.3 Molecular control of Wolffian duct budding

The initiating process of metanephric kidney development, namely the formation of the UB from the WD, is a process that has only recently begun to be understood. Various knockout animal models have improved the understanding of the interactions between positive and negative regulators of this process. Numerous genetic mutations result in kidney agenesis due to lost GDNF expression. GDNF signaling is one of the principle components of budding.

1.3.1 GDNF

GDNF, a paracrine growth factor produced in the MM, binds to its receptors on the WD, which then activates signaling in the WD cells to form into the UB (Figure 1.5). GDNF first binds to its receptor GDNF family receptor $\alpha 1$ (GFR $\alpha 1$), a GPI-linked receptor, which then recruits Ret, a receptor tyrosine kinase. GFR $\alpha 1$ binds the ligand but is not thought to signal without Ret as GFR $\alpha 1$ does not completely cross the plasma membrane. Conversely, Ret delivers

the intracellular signals but does not bind the ligand. The co-receptors $GFR\alpha 1$ and Ret are located throughout and along the WD prior to UB formation; however, they both become localized to the budding tip(s) once the UB has formed (Costantini and Shakya 2006). GDNF activates many different downstream signaling pathways, which are discussed below.

Mutations in RET account for 40% of human cases of renal agenesis, while 5-10% are caused by GDNF mutations (Costantini and Shakya 2006). In addition to the mutations in Eya1, Pax2, and Sall1, mentioned above, mouse knockouts of Gdf11 (Esquela and Lee 2003) or a triple knockout Hox(a/c/d)11 (Wellik, Hawkes et al. 2002) also result in kidney agenesis due to insufficient GDNF formation (Figure 1.6). Although GDNF has been the central focus of attention on UB budding, it may not be the only growth factor leading to UB formation. Because 30-50% of animals deficient in Ret still form a UB (Schuchardt, D'Agati et al. 1996), there probably exists bypass mechanisms that allow for compensatory adjustment in the cases where one of the receptors is absent.

1.3.2 Balance of growth factors and inhibitors

A balance of positive and negative factors is required to form a single UB in the proper location on the WD. Without sufficient GDNF, no UB forms or the UB degenerates, leading to kidney agenesis. Similarly, knockouts of the receptors $GFR\alpha 1$ or Ret result in defective kidney formation. Knockouts of Six1 or Wt1 result in kidney agenesis (Kreidberg, Sariola et al. 1993; Xu, Zheng et al. 2003); however, GDNF is not affected, at least at the mRNA level. Whether protein levels of GDNF are affected by this knockout or if different pathways are altered remains to be determined. It is possible that Six1 or Wt1 could affect downstream regulators of budding such as bone morphogenetic protein 4 (BMP4) or Gremlin (discussed below) or they may affect an as yet undiscovered mechanism.

Excessive GDNF production results in multiple, ectopic UB formation from the WD. Deletion of *Foxc1*, a transcription factor expressed in the MM, caused an expansion in the area where GDNF and *Eya1* are expressed leading to duplex kidneys and ureters (Kume, Deng et al. 2000). Similarly knockouts of the secreted protein *Slit2* or its mesenchymal receptor *Robo2* showed anterior expansion in expression of GDNF, leading to multiple ureters that were connected to the WD instead of the bladder (Grieshammer, Le et al. 2004). This suggests that *Foxc1* and *Slit2/Robo2* are negative regulators of GDNF expression. Regulation of budding also occurs independent of GDNF production. A major factor blocking response to GDNF on the WD is BMP4, which is produced in the mesenchyme surrounding the WD (not to be confused with the MM). BMP4 knockout animals die before kidney formation; however, some heterozygous BMP4 mutants have double ureters (Miyazaki, Oshima et al. 2000). A knock out of *Gremlin*, which inhibits BMP4, results in kidney agenesis due to unabated BMP4 signaling (Michos, Panman et al. 2004). Neither *Gremlin* nor BMP4 knockout mice have altered GDNF expression, suggesting that BMP4 acts downstream of Ret signaling. Current work suggests BMP4 downregulates Ret expression or prevents its upregulation in addition to blocking one of the major Ret signaling pathways. This is described in a later chapter.

Activins are dimeric proteins that are members of the TGF- β superfamily. Activin A, which may be an endogenous inhibitor of budding, blocks Ret signaling in a similar fashion to BMP4 (Maeshima, Vaughn et al. 2006). Activin A is present in both the WD cells as well as in the mesenchyme surrounding the WD. Secreted follistatin blocks activin A signaling by binding to it with high affinity. Although the Activin A mutant does not have a reported kidney phenotype, its importance in regulation of UB formation has been inferred based on in vitro culture systems.

Sprouty1 knockouts have multiple UB formation, possible due to the increased sensitivity of the WD to GDNF or FGFs (Basson, Akbulut et al. 2005). *Sprouty1* suppresses

Ras/Erk MAP kinase signaling (Kim and Bar-Sagi 2004). Whether the knockouts are more sensitive to GDNF expression or to secreted FGFs remains to be determined. Sprouty1 has also been proposed to regulate a Gdnf/Ret/Wnt11 positive feedback loop during UB branching (Basson, Watson-Johnson et al. 2006).

Therefore, there are many mechanisms by which the formation of a single UB is regulated (Figure 1.6, Table 1.1). Both positive and negative regulators play a role in assuring that only a single UB forms at the correct location on the WD.

1.3.3 Receptor tyrosine kinase signaling (Ret & FGFR)

Ret, the signaling receptor for GDNF, is a receptor tyrosine kinase which can activate various signaling pathways in cell culture models including RAS/extracellular signal-regulated kinase (ERK), phosphatidylinositol 3-kinase (PI3-kinase)/Akt, p38 mitogen activated protein kinase (MAPK), and c-Jun N-terminal kinase (JNK) pathways (Figure 1.7, reviewed in (Takahashi 2001)). This will be discussed further in the next chapter.

Although GDNF signaling is very important for budding of the WD, it may not be the only signaling molecule. The failures of Six1 or Wt1 to form a UB despite normal expression of GDNF supports this hypothesis. Recent data suggest that fibroblast growth factors (FGF) may also be involved in budding (Maeshima, Sakurai et al. 2007). FGFs are involved in cell growth, chemotaxis, cell migration, differentiation, cell survival, and apoptosis (Bottcher and Niehrs 2005). There are 22 members of the FGF family that bind to four receptors with various isoforms. The FGF Receptors (FGFR), similar to cRet, are receptor tyrosine kinases. As such, FGFRs signal through Ras/MAPK, PLC γ /Ca²⁺, and PI3-kinase/Akt (reviewed in (Bottcher and Niehrs 2005)). FGFR1 is expressed in undifferentiated MM, condensed MM and developing nephrons, while FGFR2 is expressed in the UB (reviewed in (Bates 2007)). Lost expression of

FGF7, FGF10 or FGFR2IIIb results in fewer nephrons and renal hypoplasia (Hatini, Huh et al. 1996; Qiao, Uzzo et al. 1999).

1.3.4 GDNF-independent budding

Ret-independent signaling was shown in cell lines that did not express Ret (Poteryaev, Titievsky et al. 1999; Trupp, Scott et al. 1999). Upon stimulation with GDNF, Src-type kinases were activated in these cells, which in turn triggered activation of MAPK, CREB, and phospholipase C γ ; however, Ras/ERK pathways were not activated. Further studies implicated the involvement of cMet, the HGF receptor in this Ret-independent signaling (Popsueva, Poteryaev et al. 2003).

Although most mice lacking GDNF or its receptors GFR α 1 and Ret have kidney agenesis, there is still a large percentage (20-50%) that nevertheless form a UB and then rudimentary kidneys (Schuchardt, D'Agati et al. 1994; Moore, Klein et al. 1996). There may be a compensatory mechanism that bypasses GDNF signaling to form a UB. Endogenous FGF7 and follistatin may be one of the mechanism by which budding is achieved without GDNF (Maeshima, Sakurai et al. 2007). Further discussion on this topic will be addressed chapter 4.

1.4 Microarrays in the study of renal development

Microarrays allow measurement of genome-wide transcriptional profiles, giving vast amounts of data. They have been successfully utilized to discover novel agents of kidney development, such as CLF-1 (Schmidt-Ott, Yang et al. 2005), mentioned previously. Short DNA segments (probes) are affixed to a solid surface of the microarray. Fluorescently labeled cDNA amplified from mRNA hybridizes to the appropriate probes, allowing measurement not only of

the presence or absence of a specific gene but also their relative quantities. Patterning hundreds of thousands of probes on a microarray allows for the measurement of mRNA of the entire genome, termed the transcriptome. Measurement of mRNA levels in different states should give clues to the differential expression of genes and possibly signaling pathways.

Some problems exist with microarrays, such as low signal-to-noise ratios and high rates of false positive signals, making verification of results via quantitative PCR (qPCR) essential. Another confounding factor is the widely varying basal expression level for many genes, making measurement of a baseline or selecting a reference gene more difficult (Vandesompele, De Preter et al. 2002). An additional complication is that some growth factors can operate at very low concentrations and that mRNA expression level may not accurately correlate to protein levels (Hack 2004).

1.4.1 Microarray analysis of kidney development

Our lab was involved in a seminal work to define patterns of gene expression during development of the metanephros (Stuart, Bush et al. 2001). Microarrays from embryonic day 13, 15, 17 and 19, newborn, 1 week old and adult rat kidneys showed 5 distinct patterns of gene expression, with groups of genes having similar patterns of expression. Many genes known to modulate kidney development were in groups that showed high initial expression followed by a decrease in expression with time. A further study comparing microarrays of in vitro models of kidney development were utilized to decouple branching of the UB and induction of the MM. This demonstrated differential patterns in gene expression in development of the UB and the MM (Stuart, Bush et al. 2003). Another group recently used a similar approach to find novel regulators of kidney development (Schmidt-Ott, Yang et al. 2005; Schmidt-Ott, Masckauchan et al. 2007). In this present study, microarray analysis of numerous budded and nonbudded conditions were obtained and analyzed to find genes and networks essential for bud formation.

Chapters 2 and 3 will discuss this in further detail. This method has identified a novel component in WD budding, neuropeptide Y.

1.5 NPY

Neuropeptide Y (NPY) is one of the most abundant neuropeptides. NPY, which is distributed in both the peripheral and central nervous systems, was initially identified in porcine brain extracts (Tatemoto, Carlquist et al. 1982). It was named neuropeptide Y due to its many tyrosine (Y) residues. NPY is involved in the regulation of various physiological functions such as cardiovascular response, circadian rhythms, food intake and hormone secretion. NPY has also been implicated to play a role in several disorders such as epilepsy, depression, anxiety and alcohol dependence.

1.5.1 NPY structure and localization

NPY is a conserved, linear 36-amino acid polypeptide (Figure 1.8) that is derived from a 97-amino acid precursor (Minth, Bloom et al. 1984). It shares structural similarities to peptide YY (PYY) and pancreatic polypeptide (PP), which have all been proposed to be members of a peptide family (Tatemoto 1982). The structural homology of NPY to PYY and PP is 69% and 50%, respectively (Figure 1.9)(Tatemoto 1982). NPY is a major peptide in the sympathetic nervous system, where it is co-stored and co-released with catecholamines (McDonald 1988). In the central nervous system, NPY was found at extremely high concentrations, but with uneven distribution in rat and human brains (Allen, Adrian et al. 1983).

1.5.2 NPY receptors and signal transduction

NPY and its homologues signal through a group of receptors belonging to the class A (rhodopsin-like) G protein coupled receptor (GPCR) family with seven transmembrane domains. Five members have been cloned: Y₁, Y₂, Y₄, Y₅, and y₆. The putative Y₃ receptor is characterized by its high affinity for NPY but low affinity for PYY; however, the existence of the Y₃ receptor has not been proven as no clone has been produced (Michel, Beck-Sickinger et al. 1998). The y₆ receptor is present in chicken, rabbit, cow, dog and mouse, but is not present in rats (Burkhoff, Linemeyer et al. 1998). In primates and humans, the y₆ receptor is nonfunctional due to a stop codon mutation (Matsumoto, Nomura et al. 1996). The five cloned receptors are relatively promiscuous with respect to ligands, with NPY, PYY and PP binding each receptor to varying degrees. The NPY receptors couple to a single G protein belonging to the G_{i/o} class; therefore, in most cell culture assays, the NPY receptors are sensitive to pertussis toxin (PTX). However, in some cases NPY response has been PTX-insensitive (Colmers and Pittman 1989; Foucart and Majewski 1989). It is not clear if this represents a distinct mechanism or merely the failure of PTX to fully inactivate the receptors in certain cell types.

Inhibition of adenylyl cyclase is usually found in NPY signaling; however, this cannot explain many of the functional responses after stimulation of NPY receptors. In neurons inhibition of Ca²⁺ channels occurs (Ewald, Sternweis et al. 1988), whereas stimulation of these channels occurs in vasculature (Michel and Rascher 1995). Activation of K⁺ channels in cardiomyocytes (Millar, Weis et al. 1991), or inhibition of K⁺ channels in vascular smooth muscle cells (Xiong and Cheung 1995) results from NPY receptor stimulation. Therefore, NPY's action is dependent on the type of cell.

The Y₁, Y₂, Y₄, and Y₅ receptors increased mitogen-activated protein kinase (MAPK) activity in transfected cells (Mannon and Raymond 1998; Nie and Selbie 1998; Mannon and Mele 2000; Mullins, Zhang et al. 2002). NPY has also been shown to increase phosphorylation of Akt

in enteric neurons (Anitha, Chandrasekharan et al. 2006). NPY expression has been shown to be modulated by various growth factors: brain-derived neurotrophic factor in cortical neurons, nerve growth factor in avian sympathoadrenal cells, and GDNF in enteric neurons (Barnea, Cho et al. 1995; Barreto-Estrada, Medina-Ortiz et al. 2003; Anitha, Chandrasekharan et al. 2006).

1.5.3 NPY in the kidney

Renal function is regulated by both neuronal and hormonal systems to maintain homeostasis of the organism. NPY and PYY can regulate renal function directly via receptors in collecting tubules and renal vasculature where NPY produces potent renal vasoconstriction. They can also indirectly influence renal function via activation of NPY receptors in specific brain regions. NPY was detected in almost all renal sympathetic neurons (Chevendra and Weaver 1992) across many species; however, whether neurons are the only source of renal NPY is not presently known. Y1, Y2 and Y5 receptors appear to play a role in regulation of renal function. In humans the Y1 receptor is expressed in the collecting ducts, loop of Henle, and the juxtaglomerular apparatus. However, there appears to be large variations in receptor expression across various species. For example, rabbit kidneys express abundant Y2 receptors, whereas rat and human kidneys express little to no Y2.

Contraction of renal vasculature by NPY and its homologues has been demonstrated both in vitro in isolated perfused kidneys and in vivo by intrarenal and systemic injection. The effect appears to be through activation of the Y1 receptor. With decreased renal blood flow, water and electrolyte excretion would also be expected to decrease. However, in rats and humans, administration of NPY or PYY increased urine formation (Playford, Mehta et al. 1995; Bischoff, Erdbrugger et al. 1996). Conversely, NPY antagonists enhanced renal blood flow; however, they did not alter urine production or sodium excretion. NPY also inhibits release of renin, though it is

not clear if the effect is mediated by the Y1 or the Y5 receptor (Hackenthal, Aktories et al. 1987). Inhibition of noradrenaline release by NPY is mediated by the Y2 receptor (Bischoff and Michel 1998). End-stage renal disease is associated with elevated plasma NPY concentrations in some studies (Bald, Gerigk et al. 1997), but was not statistically significant in others (Klin, Waluga et al. 1998).

The NPY knockout mouse has no reported kidney phenotype (Erickson, Clegg et al. 1996). Similarly, knockouts of various NPY receptors also have no kidney phenotype reported. However, the lack of obvious phenotypes may be due to the many redundancies in the NPY system, which could lead to compensatory changes during gestation. It is possible that the lack of NPY or one of the receptors may be compensated for by upregulation of PYY or another receptor, such as what occurs in NPY Y1 receptor knockout mice which have increased expression of the Y2 receptor (Wittmann, Loacker et al. 2005).

1.5.4 NPY in development

The role of NPY in development has been demonstrated in enteric neurons, where it was shown to modulate neuronal survival and proliferation (Anitha, Chandrasekharan et al. 2006). It was found to act in an autocrine fashion as a result of GDNF-induced expression. NPY was also shown to be a neuroproliferative factor in postnatal neuronal precursor cells in the olfactory epithelium (Hansel, Eipper et al. 2001). In this work the role of NPY in the development of the kidney is explored.

1.6 Scope of the Dissertation

WD budding is important because without this initial step, the metanephric kidney will not develop. Much progress has been made in understanding the genetic alterations that lead to its disruption; however, that has largely been limited to the single gene level. How genes interact or what cell signaling events occur during budding are largely unknown. This project has aimed to further the knowledge of what occurs during the budding process.

Chapter 2 discusses various in vitro culture systems utilized to study WD budding, focusing on which Ret-mediated pathway(s) are important for budding. We ascertained that the PI3-kinase/Akt pathway was essential for budding of the WD. We next utilized microarray analysis of various budding and nonbudding conditions to determine which genes or network of genes were involved in the budding process. Using a fold-change analysis we came up with a small list of genes that were directly or indirectly related to Ret signaling: Ret, Lim1 (a transcription factor shown to be important in tubular formation and Ret expression), retinaldehyde dehydrogenase (an enzyme that regulates retinoic acid, which in turn regulates Ret via renal stromal cells), and NPY (which we believe to also be involved in ret signaling). That we were able to narrow a list of 31,000 probe sets down to 4 apparently related genes attests to the power of microarray analysis.

In Chapter 3, the role of NPY in WD budding is further investigated. We started with a more limited in vivo microarray set with two unbudded and one budded microarray data set (three pooled biological replicates) and analyzed which genes are important for budding. We confirmed that NPY correlated with budding using only in vivo microarray data. We tested various receptor inhibitors and utilized siRNA to downregulate NPY, which diminished budding number and/or size. Next we explored which pathways were reactivated when NPY rescued BMP4 mediated

budding inhibition and found phospho-Akt restored in the NPY treated WDs compared to those with just the budding inhibitor BMP4.

GDNF-independent budding has been mentioned several times in this introductory chapter. In Chapter 4, the transcriptome from kidneys formed from mutant mice deficient in Ret were compared to those from wild-type mouse kidneys of the same age to determine what differences existed in these kidneys. Initial clustering showed that the variation between replicates of the wild-type kidneys were greater than the difference between the knockouts and wild-types. This suggests that only subtle changes occur during this Ret-independent budding mechanism. In vitro work to simulate knockout and wild-type budding was used to explore which signaling pathways were essential for budding in the absence of GDNF-Ret signaling. Here we found JNK signaling to be superfluous in GDNF-mediated budding but was essential in the absence of GDNF.

Chapter 5 provides future directions for this project. In this study we focused on the initial budding event. However, as previously mentioned iterative branching of the UB may involve similar or the same pathways as budding, suggesting that the same set of genes will be activated. Preliminary experiments implicate a role for NPY in UB branching. Recently, we were able to induce the WD to undergo limited branching morphogenesis in our culture system (without having to utilize a 3D matrix or conditioned media). This system may offer a promising platform in which to study the similarities and differences between budding and branching. RNA interference against candidate genes, such as Gap43, may help to screen candidate genes. Increasing our knowledge of the initial budding event may possibly lead to advances in tissue engineering or regenerative medicine for kidney replacement or regrowth.

1.7 Figures

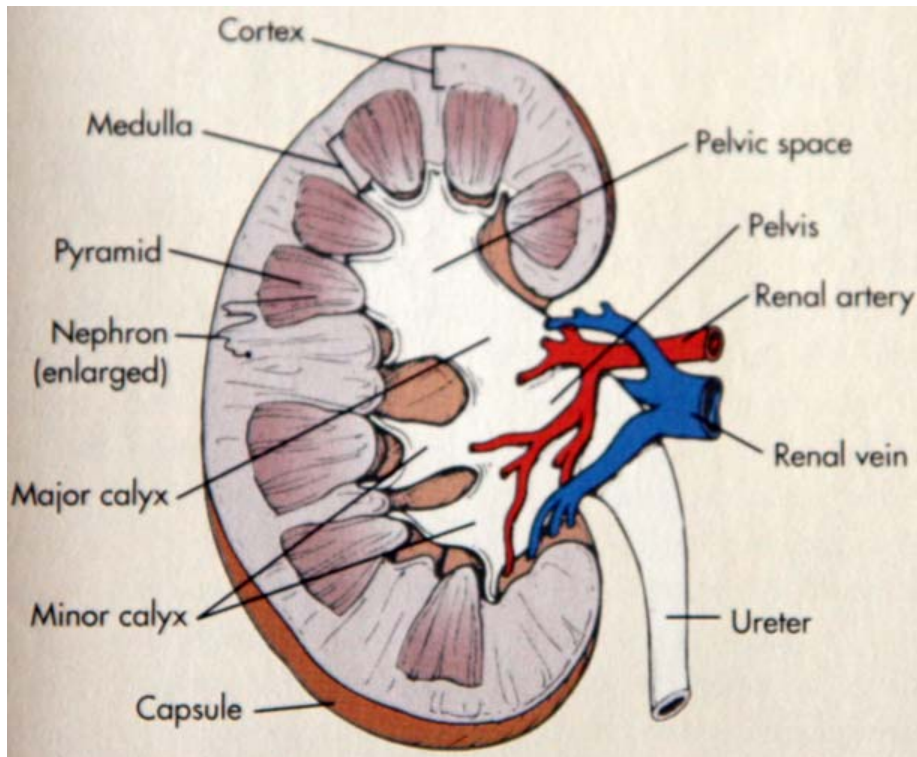


Figure 1.1: Structure of the kidney

This cross-sectional diagram of the kidney shows various components of the human kidney. The cortex forms the outer layer of the kidney, with the medulla comprising the inner layers. Collecting ducts merge into minor calyces which send urine to two or three major calyces, the renal pelvis and then down the ureter. Adapted from (Berne and Levy 2000)

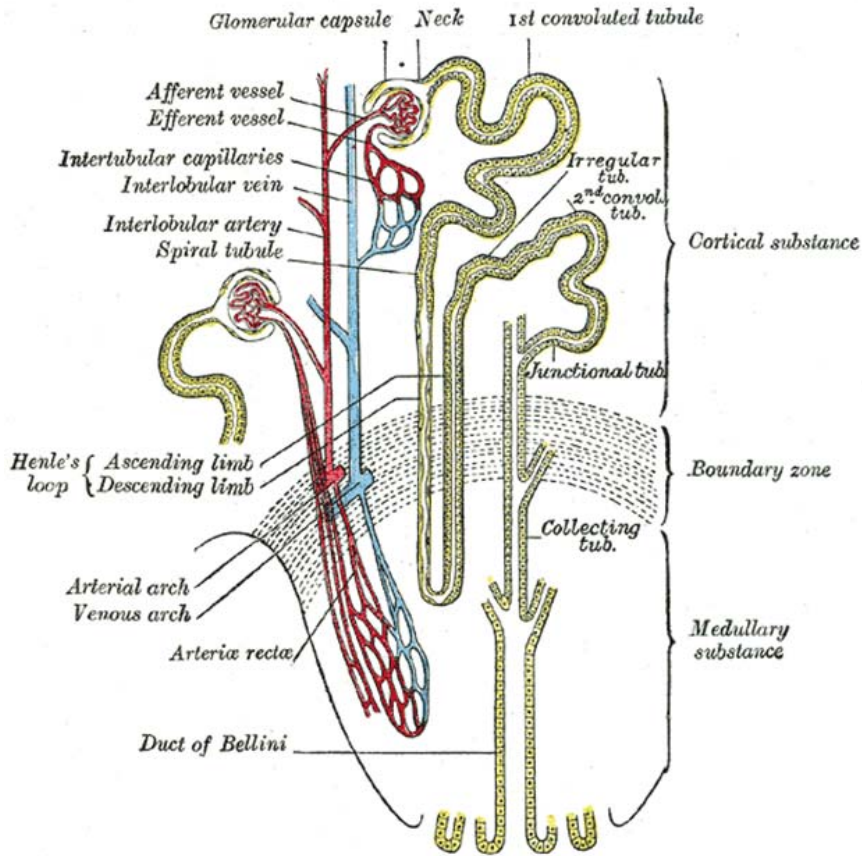


Figure 1.2: Nephron structure

Each nephron is composed of glomerular capillaries, Bowman's capsule, proximal tubule, loop of Henle, distal tubule and collecting duct. Afferent and efferent blood vessels are intertwined with the nephron to aid in filtration and reabsorption. (adapted from (Gray and Lewis 1918))

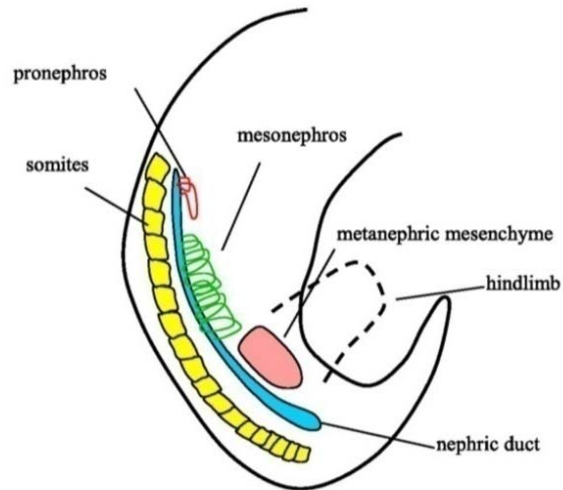


Figure 1.3: Early kidney development

Three phases of kidney development are the pronephros, mesonephros and metanephros, which form successively in mammals. The nephric duct (also called the Wolffian duct) and metanephric mesenchyme both form from intermediate mesoderm. (Adapted from (Boyle and de Caestecker 2006)).

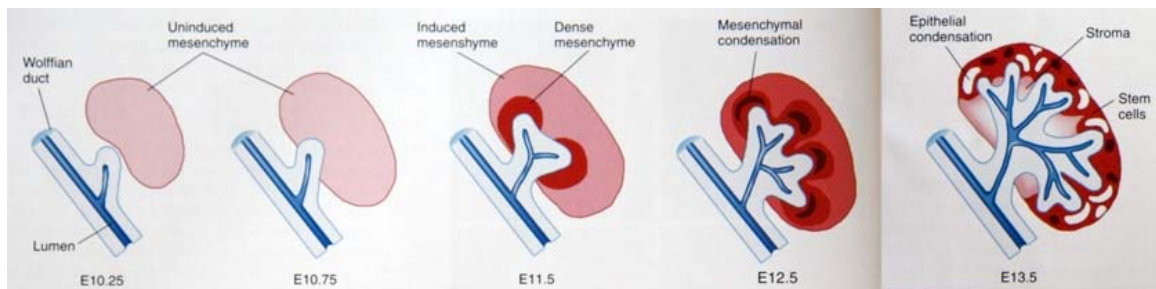


Figure 1.4: Mutual induction of UB and MM during kidney morphogenesis in mouse gestation days.

The WD forms an initial bud at approximately E10. This bud then invades the uninduced mesenchyme at E10.75. By E11.5 the UB had undergone its first branching event and mesenchyme has condensed around the tips of the UB. Later development leads to further rounds of UB branching and the epithelial condensation of mesenchyme (Adapted from (Davies and Bard 1998)).

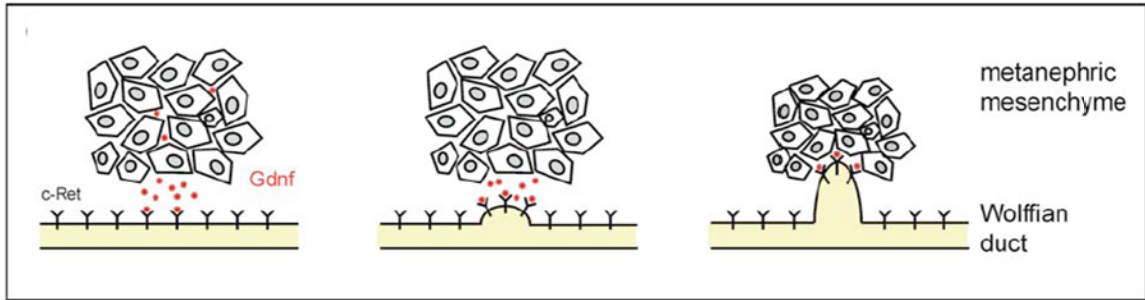


Figure 1.5: GDNF produced in the MM

GDNF from the MM travels to its receptors on the WD which then causes the WD to bud into the WD (Adapted from Brodbeck & Englert, 2004).

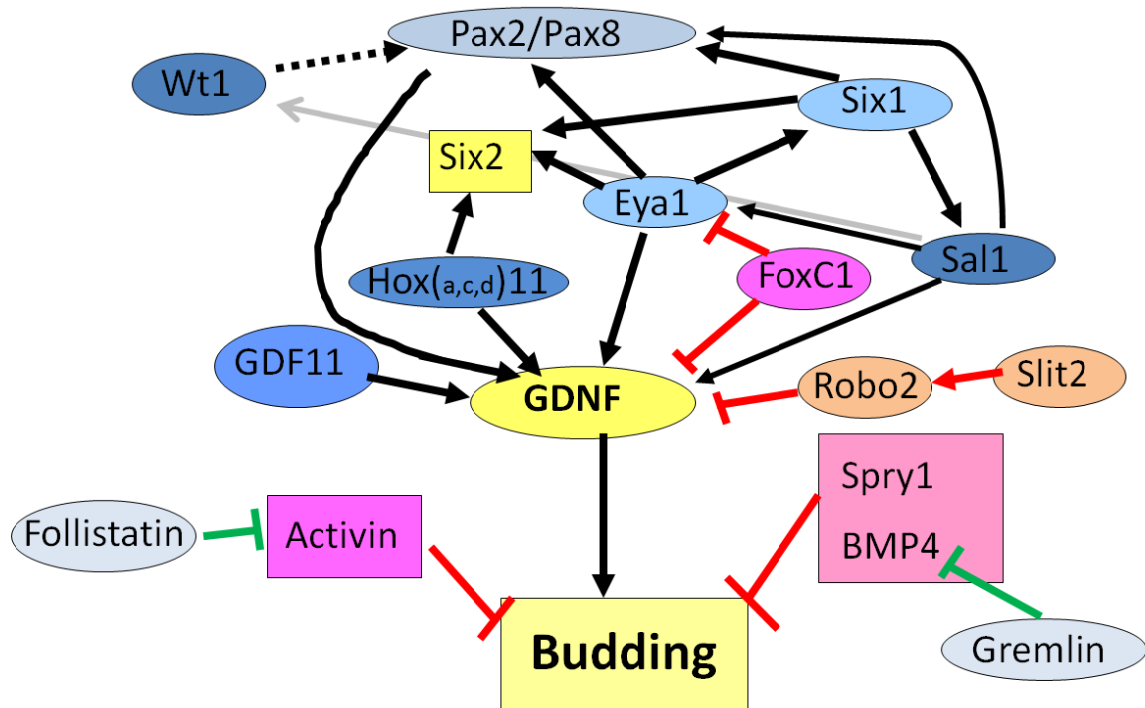


Figure 1.6: GDNF-centric transcriptional network model.

Genes regulating GDNF expression and budding. Arrows indicate activation while lines with a bar at the end indicate inhibition. Blue shaded genes increase or activate GDNF or budding. Red or orange shaded genes block GDNF expression or budding. Inhibitors of inhibitors, such as Gremlin or Follistatin, have green inhibition bars (adapted from (Brodbeck and Englert 2004)).

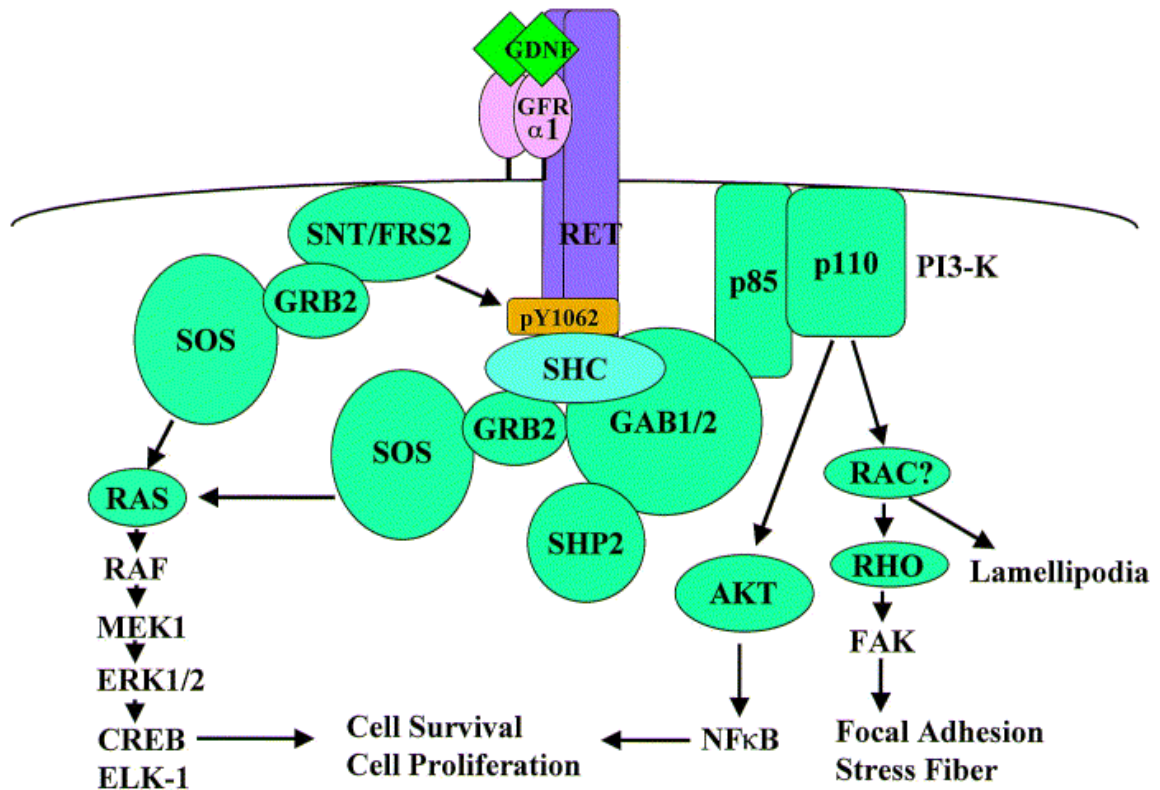


Figure 1.7: Ret signaling.

GDNF attaches to its receptor GFR α 1, which then recruits the signaling receptor Ret. Ret activates various signaling pathways such as MEK, PI3-kinase, p38 MAPK and JNK some of which are shown in the diagram (Adapted from (Takahashi 2001)).

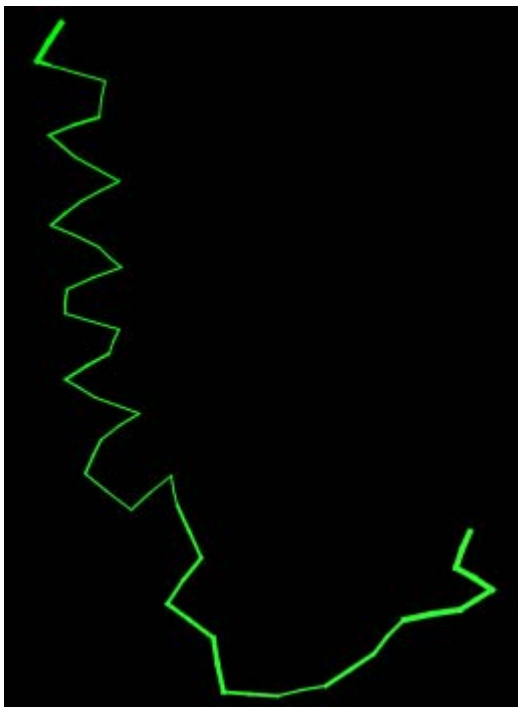


Figure 1.8: NPY structure from Protein Data Bank using QuickPDB viewer.

The 36 residues: YPSKPDNPGEDAPAEDLARYYSALRHYYINLITRQRY begin at the lower right-hand side and continue down the peptide to the upper left-hand side of the figure.

	1	10	20	30	homology
NPY	<u>Y</u> <u>P</u> <u>S</u> <u>K</u> <u>P</u> <u>D</u> <u>N</u> <u>P</u> <u>G</u> <u>E</u> <u>D</u> <u>A</u> <u>P</u> <u>A</u> <u>E</u> <u>D</u> <u>L</u> <u>A</u> <u>R</u> <u>Y</u> <u>Y</u> <u>S</u> <u>A</u> <u>L</u> <u>R</u> <u>H</u> <u>Y</u> <u>I</u> <u>N</u> <u>L</u> <u>I</u> <u>T</u> <u>R</u> <u>Q</u> <u>R</u> <u>Y</u>	100%			
PYY	<u>Y</u> <u>P</u> <u>A</u> <u>K</u> <u>P</u> <u>E</u> <u>A</u> <u>P</u> <u>G</u> <u>E</u> <u>D</u> <u>A</u> <u>S</u> <u>P</u> <u>E</u> <u>E</u> <u>L</u> <u>S</u> <u>R</u> <u>Y</u> <u>Y</u> <u>A</u> <u>S</u> <u>L</u> <u>R</u> <u>H</u> <u>Y</u> <u>L</u> <u>N</u> <u>L</u> <u>V</u> <u>T</u> <u>R</u> <u>Q</u> <u>R</u> <u>Y</u>	69%			
PP	<u>A</u> <u>P</u> <u>L</u> <u>E</u> <u>P</u> <u>V</u> <u>Y</u> <u>P</u> <u>G</u> <u>D</u> <u>D</u> <u>A</u> <u>T</u> <u>P</u> <u>E</u> <u>Q</u> <u>M</u> <u>A</u> <u>Q</u> <u>Y</u> <u>A</u> <u>A</u> <u>E</u> <u>L</u> <u>R</u> <u>R</u> <u>Y</u> <u>I</u> <u>N</u> <u>M</u> <u>L</u> <u>T</u> <u>R</u> <u>P</u> <u>R</u> <u>Y</u>	50%			

Figure 1.9: Comparison of amino acid sequences of porcine NPY, PYY, and PP.

PYY and PP share 69% and 50% amino acid identity, respectively. Identical amino acids are underlined (adapted from (Tatemoto 1982)).

Table 1.1: Knockout mouse strains with budding defect phenotypes. Genes expressed in the metanephric mesenchyme are listed first.

Gene	Early Expression	Kidney Phenotype	Molecular alterations	MM Competence	Disease	Ref
<u>Eya-1</u>	E8.5 IM E10.5 ND,U-MM E11.0 Cap MM	Agenesis, MM not specified from IM	Six1, Six2, Pax2, Gdnf lost	No MM formed	BOR syndrome	1*
<u>FoxC1/2</u>	E9.5 MN E10 U-MM E11.0 Stromal MM	Duplex kidney	Eya1, Gdnf expanded	Yes		2*
<u>Gdf11</u>		No UB formation	Gdnf lost	?		3*
<u>Gdnf</u>	E10 MM	No UB formation, MM apoptosis	Pax2 normal			4*
<u>Hox (a,b,c)11</u>	E10.5 U-MM E11.0 Stromal MM	No UB formation, MM apoptosis	Six2, Gdnf lost Eya1 normal	?		5*
<u>Pax2</u>	E8.5 IM, ND E10.5 U-MM E11.0 UB, Cap MM	Agenesis, failure of UB outgrowth	Gdnf lost	No	Renal coloboma	6*
<u>Pbx1</u>	E10.5 U-MM E11.0 Cap & stromal MM	Expansion of cap MM, UB branching reduced, hypoplasia	Pax2, Wt1 expanded	Reduced		7*
<u>Rara/β2</u>	E11.5 stromal MM	Hypoplasia, agenesis	Pax2, Wt1, Gdnf, Bmp7 normal	Yes		8*
<u>Sall1</u>	E9.5 MN, ND E10.5 U-MM E11.0 Cap MM	Agenesis (variable), failure of UB outgrowth	Pax2, Wt1, Eya1, Gdnf reduced	Yes	Townes-Brocks syndrome	9*
<u>Six1</u>	E10.5 U-MM E11.0 Cap MM	Agenesis, failure of UB outgrowth	Pax2, Six2, Sall1 absent Eya1, Gdnf, Wt1 normal	No		10*
<u>Wt1</u>	E10.5 U-MM	Agenesis	Six2, Gdnf, Pax2 normal	No	Denys-Drash syndrome Frasier syndrome	11*
<u>GFRα1</u>	UB, MM	Bilateral Agenesis (76%); unilateral rudiment (23%)				12*
<u>Lim1</u>	UB	Bilateral Agenesis				13*
<u>Ret</u>	ND, UB	Bilateral Agenesis (58%); unilateral agenesis (31%)				14*
<u>Slit2</u> <u>Robo2</u>	ND MM	Multiple UB	Gdnf expanded			15*
<u>Sprouty1</u>	ND	Multiple UB	Gdnf normal			16*

Underlined text indicates increased budding.

IM, intermediate mesoderm; ND, nephric duct; MN, mesonephros; MM, metanephric mesenchyme; U-MM, uninduced MM; UB, ureteric bud.

1* (Xu, Adams et al. 1999), 2* (Kume, Deng et al. 2000), 3* (Esquela and Lee 2003), 4* (Moore, Klein et al. 1996), 5* (Wellik, Hawkes et al. 2002), 6* (Brophy, Ostrom et al. 2001), 7* (Schnabel, Godin et al. 2003), 8* (Mendelsohn, Batourina et al. 1999), 9* (Nishinakamura, Matsumoto et al. 2001), 10* (Xu, Zheng et al. 2003), 11* (Kreidberg, Sariola et al. 1993), 12* (Cacalano, Farinas et al. 1998), 13* (Shawlot and Behringer 1995), 14* (Schuchardt, D'Agati et al. 1996), 15* (Grieshammer, Le et al. 2004), 16* (Basson, Akbulut et al. 2005)

Table 1.2: Early branching genes (adapted from (Shah, Sampogna et al. 2004))

Gene	Location of expression	Mutant mouse phenotype
Emx2	MM, UB	Bilateral agenesis secondary to failure of UB branching. Outgrowth normal(Miyamoto, Yoshida et al. 1997)
Fgf7	S	30% fewer nephrons(Qiao, Uzzo et al. 1999)
Fgf10	MM	Hypoplasia (Ohuchi, Hori et al. 2000)
Foxd1 (BF2)	S	Hypoplasia(Hatini, Huh et al. 1996)
Gdnf heterozygotes	MM	Dysplasia; 30% fewer nephrons(Cullen-McEwen, Drago et al. 2001)
Heparan sulfate 2-sulfotransferase	MM, UB	Bilateral agenesis (Bullock, Fletcher et al. 1998)
Integrin α 8	MM	Bilateral dysgenesis (Muller, Wang et al. 1997)
Laminin α 5	MM	Dysgenesis; decreased UB branching (Miner and Li 2000)
Pod1	MM	Hypoplasia and 61% decreased branching(Quaggin, Schwartz et al. 1999)
Rara/Rarb2	S	4x decrease in UB tips (Mendelsohn, Batourina et al. 1999)
Wnt4	MM	Failure of MET in MM (Stark, Vainio et al. 1994)
Wnt11	UB	36% fewer nephrons (Majumdar, Vainio et al. 2003)

MET - mesenchymal to epithelial transformation, MM – metanephric mesenchyme, S – stroma, UB - ureteric bud

CHAPTER 2

WD Budding In Vitro

Abstract

The initiating step in metanephric kidney development is budding of the Wolffian duct (WD). This process has been modeled in vitro to assay the effects of positive and negative regulators of budding. The GDNF co-receptor Ret plays a key role in GDNF signaling and thus in WD budding; however, the signaling pathways activated by Ret have not been thoroughly studied. The PI3-kinase/Akt signaling pathway was found to be essential for budding but other Ret stimulated pathways appeared to be dispensable. Microarray analysis of numerous budded and unbudded conditions was used to examine the gene changes in budding or budding suppression and revealed a cluster of genes related to GDNF-Ret signaling involved in budding.

2.1 Introduction

Wolffian Duct (WD) budding is the first step in metanephric kidney development. This is a critical phase of kidney development as the kidney will not form if the ureteric bud (UB) does not emerge from the WD. Various knockout animals displaying defective UB formation were discussed in the previous chapter. These studies have provided a wealth of information about genes and gene products involved in kidney development, nevertheless such studies are not without their own limitations. In addition to the time and expense required to generate and maintain a viable mutant animal, knockout of a number of genes are early embryonic lethal. This necessitates the generation of a conditional knockout, which requires tissue-specific promoters as well as the use of a separate transgenic mouse expressing the recombinase gene. Other genes have subtle effects when knocked out, such as cadherins, which show only slight changes in

nephron structure in the adult kidney (Dahl, Sjodin et al. 2002). Other genes have functional redundancy so there is no effect unless all the homologues are knocked out together, such as the *Hoxa11/Hoxb11/Hoxc11* cluster (Wellik, Hawkes et al. 2002), which was mentioned in chapter 1. Sometimes there is a strain effect, with an example being the *Wnt4* knockout kidney which has no epithelial differentiation of metanephric mesenchyme (MM) in pure genetic backgrounds; however, in mixed backgrounds the MM is differentiated, although the kidneys are underdeveloped (Stark, Vainio et al. 1994). Also, germline removal of a gene might cause secondary effects not directly linked to the actual gene function in the wild-type animals.

The opposite end of the spectrum is to study ureteric bud formation utilizing single cell cultures (Cantley, Barros et al. 1994; Montesano, Soriano et al. 1999). Although much information has been derived from such systems, the interaction between heterogeneous cells (such as an interface where the MM and UB interact) cannot be studied with such a simple system. An alternative to single cell cultures or whole animal mutations is an *in vitro* tissue culture system. The WD can be isolated from the embryo at E13.5 in the rat (Figure 2.1) and induced to bud *in vitro*, making systematic study of WD budding possible. Three variations of the WD culture system were described initially: whole WD culture, WD + intermediate mesoderm (WD(+IM)) culture and isolated WD (iWD) culture (Rosines, Sampogna et al. 2007). The WD can be isolated before or after the UB emerges; however, it begins to degenerate at later stages of development in females and forms seminiferous tubules in males. The entire length of the WD is capable of budding, which explains why mutations causing misexpression of GDNF can lead to multiple ureters (Maeshima, Sakurai et al. 2007).

2.1.1. Whole WD culture

The WD was originally cultured in vitro with minimal removal of the surrounding tissue (mesonephros and gonadal ridge). In this WD system GDNF-soaked heparin beads or exogenous GDNF added to the culture media was sufficient to elicit budding (Sainio, Suvanto et al. 1997; Maeshima, Vaughn et al. 2006). However, components such as the mesonephric tubules and gonadal ridge remain in the culture system. There may be secreted factors from these attached tissues that could affect budding (Maeshima, Sakurai et al. 2007). Therefore this culture system will not be discussed further.

2.1.2 WD(+Intermediate Mesoderm) culture

The second WD culture system is one where the WD is separated from the gonadal ridge and mesonephric tubules (Figure 2.2). A layer of mesenchymal tissue from the intermediate mesoderm (IM) remains attached to the WD epithelium (Figure 2.3). These WD(+IM) are cultured at the air/medium interface on top of porous filters, allowing contact with growth factors in the culture media (Rosines, Sampogna et al. 2007). In this culture system GDNF alone is usually not sufficient to induce the WD to bud; additional factors appear to be required for budding similar to the case for the isolated UB culture (Qiao, Bush et al. 2001). Supplementation of an FGF, such as FGF1 or FGF7, in addition to GDNF was found to elicit budding in this culture system (Maeshima, Sakurai et al. 2007). The studies described below utilized this WD(+IM) culture system.

2.1.3 Isolated WD (iWD) culture

The third WD culture system involves culturing the WD epithelium free from any attached intermediate mesodermal cells. This culture system is free from influences from the

mesenchymal cells; however, the WD epithelium will not maintain its tubular structure on top of a filter in 2D culture in vitro. In order to bud in vitro, the iWD must be embedded in a 3D matrix, such as Matrigel, a heterogeneous mixture of growth factors and structural proteins such as laminin and collagen secreted by mouse tumor cells. Growth factors (GDNF and FGF1) are added to the culture medium (Figure 2.4). The lumen of the WD is visible as a dark line in the center of the WD (arrowhead, Figure 2.4B). Residual attached mesenchymal cells that were not removed are also visible (arrow, Figure 2.4B). The WDs grown with GDNF and FGF1 can form multiple buds after 2 to 3 days in culture (Figure 2.4C).

2.2 Signaling pathway studies

GDNF has the potential to activate many signaling pathways upon binding to its receptors (Figure 2.5). In order to identify which of these pathways are activated for Wolffian duct budding two experimental approaches were designed. First, we utilized the WD(+IM) culture system from E13.5 rats. This WD system allowed for the investigation of various stimulatory and inhibitory signaling pathways by observing budding from the WD epithelium (Figure 2.6). Initial analysis was based on a quantitative digital readout of budding or no budding from the WD compared to controls cultured without addition of signaling inhibitors.

The second step was to obtain microarray data from numerous positive and negative budding conditions to identify genes upregulated in the budding conditions. We obtained three in vivo budding and unbudded conditions as well as 6 cultured conditions based on the initial inhibitor work with both budding and nonbudding phenotypes.

2.2.1 Inhibitor studies

We first investigated the effect of blockade of several signaling pathways through which Ret is reported to signal (Takahashi 2001). Inhibitor results are summarized in Figure 2.7. Blockade of p38 MAPK, MEK, JNK, or PKC did not inhibit budding. These GDNF stimulated pathways, were not essential for bud formation; however, they may affect other aspects of GDNF signaling in kidney development such as a decrease in iterative branching of the UB as with blockade of the MEK pathway (Watanabe and Costantini 2004). There are conflicting reports on the effect of p38 MAPK on branching of the UB. One group reported a decrease in branching with p38 MAPK inhibition (Tang, Cai et al. 2002), while another group reported a decreased size of the kidney but with the same number of branching points (Hida, Omori et al. 2002). These two conflicting reports may be reconciled because the first group used an earlier kidney, which is more sensitive to growth factors and inhibitors, as the starting point for their culture.

PI3-kinase was previously found to be important in WD budding (Tang, Cai et al. 2002), however, that study utilized the whole WD culture system, which may include influences from the remaining mesonephros or gonadal ridge tissue. Therefore, we decided to test various steps in the PI3-kinase/Akt pathway with our WD(+IM) culture system. Similar to previous results, blockade of various steps within the PI3-kinase pathway (i.e: PI3-kinase, Akt, or IKK) inhibited budding.

The mammalian target of rapamycin (mTOR) is related to the PI3-kinase/Akt pathway. Akt is stimulated by mTOR, so blocking mTOR may affect Akt signaling. Addition of rapamycin, a bacterial protein that inhibits mTOR, at high levels (~1 μ M) blocked WD budding, but the results were inconsistent at lower concentrations.

In addition to investigating the pathways with known stimulation via Ret, we explored several other pathways with the in vitro WD budding cultures. Src is a family of tyrosine kinases similar to the v-src gene in the retrovirus Rous sarcoma virus (RSV). Inhibition of Src via PP2

(4-Amino-5-(4-chlorophenyl)-7-(t-butyl)pyrazolo[3,4-d]pyrimidine) or Herbimycin A inhibited budding. PP3 (4-Amino-7-phenylpyrazol[3,4-d]pyrimidine), a negative control for PP2, had no effect on budding. As mentioned in Chapter 1, GDNF was found to activate Src-type kinases in cells that did not contain Ret, suggesting that Src might be directly or indirectly activated by GFRa1 without complexing with Ret. Some cross talk between PI3-kinase and Src was previously reported (Castoria, Migliaccio et al. 2001), suggesting that inhibition of Src will affect PI3-kinase. Whether or not this is the case in WD budding remains to be determined.

BMP4 and activin A are TGF-beta family members believed to act as endogenous inhibitors of budding (Tang, Cai et al. 2002; Michos, Panman et al. 2004; Maeshima, Vaughn et al. 2006). Addition of either BMP4 or activin A prevented budding from occurring in the cultured WD. In addition, increasing levels of protein kinase A (PKA), which serves as the major mediator of intracellular 3'-5'-cyclic adenosine monophosphate (cAMP) signaling in eukaryotic cells, through the addition of cAMP analogues also blocked budding (Tee, Choi, et al. unpublished work).

2.3 Microarray analysis

The results of the inhibitor studies indicated that a variety of growth factor and/or intracellular signaling pathways are, apparently independently, modulating the budding process. This suggested there might be common genes regulating UB formation. To explore this, we performed a microarray-based screen of genes that are expressed in a variety of budding and nonbudding conditions.

2.3.1 Affymetrix microarrays

The microarray datasets in the experiments that follow were obtained using the Affymetrix microarray chips and software platform. Affymetrix GeneChips are patterned with 25-base-pair long oligonucleotide probes that either form a perfect match (PM) or have a single base-pair mismatch (MM) that acts as negative controls. Multiple probes per probe set targeting different regions of the transcript provide robustness and resistance to minor defects to the microarray since the probes are scattered across the surface of the chip. Not all probes in a probe set will bind their target similarly due to differences in sequence and hybridization characteristics, but that can be improved by utilizing suitable design algorithms. The GeneChip Rat Genome 230 2.0 Array has approximately 31,000 probe sets on a silicon chip with an 11 micron feature size, allowing a high enough probe density to fit the entire genome on a single microarray.

The first step in obtaining the transcriptome is to purify RNA from the sample. The RNA is then amplified to cDNA using either one or two rounds of amplification depending on the amount of starting RNA available. The cDNA is then labeled with a fluorescent probe and allowed to hybridize to the microarray. An optical scanner obtains an image of the hybridized chip and analysis of the image leads to quantification of expression data. This data can then be analyzed by various methods.

Affymetrix has 12 unique PM probes and 12 MM probes in each probe set. Based on the hybridization to the PM probes and MM probes, three flags are generated: present (P), marginal (M) and absent (A). The flags are computed using a Wilcoxon signed rank test on the $(PM - MM)/(PM + MM)$ values of the probes within the probe set to determine if the difference between the signals of the PM and MM probes are statistically significant (Liu, Mei et al. 2002). Probe sets with a p-value greater than a set threshold (Higher Critical p-value) get an absent flag. Those with an intermediate p-value (between Lower Critical and Higher Critical p-values) are given a marginal flag, and the remaining probe sets are given a present flag.

2.3.2 Microarray samples

In order to identify novel factors that modulate the budding process, we obtained genome-wide transcriptional profiles of WDs with either a budded or nonbudded phenotype utilizing the Affymetrix Rat Genome Array 230 2.0. We selected three budded conditions (isolated UB, cultured WD(+IM) induced to bud with GDNF plus FGF1 and cultured WD(+IM) induced with GDNF plus FGF7) and six unbudded conditions all from, or derived from, embryonic day 13 (E13) rat tissue. The six unbudded conditions fell into two different groups: (1) uncultured iWD and WD(+IM), and (2) four cultured conditions with budding inhibited (with GDNF and FGF1 and either BMP4, activin A, Akt inhibitor IV, or dibutyryl-cAMP). Three biological replicates were performed for each condition. We obtained approximately 2-5 μg of total RNA for each of the replicates from each condition which required approximately 300 iWDs, 150 WD(+IM)s, 60-90 cultured WDs, and 300 isolated ureteric buds (Figure 2.8A).

Self-organizing maps (SOM) are useful for visualizing complicated, multidimensional data, such as multiple DNA microarrays. A small two dimensional representation of the data is produced by a type of unsupervised learning algorithm (Tsigelny, Kouznetsova et al. 2008). In this case, greater than 30,000 probe sets on the microarray was reduced to a 24x26 array. The SOMs representing the microarray data show overall similarities (via visual inspection) in pattern between the budded WDs cultured with FGF1 or FGF7 and with the two uncultured WDs (Figure 2.8B). This suggests that although the phenotype between FGF1 and FGF7 appears different, the molecular changes are largely similar. Similarly, BMP4 and activin A, which both signal through SMADs have SOMs that are roughly similar in pattern.

2.3.3 NMF

We analyzed each sample replicate via nonnegative matrix factorization (NMF), which is used for computer pattern recognition in image and natural language processing (Devarajan 2008). A matrix X is factorized into two matrices, W and H . The matrix X has the dimensions “ i ” and “ j ,” which for microarrays represent the number of conditions and the number of probe sets on the array, respectively. NMF compresses the data into the specified number of metagenes consisting of hundreds or thousands of genes in order to acquire an “overview” of the data, rather than viewing individual genes. The number of metagenes “ k ” is selected to reduce the amount of data (usually “ k ” \ll “ j ”, i.e. the number of metagenes is much less than the number of genes on the array). The W matrix will have the dimensions “ $j \times k$ ” and the H matrix, which represents the data in metagene format will have the dimensions “ $i \times k$ ” (Brunet, Tamayo et al. 2004). We analyzed 2-10 metagenes; the data for 5 metagenes is shown (Figure 2.9A). Utilizing NMF analysis, we were able to discern variations within our replicate samples. We were satisfied that the homogeneity within triple replicates was well-maintained until the number of metagenes increased beyond 7-8, beyond which point some samples within the biological triplicates partitioned into different groups. Thus, although a more traditional “Tree” view of the microarray data (with the replicates merged into one) shows no obvious correlation between budded and non-budded samples (Figure 2.9B) the NMF analysis indicated internal consistency of the data.

2.3.4 Fold-change analysis

To isolate genes that were upregulated in the budding conditions, we initially focused on ~ 400 genes that were upregulated more than two-fold in the three conditions in which budding could be induced in vitro or occurred naturally in vivo (isolated UB and the two budded, cultured WDs) compared with the uncultured WD(+IM)s (Figure 2.9C). We further reduced the genes

selected from this subset by ignoring those genes that were downregulated less than two-fold in the four conditions in which budding was blocked following treatment with signaling pathway inhibitors (compared to the WDs cultured with GDNF and FGF1); this analysis resulted in a small set of 9 genes remaining (Figure 2.9D, Table 2.1). Of the 9 genes, 4 have not been well-characterized to date, and one, Pou3f3 (Brn1), had an absent flag in all conditions except the isolated UB, suggesting this was a false positive signal. The potential in vivo relevance of this in vitro screen is supported by the fact that three of the remaining characterized genes were related to GDNF-Ret signaling: Ret, Lim 1 (a transcription factor shown to be important in tubular formation and Ret expression (Kobayashi, Kwan et al. 2005)), and retinaldehyde dehydrogenase (an enzyme that regulates retinoic acid, which in turn regulates Ret (Moreau, Vilar et al. 1998)). The remaining gene, the only one that encoded a secreted product, was Neuropeptide Y (NPY) which, as shown in chapter 3, is also likely to be involved in GDNF signaling.

2.3.5 ANOVA + Pattern Matching

The data was also analyzed using ANOVA and pattern matching which does not require arbitrarily setting a fold-change threshold (Pavlidis and Noble 2001; Pavlidis 2003). The patterns were budded or non-budded (Figure 2.10A), with the output being a P-value for each gene (the lower the P-value the greater the likelihood that the gene is relevant). More than 1500 genes were found to have a P-value less than 0.05 (Figure 2.10B), 296 of which had a P-value less than 0.01 (Figure 2.10C), while 18 genes had a P-value less than 0.001 (Figure 2.10D, Table 2.2). Interestingly, using this analysis, NPY had the lowest P-value (3.8×10^{-7}). The ANOVA method does not distinguish between positive correlation and negative correlation; however, a simple fold change analysis can determine this (c.f. top and bottom line graphs in Figure 2.10B-D). All 9 genes selected by the 2-fold change criteria were also selected by the ANOVA method when the

P-value was set to 0.05. Seven of the 9 had a P-value of 0.01 or less (Table 2.1), and only 3 genes had a P-value of 0.001; NPY was again found in this group.

2.3.6 NPY from microarray data

That these two independent methods of data analysis identified NPY from among the several thousand genes present on the array supports the role of NPY in the budding process. Moreover, we analyzed the expression of NPY in the developing embryonic kidney from microarrays and found that its highest levels of expression are at the initiation of UB formation providing some in vivo validation of the in vitro analysis (Figure 2.11). Given these results, further studies on NPY in WD budding were performed to elucidate its role in the budding process.

2.4 Discussion

Among the various WD model systems, the WD(+IM) and iWD culture set-ups are most useful since they are not influenced by factors secreted by mesonephric tubules or the gonadal ridge; nevertheless, there are trade-offs between these two. For example, while the iWD system is free from the influence of mesenchymal cells, it is possible that there are unknown growth factors present in the Matrigel matrix in which the WD is embedded. WDs appear to behave similarly in their response to growth factors and inhibitors in these two in vitro culture. The mesenchymal cells may support budding in the WD(+IM) system by secreting growth factors and/or by providing a matrix for the WD epithelium to maintain its tubular structure, although this remains to be determined.

Generally, these WD systems, when stimulated with GDNF and FGFs, will lead to the formation of supernumerary buds, but not branched buds. However, modifying the growth factors (such as with the addition of conditioned media from BSN cells, an immortalized cell line derived from mouse MM cells (Sakurai, Barros et al. 1997)) will lead to generation of branched structures on the 2D filter (Figure 2.12) or in the 3D matrix. The beginning of the branched structure might already be present on the luminal side before it becomes apparent on the outside (basolateral surface) of the bud (c.f. the simple lumen in Figure 2.6B with the T-shaped lumen in Figure 2.6C). Further investigation will be necessary to ascertain this.

It is not known why buds form in a periodic fashion along the length of the WD rather than the entire WD expanding in a single, large bud. There could be some local inhibition of budding on cells adjacent to the bud. This process may be mediated by rho kinase, as its inhibition leads to a swollen, expanded WD (data not shown). Activin A is another candidate for autocrine budding inhibition (Maeshima, Vaughn et al. 2006). Activin A could be released by the budding WD epithelium, preventing lateral areas from also budding. A complimentary explanation is that the budding process is a self-regulating auto-catalytic process, with increased expression of the receptors Ret and GFRa1 on the forming bud leading to increased sensitivity to GDNF. Perhaps a combination of these two processes occurs during budding.

The PI3-kinase/Akt pathway is essential for budding (Tang, Cai et al. 2002). Blockade of PI3-kinase, Akt or IKK all inhibited budded in vitro. This pathway may be activating cellular proliferation, cytoskeletal rearrangement, and/or migration to support the budding program. The other pathways stimulated by GDNF, such as the MEK/ERK, p38 MAPK and JNK pathways do not appear to be essential for in vitro epithelial budding. It is possible that these pathways modulate other aspects of GDNF signaling in kidney development such as iterative UB branching which is decreased when the MEK/ERK or p38 MAPK pathways are blocked (Tang, Cai et al.

2002; Watanabe and Costantini 2004). There could be a redundancy in the activated pathways, i.e. where two or more signaling pathways need to be quenched before an effect on budding is seen. Initial studies with the combination of MEK and JNK inhibition did not result in budding inhibition; however.

By obtaining a gene expression profile of assorted budded and unbudded conditions, we were able to identify genes that specifically correlated with budding. We analyzed our data with several software tools to first obtain an overview of the data and then to find specific genes regulating the budding process. In order to increase the sensitivity of detecting genes that correlate with budding, we then analyzed the data using a fold-change analysis. Under relaxed conditions, a 1.5-fold expression change threshold or when genes that were downregulated in only 3 of the 4 inhibited conditions were selected, the number of genes that were significant to the budding process was 56 and 34 genes, respectively. A gene that appears in both of these relaxed conditions is *Wnt11*, which is involved in reciprocal signaling with GDNF to form the UB and regulate branching; *Wnt11*^{-/-} mutant animals were reported to have smaller kidneys (Majumdar, Vainio et al. 2003). When the data was analyzed using the more stringent two-fold threshold, the number of significantly changed genes was reduced to 9. Further increasing the stringency to 3-fold or higher resulted in no genes being selected. We also analyzed the data with a method that did not rely on a specified fold-change number utilizing ANOVA and pattern matching (Pavlidis and Noble 2001; Pavlidis 2003). This analysis largely correlated with the fold-change analysis except that it was able to select additional genes that varied less than the arbitrary threshold. By both these analyses, NPY was the gene that had the strongest correlation (lowest P-value) with budding, which will be investigated in detail in Chapter 3.

2.5 Methods

2.5.1 Reagents

Recombinant human activin A, BMP4, rat glial-cell-derived neurotrophic factor (GDNF), FGF7, and follistatin were from R&D systems (Mineapolis, MN). Recombinant FGF1 was from Calbiochem (EMD, San Diego, CA). Akt inhibitor IV, dibutyryl-cAMP, PD169616, SB203580, JNK inhibitor II, PD98059, MEK inhibitor II, LY294002, Calphostin C, IKK-2 inhibitor IV were from CalBiochem. DMEM/F12 was purchased from Gibco (Invitrogen, Carlsbad, CA). Fetal bovine serum (FBS) was from Biowhittaker (Walkersville, MD). Flouroscein labeled Dolichos biflorus agglutinin was from Vector Labs (Burlingame, CA). Goat anti-GRF α 1 was from R&D Systems. Anti-ZO-1 and anti-E-Cadherin were from Zymed (Invitrogen). Alexa Fluor 488 or 594 secondary antibodies were from Molecular Probes (Invitrogen). Matrigel was from BD Biosciences. All other reagents were from Sigma.

2.5.2 WD isolation and culture

Wolffian duct (WD) cultures were performed as previously described (Maeshima, Vaughn et al. 2006). Briefly, embryos from time pregnant Sprague-Dawley rats (Harlan, Indianapolis, IN) at day 13 of gestation were utilized for all cultures. The WDs along with a thin layer of attached mesodermal mesenchymal cells were dissected using a stereomicroscope and fine forceps (FST, Foster City, CA). The WDs were placed on 0.4 μ m pore sized Transwell filters (Costar, Cambridge, MA) in 12 or 24-well tissue culture dishes. Culture medium consisting of DMEM/F12, 10% FBS, and growth factors was added below the Transwell.

P38 MAPK was inhibited via addition of 1 μ M PD169316 or 10 μ M SB203580. MEK/ERK was inhibited with addition of 20 μ M PD98059 or up to 100 μ M MEK inhibitor II. JNK was blocked with 5 μ M JNK inhibitor II, and PKC was blocked with 1 μ M Calphostin C.

PI3-kinase was inhibited with 10-20 μ M LY294002, Akt was inhibited with 5 μ M Akt inhibitor I, IV, or VIII, and IKK was blocked with IKK-2 inhibitor IV.

2.5.3 Immunohistochemistry

Cultured WDs were fixed with 4% paraformaldehyde (PFA) for 1-2 hours at room temperature, followed by incubation with the primary antibody in blocking solution overnight at 4C. Three rinses in phosphate buffered saline (PBS) with 0.1% Tween (PTW) was followed by incubation with the secondary antibody in blocking solution with 10% donkey serum overnight at 4C. The samples were then thoroughly rinsed with PTW and view with a confocal microscope (Nikon D-Eclipse C1).

2.5.4 Microarray preparation and analysis

RNA from the various tissues was isolated with the Abion RNAquous Micro Kit (Applied Biosystems) following the manufacturer's protocol. The purified RNA was processed by the UCSD Microarray Core facility and hybridized to the Rat Genome 230 2.0 Array (Affymetrix). Data normalization and fold-change analysis was performed with Genespring GX (Agilent).

NMF was performed using the GenePattern server and client software (Brunet, Tamayo et al. 2004; Reich, Liefeld et al. 2006). The data was preprocessed to remove genes that did not vary by 3-fold or 300 units, which reduced the data set to 21,000 genes. (5-fold and 500 unit preprocessing resulted in 10,000 genes; however the analysis was similar.) The number of metagenes was set to 5 and the rest of NMF variables were kept at the default values. For NMF Consensus clustering the number of metagenes was varied between 2 and 10.

ANOVA and pattern matching (Pavlidis and Noble 2001; Pavlidis 2003) was performed with data normalized with Genespring GX. The pattern was set as budding or non-budding. The budding sample was the isolated ureteric bud and WDs cultured with GDNF+FGF1 and GDNF+FGF7. The six non-budding samples were the two uncultured, unbudded WDs (iWD and WD(+IM)), and the four WDs cultured with GDNF, FGF1 and either BMP4, Activin A, Akt inhibitor IV, or dibutyryl-cAMP. The test type was set to parametric test, without assuming equal variances. The false discovery rate was varied between 0.05 and 0.001. No multiple testing correction or post hoc testing were performed. The software reported the P-value for each gene.

The data was normalized to unity per chip and per gene. Self-organizing maps (SOM) were generated in Genespring by selecting a matrix of 24 by 26 with a neighborhood radius of 25 and 310,000 iterations.

2.6 Figures

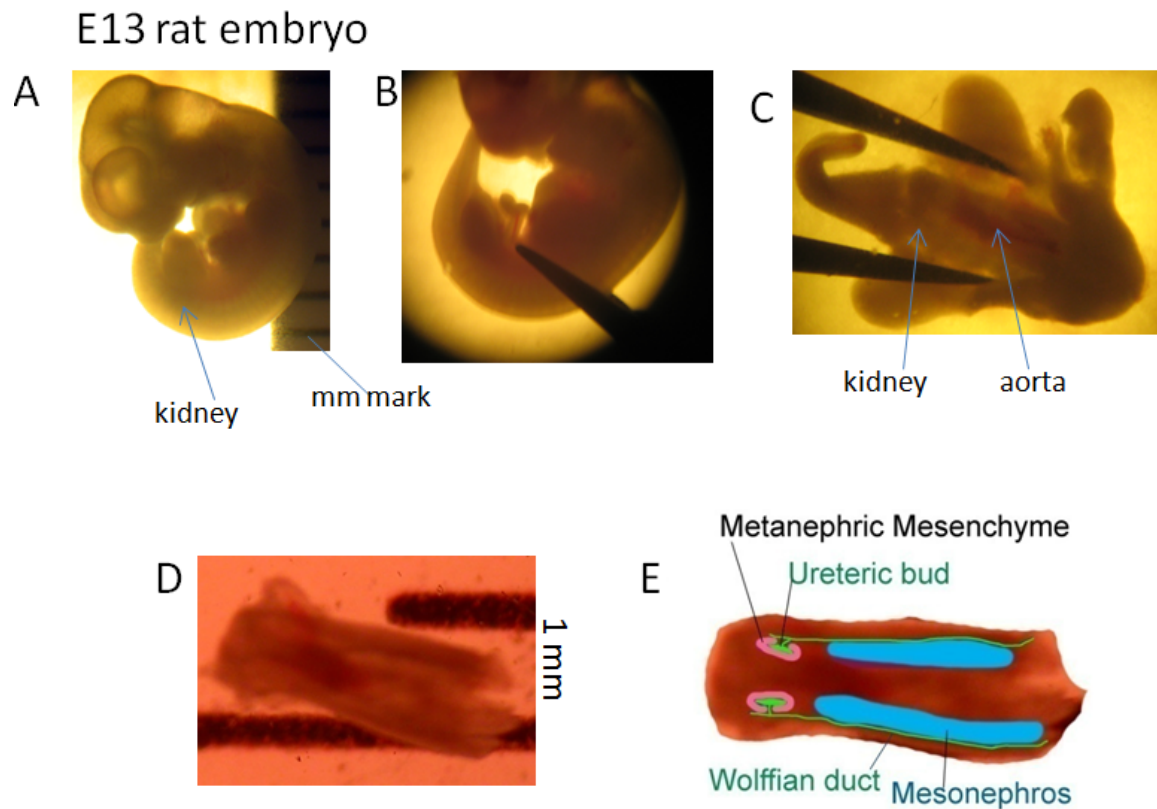


Figure 2.1: Removal of WD & kidneys from embryo.

(A) E13 rat embryo. (B) The lower section of the embryo is separated from the rest of the embryo and then rotated to allow view of the WD and kidneys. (C) Forceps are used to open the abdominal cavity, exposing the WDs and kidneys. The aorta can be seen between the WDs. (D) The WDs and kidneys are removed from the embryo by carefully pinching under the WD and pulling the tissue loose. (E) Previous image with MM, UB, WD, and mesonephros labeled.

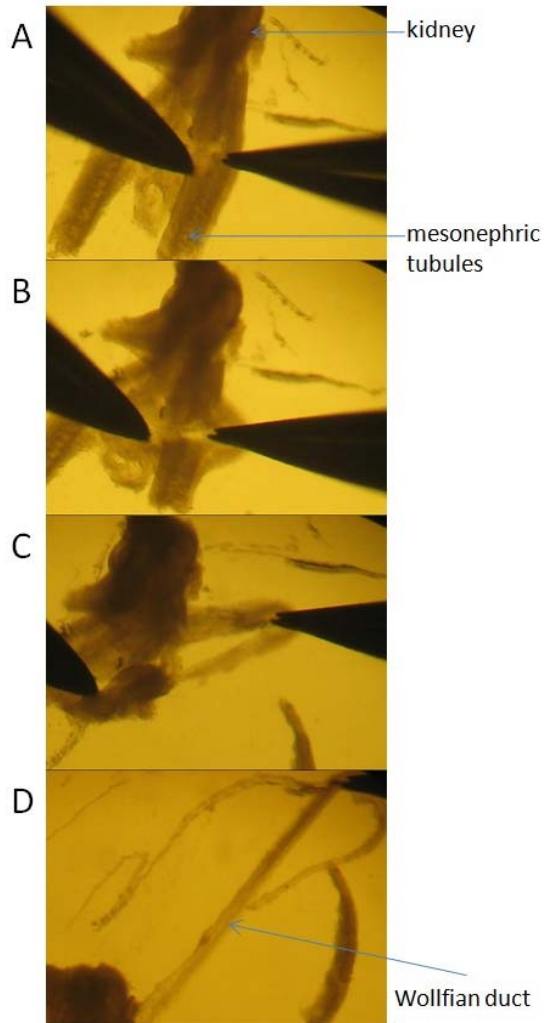


Figure 2.2: Separation of WD(+IM)

(A) One pair of forceps (left) is used to stabilize the tissue while the other is pressed between the WD and mesonephric tubules. (B-D) The WD is gently pulled away from the rest of the tissue. The attached intermediate mesoderm can be seen to the left of the WD epithelium in D.

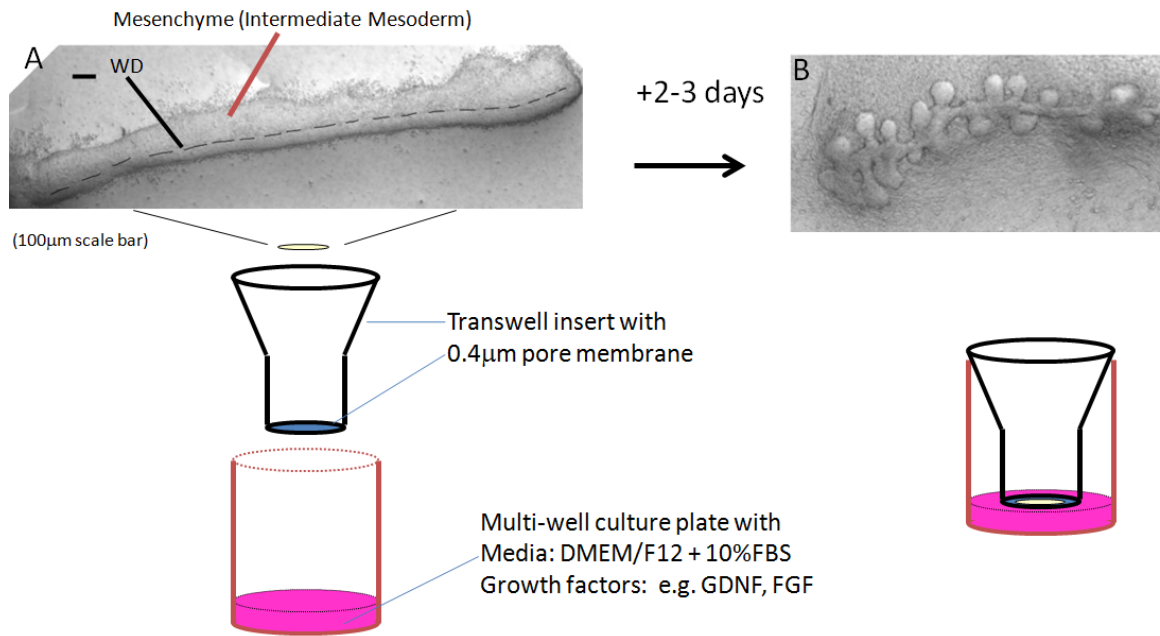


Figure 2.3: WD(+IM) culture system.

(A) WD(+IM) culture at day 0 (freshly dissected and placed on top of a transwell filter. 100 µm scale bar. (B) After 2-3 days in culture the WD epithelium will form multiple buds. (C) Schematic of culture apparatus. WDs are placed on top of the porous membrane of the Transwell insert. Culture media with growth factors contact the bottom of the porous membrane, allowing movement of nutrients and wastes between the growing tissue and media.

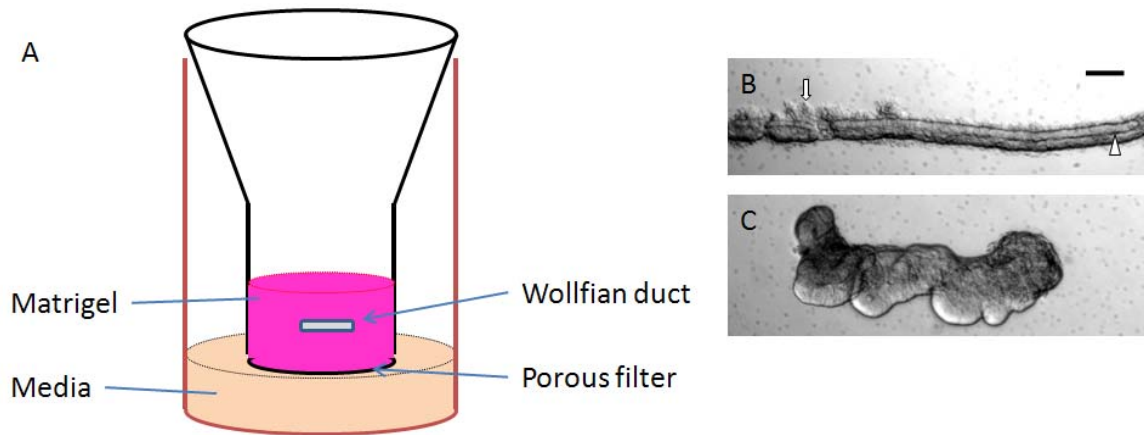


Figure 2.4: Isolated WD (iWD) culture system.

(A) Schematic of iWD culture system. In this case Matrigel is placed directly inside the Transwell and on top of the filter and the iWD is embedded within the extracellular matrix (ECM) gel. (B) WD at day 0 suspended in Matrigel. Lumen (arrow head) and attached mesenchymal cells (arrow). 100 μm scale bar. (C) WD after 2 days in culture with GDNF and FGF1.

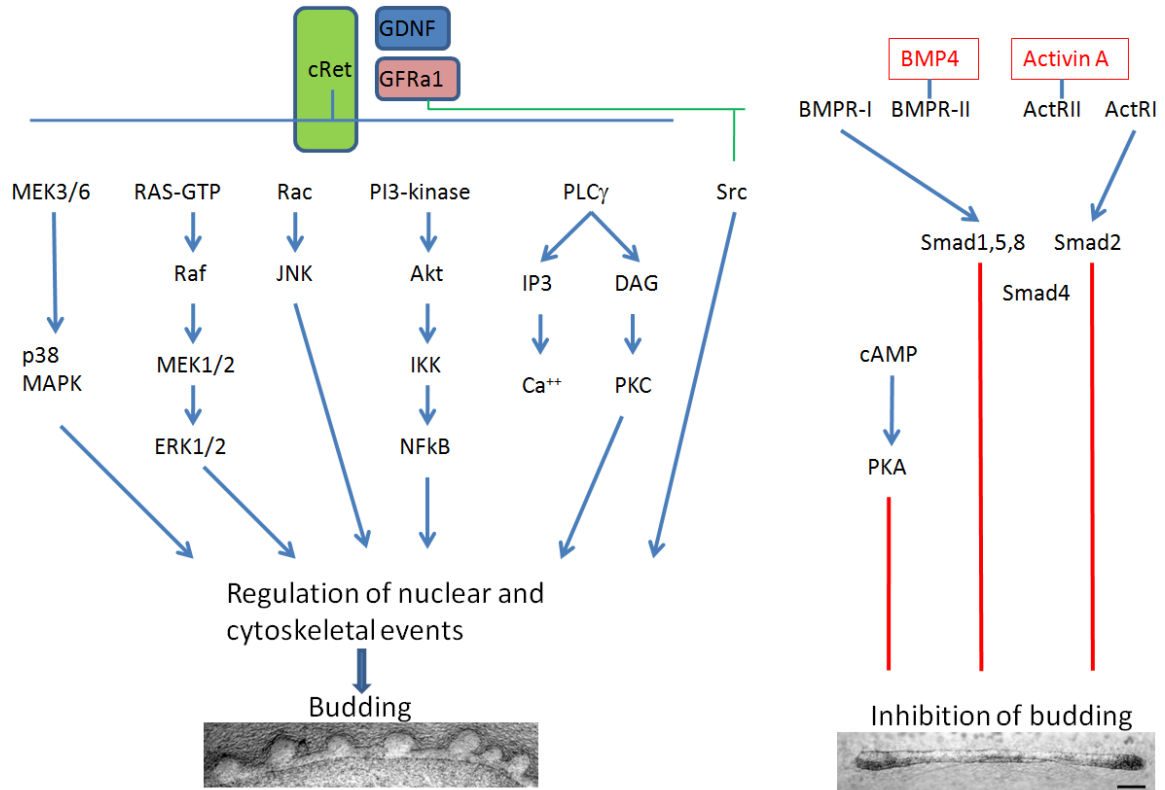


Figure 2.5: GDNF signaling in budding or inhibition of budding.

Schematic of various signal transduction pathways which are potentially activated via GDNF-GFR α 1-Ret. Inhibition of various downstream pathways that signal from Ret resulted in either no effect on budding or inhibition of budding. Endogenous inhibitors of budding, BMP4 and activin A, as well as increased PKA activity blocks budding. Sample budded WD and unbudded WD (bottom left and bottom right, respectively). 100 μ m scale bar.

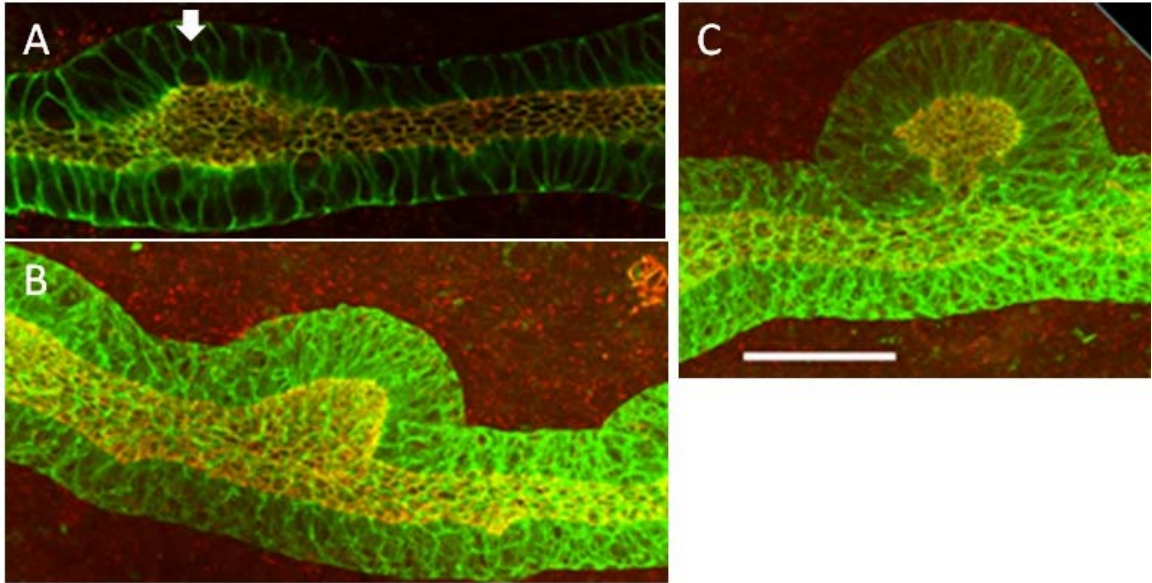


Figure 2.6: WD budding.

60x confocal images of WDs at various stages of budding. (A) Single confocal slice of a bulging WD. Round cells are dividing (arrow). (B) & (C) Confocal stacks. Red is ZO-1, which stains a tight-junction protein found in the lumen of the WD. A continuous lumen is seen in both the tubular WD and the budding section. Green is E-cadherin, an epithelial marker. 50 μm scale bar.

Ret pathway	Compound(s)	Effect on budding
p38 MAPK	PD169316 SB203580	No inhibition
MEK/ERK	PD98059 MEK inhibitor II	No inhibition
JNK	JNK inhibitor II	No inhibition
PKC	Calphostin C	No inhibition
PI3-kinase	LY294002	Inhibition
AKT	AKT inhibitor IV	Inhibition
IKK	IKK-2 inhibitor IV	Inhibition
Non-Ret pathways		
Src	Herbimycin A	Inhibition
	PP2	Inhibition
BMP4	BMP4	Inhibition
Activin A	Activin A	Inhibition

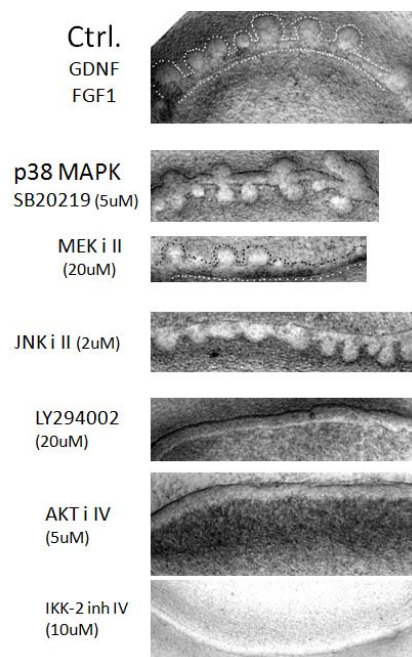


Figure 2.7: Summary of pathway inhibitors added to WDs cultured with 125 ng/ml GDNF and 125 ng/ml FGF1.

Addition of inhibitors to p38 MAPK, MEK/ERK, JNK or PKC did not inhibit budding when WDs were cultured with 125 ng/ml GDNF and 125 ng/ml FGF1. However, blockade of the PI3-kinase/Akt/IKK pathway blocked budding. Other pathways (not directly related to Ret signaling) that also inhibited budding were inhibition of Src or addition of BMP4 or Activin A. Sample images of WDs cultured with the inhibitors for 3 days are shown (Right).

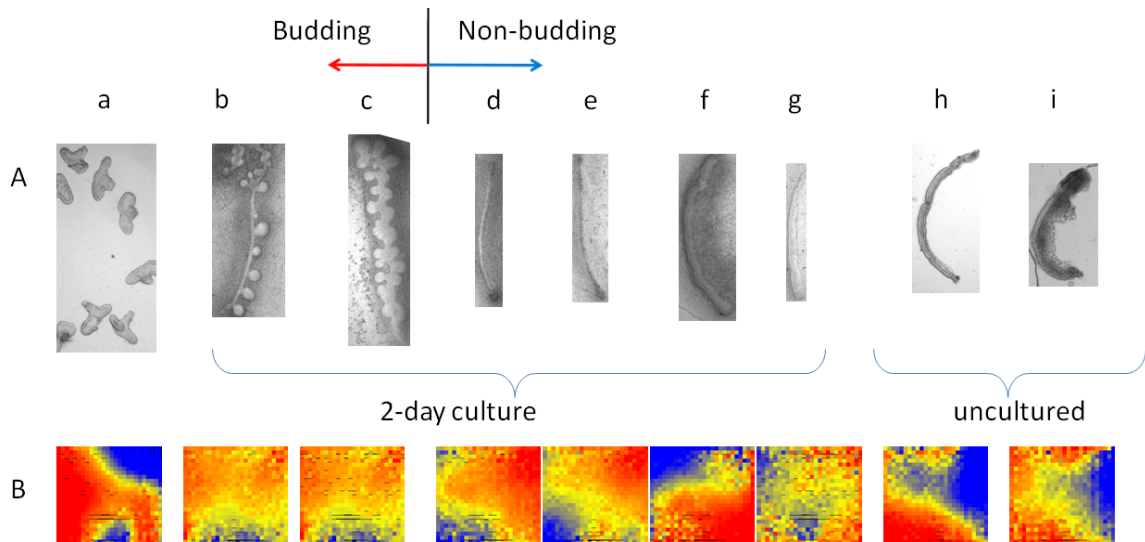


Figure 2.8: Microarray conditions of Wolffian ducts.

(A) Microarray sample images: (a) uncultured budded isolated UB; WDs cultured for 2 days in (b) 125 ng/ml GDNF+FGF1, (c) 125 ng/ml GDNF + 50 ng/ml FGF7; WDs cultured with 125 ng/ml GDNF+FGF1 + a budding inhibitor (d) 100 ng/ml BMP4, (e) 100 ng/ml Activin A, (f) 5 μM Akt inhibitor IV, (g) 200 μM dbcAMP; Uncultured, unbudded WDs (h) isolated WD (without attached mesenchymal cells) (i) WD+Intermediate Mesoderm (with attached mesenchymal cells). (B) Self-organizing maps (SOM) of the microarray for the conditions (a-i) above.

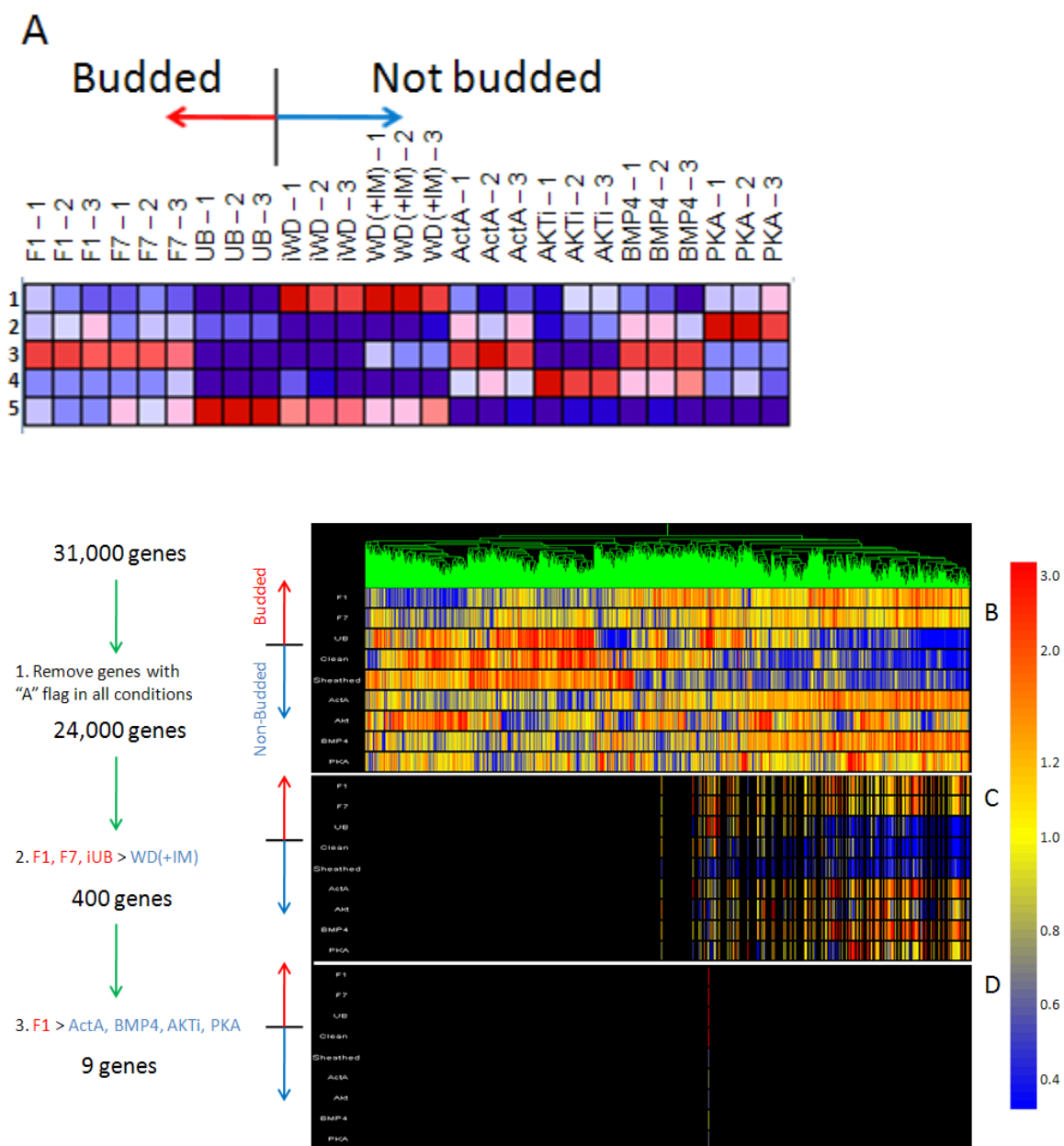


Figure 2.9: Microarray Analysis

(A) Nonnegative Matrix Factorization (NMF) was applied to the microarray data that was preprocessed to include genes that changed at least 3-fold and by 300 units. The data was factored into 5 metagenes. (B-D) Microarray tree of budded and non-budded samples (B) Genes without an Absent flag in all conditions ~24,000 genes (C) ~400 genes upregulated 2-fold in budded F1 and F7 vs. sheathed WDs (D) subset of 9 genes upregulated in budded WDs as described in the text.

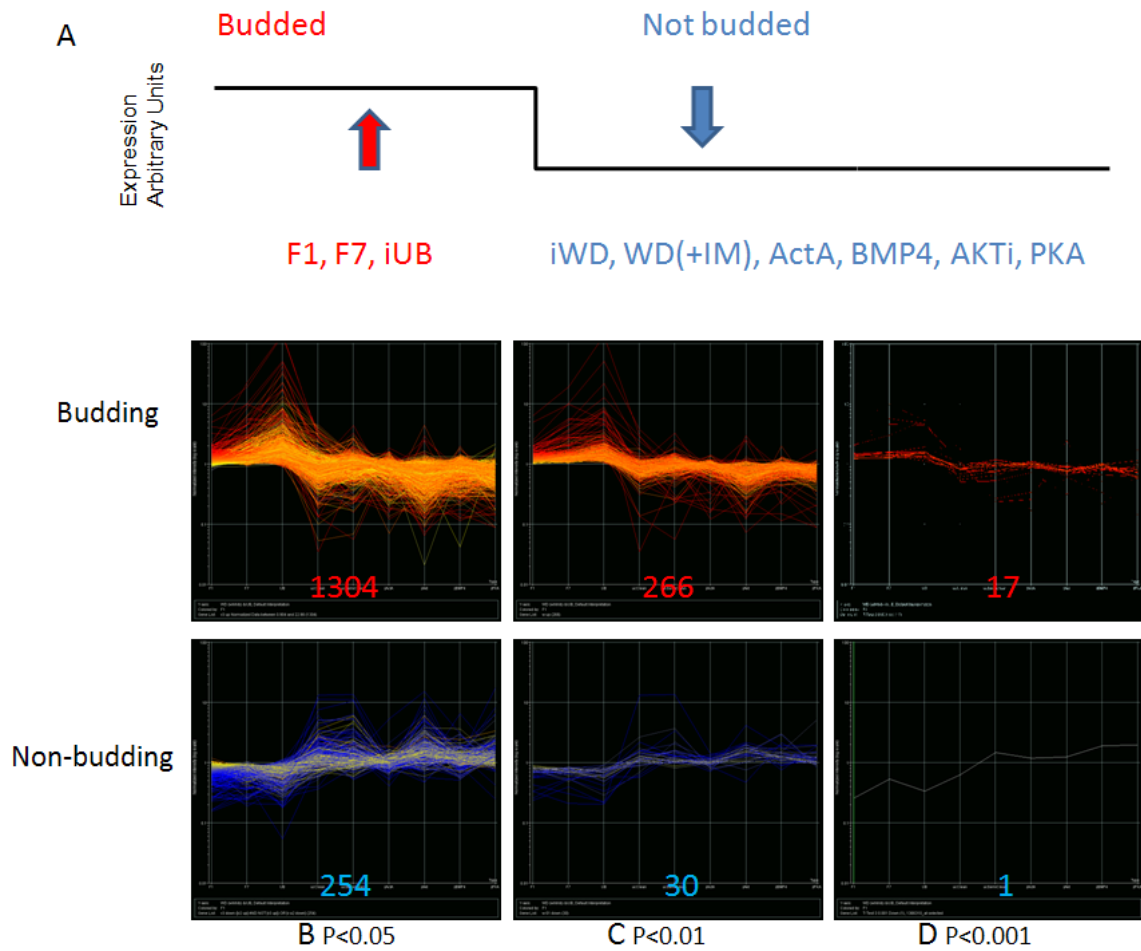


Figure 2.10: ANOVA and pattern matching

(A) Pattern set for ANOVA analysis (B-D) Line graph corresponding to budding (top) or non-budding (bottom) for (B) $P < 0.05$ 1558 genes: 1304 up (top), 254 down (bottom), (C) $P < 0.01$ 296 genes: 266 top, 30 bottom, (D) $P < 0.001$ 18 genes: 17 top, 1 bottom.

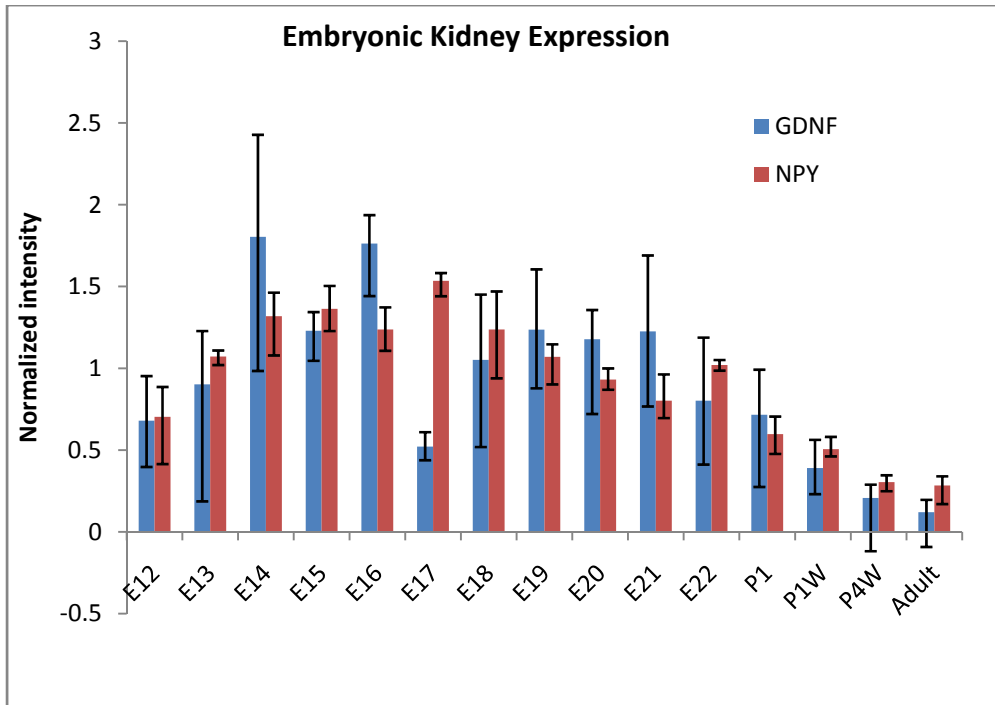


Figure 2.11: NPY and GDNF expression patterns in developing kidneys.

Normalized gene expression of GDNF and NPY in rat kidneys from E12 to adult from Rat 230 2.0 microarrays with 3 to 4 biological replicates. E12 was the Wolffian duct, mesonephros, and MM area. The remainder of the time points were isolated embryonic kidneys.

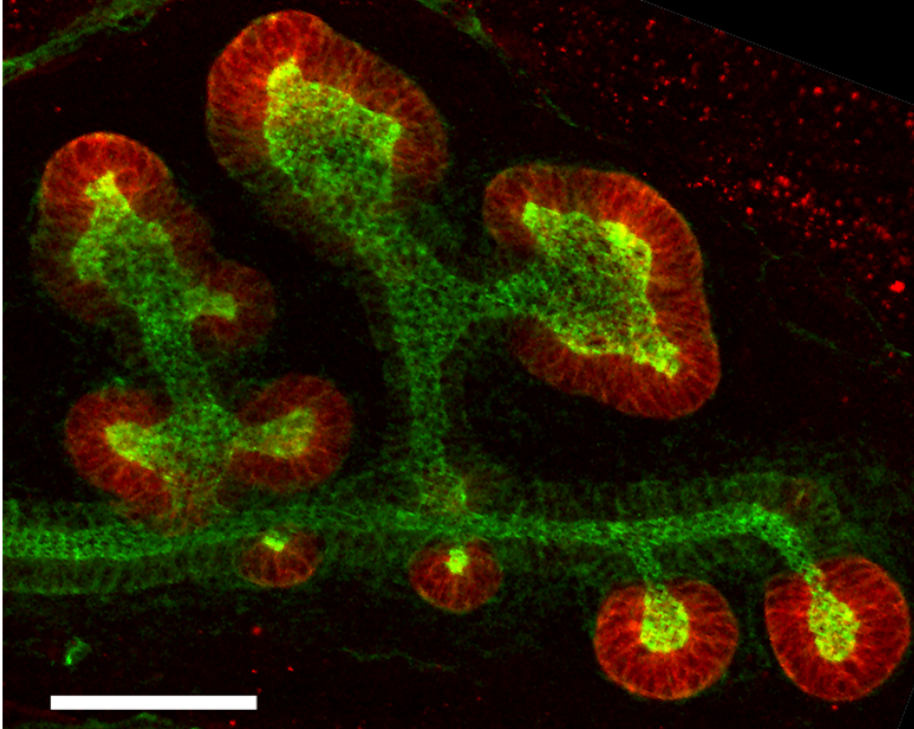


Figure 2.12: WD branching on filter.

WDs were cultured with recombinant human GDNF with FGF1 for 3 days. 10x confocal image. Red pseudo-color indicates the GDNF receptor $GFR\alpha 1$. Green stains E-cadherin and ZO-1. 100 μm scale bar.

Table 2.1: Genes upregulated in budded conditions and downregulated in non-budding samples.

<u>Probe Name</u>	<u>Description</u>	<u>P-value</u>
1368718_at	Aldehyde dehydrogenase family 1, subfamily A4	0.0268
1389982_at	LIM homeobox protein 1	0.00842
1387154_at	Neuropeptide Y	3.81e-7
1392158_at	POU domain, class 3, transcription factor 3	0.012
1371112_at	Ret proto-oncogene 4 transcribed loci	0.00317

Table 2.2: ANOVA and pattern matching. Genes with P<0.001

Probe Name	P-value	Description
1387154_at	3.81e-7	neuropeptide Y
1376639_at	1.36e-5	ring finger protein 126
1387861_at	0.000142	amino-terminal enhancer of split
1390393_at	0.000179	Transcribed locus
1367453_at	0.00023	cell division cycle 37 homolog (S. cerevisiae)
1370007_at	0.000325	protein disulfide isomerase associated 4
1390031_at	0.000325	similar to hypothetical protein FLJ14466
1367868_at	0.000406	adhesion regulating molecule 1
1390490_at	0.000406	similar to Btk-PH-domain binding protein
1368126_at	0.000433	acetoacetyl-CoA synthetase
1386310_at	0.000644	Transcribed locus
1388341_at	0.000691	RAN GTPase activating protein 1
1385389_x_at	0.000935	Transcribed locus
1393783_at	0.000935	Similar to contactin associated protein-like 2 isoform a
1399041_at	0.000948	similar to OPA3 protein
1372402_at (predicted)	0.000948	N-acetylneuraminic acid synthase (sialic acid synthase)
1370031_at	0.000952	golgi SNAP receptor complex member 2
1371620_at	0.000993	similar to px19-like protein

CHAPTER 3

Neuropeptide Y Functions as a Facilitator of GDNF-induced Budding

Abstract

Budding of the Wolffian duct is the first step in the formation of the metanephric kidney. This initial step is dependent on GDNF; however, what happens after GDNF signals through its receptor Ret is not well understood. GDNF by itself is insufficient to induce robust epithelial budding of the isolated Wolffian duct in vitro. Thus, additional factors, presumably secreted peptides or polypeptide growth factors, must be involved. To approach this question, we analyzed microarray data from in vivo budding and non-budding conditions. We performed non-negative matrix factorization followed by gene ontology filtering and then network analysis to determine interactions between genes. The GDNF receptors GFR α 1 and Ret appeared in the network as well as other genes implicated in development of the kidney and other organs. We found that the secreted polypeptide neuropeptide Y (NPY), had a high degree of connectedness to genes with developmental roles. ANOVA plus pattern matching augmented this process to determine which set of genes were most highly regulated during the budding process. NPY, the highest scoring gene product, correlated most significantly to the budded condition (out of over 28,000 genes). Although NPY was upregulated in GDNF-dependent budding, it was not upregulated in GDNF-independent budding; moreover, it was down regulated when GDNF-dependent signaling (and budding) was inhibited. When NPY was added to the isolated Wolffian duct cultured in vitro, GDNF-dependent (but not GDNF-independent) budding was markedly

augmented; conversely, inhibition of the NPY receptors or perturbation of NPY expression inhibited budding, confirming that NPY facilitates this process. Addition of BMP4 decreased GDNF-dependent budding; through down regulation of Ret expression, mislocation of GFR α 1 and/or blocking the PI3-kinase/Akt signaling pathway. Addition of NPY to these BMP4-treated WDs rescued budding with a corresponding increase in phosphorylated Akt as well as Ret expression and GFR α 1 localization to budding zones. This suggests that NPY acts through the budding pathway reciprocally regulated by GDNF and BMP4. The formation of the ureteric bud may be a result from a combination of upregulation of the GDNF receptors along with genes that support GDNF signaling in a feed-forward loop and/or by counteracting the inhibitory pathway regulated by BMP4.

3.1 Introduction

The initiating step in kidney development is the formation of the ureteric bud from the Wolffian duct (WD). Glial cell line-derived neurotrophic factor (GDNF), produced in the metanephric mesenchyme (MM), interacts with its receptors on the WD where it binds to the GPI-linked co-receptor GFR α 1 which then signals through the receptor tyrosine kinase Ret (Sariola and Saarma, 2003). GDNF is expressed in the MM adjacent to the caudal portion of the WD while Ret and GFR α 1 are expressed throughout the WD prior to the formation of the ureteric bud (UB). After the UB emerges from the WD, the expression of Ret and GFR α 1 becomes limited to the UB (Costantini and Shakya, 2006). GDNF signaling appears to be the central modulator of UB formation; mice lacking GDNF or its receptors GFR α 1 or Ret are characterized by kidney agenesis (Schuchardt et al., 1994; Schuchardt et al., 1996). Similar phenotypes are found in mice in which upstream mediators of GDNF expression, such as Eya1, Six1, Pax2 and Gdf11 are knocked out (reviewed in (Brodbeck and Englert, 2004; Li et al., 2003; Sampogna and

Nigam, 2004; Shah et al., 2004)). The proper expression of GDNF is also important in limiting the formation of the UB to a single site; transgenic misexpression of GDNF throughout the WD in vivo (Shakya et al., 2005) or application of GDNF-soaked beads next to the WD in organ culture (Sainio et al., 1997) caused multiple, ectopic UB's to emerge. BMP4, one of the endogenous inhibitors of budding, regulates the budding process downstream of GDNF expression (Costantini and Shakya, 2006); however, the mechanism of this inhibition has not yet been clarified. In some cases, GDNF signaling might be bypassed through activation of signaling pathways via stimulation from FGF-family growth factors; this may explain why some *Ret* and *Gfra1* knockout animals manage to form rudimentary kidneys (Maeshima et al., 2007).

Microarray analysis of gene expression during kidney organogenesis has revealed broad patterns of expression changes (Stuart et al., 2001; Tsigelny et al., 2008). Further analysis of the in vitro cultured kidney components (UB and MM) demonstrated differences in gene expression within the various compartments of the kidney suggesting there are distinct gene networks responsible for UB branching and MM induction (McMahon et al., 2008; Stuart et al., 2003). Similar analyses have aided in the identification of novel regulators of kidney development (Schmidt-Ott et al., 2007; Schmidt-Ott et al., 2005). These and other studies demonstrate the utility of microarray analysis to investigate developmental systems. Various methods of unsupervised data clustering exist, such as hierarchical clustering (HC), self-organizing maps (SOM) and nonnegative matrix factorization (NMF) (Brunet et al., 2004; Tsigelny et al., 2008). NMF clusters many thousands of genes together into a metagene to simplify the expression pattern and to extract biological correlations in microarray data. This patterning is less dependent on initial conditions than HC and SOM clustering. Here, we performed microarray analysis on several in vivo conditions with budded and unbudded phenotypes to determine which genes are important for the initial formation of the UB. Utilizing this approach, we have identified a novel modulator of WD budding, neuropeptide Y.

Neuropeptide Y (NPY) is a linear 36 amino acid neurotransmitter expressed throughout the central and peripheral nervous systems (Tatemoto, 1982), which has been shown to play a role in the development of enteric neurons in response to GDNF (Anitha et al., 2006). NPY belongs to a family of neurotransmitters that include the homologous peptide YY (PYY) and pancreatic polypeptide (PP), which share 69% and 50% amino acid sequences, respectively. NPY and its homologues signal through five G protein coupled receptors belonging to the $G_{i/o}$ class: Y1, Y2, Y4, Y5, and y6. The existence of the Y3 receptor has not been determined and the y6 receptor is not present in rats (Burkhoff et al., 1998). The Y1, Y2, Y4, and Y5 receptors are known to increase mitogen-activated protein kinase (MAPK) in transfected cells (Mannon and Mele, 2000; Mannon and Raymond, 1998; Mullins et al., 2002; Nie and Selbie, 1998). NPY has also been shown to increase phosphorylation of Akt in enteric neurons (Anitha et al., 2006). Both of these pathways appear to be involved in GDNF signaling. NPY expression has been shown to be modulated by various growth factors: brain-derived neurotrophic factor in cortical neurons, nerve growth factor in avian sympathoadrenal cells, and GDNF in enteric neurons (Anitha et al., 2006; Barnea et al., 1995; Barreto-Estrada et al., 2003). Since NPY was the transcript which was most significantly altered in the budded and nonbudded conditions among ~30,000 transcripts, we sought to define the effect of NPY on the budding of the WD. In order to study the effect of NPY on UB formation, we utilized an in vitro culture system in which the WD without the attached mesonephros was induced to undergo budding without reliance upon artificial matrices (Maeshima et al., 2006; Rosines et al., 2007). Our results support a key role for NPY in facilitating the formation of the UB from the WD in concert with GDNF.

3.2 Results

3.2.1 A microarray-based approach identifies genes potentially involved in UB formation from the WD

In order to identify novel factors that modulate the budding process (Figure 3.1), we obtained genome-wide transcriptional profiles of rat tissue with either a budded or nonbudded phenotype utilizing the Affymetrix Rat Genome Array 230 2.0. We selected one budded condition (isolated ureteric bud, iUB) and two unbudded conditions: uncultured isolated E13 WDs with and without attached mesenchymal cells (WD with intermediate mesoderm [WD(+IM)] and isolated WD [iWD], respectively). Three biological replicates were performed for each condition.

Nonnegative matrix factorization (NMF), which is used for computer pattern recognition in image and natural language processing (Devarajan, 2008), was used to separate out the “budding genes” enriched in the iUB from those enriched in either of the two nonbudding conditions. NMF sorts the data into the specified number of metagenes consisting of hundreds or thousands of genes without input from the user. The original matrix, M , comprised of the number of samples multiplied by the number of genes on the microarray, is factored into the matrices W and H . The W matrix has the dimensions of the number of genes on the microarray multiplied by the number of metagenes. The H matrix represents the data in metagene format and has the dimensions of the number of samples multiplied by the number of metagenes (Brunet et al., 2004). The data for 4 metagenes is shown (Figure 3.2A). The genes that were enriched in the iUB were then filtered by gene ontology to select genes that were involved in signal transduction (Figure 3.2C). This reduced the number of genes to approximately 64. This reduced set of genes was then fed into Ingenuity Pathway Analysis, a hand-curated interaction dataset, which resulted in two networks containing a number of genes from the list of 64 (Figure 3.3). The first network

included the GDNF receptors Ret and GFR α 1, and was categorized as “Cellular Development” and “Nervous System Development and Function.” The second network was categorized as “Behavior, Digestive System Development & Function” and “Cell Signaling” and had 9 genes which included three secreted ligands: neurexophilin 1 (a neuropeptide-like ligand that binds to receptor-like proteins expressed on many neuronal cell surfaces (Missler et al., 1998), NXP1), neuropeptide VF precursor (a member of the neuropeptide FF family that modulates opioid tolerance and gut motility (Hinuma et al., 2000), NPVF), and neuropeptide Y (NPY) (Table 1).

The data was also analyzed using a method that compares the data using ANOVA and pattern matching without the need for arbitrarily setting a fold-change threshold (Pavlidis, 2003; Pavlidis and Noble, 2001). The pattern was set as budded or non-budded (Figure 3.4A), with the output being a P-value for each gene. Greater than 1800 genes had a P-value less than 0.001 (Figure 3.4C), 481 genes had a P-value less than 0.0001 (Figure 3.4D), and 110 genes had a P-value less than 0.00001 (Figure 3.4E). The ANOVA method does not distinguish between positive correlation and negative correlation; however, a simple fold change analysis can determine this to determine which genes positively correlate to budding. Table 2 lists selected genes upregulated in the iUB with their P-value. Using this analysis, NPY had the lowest P-value (2.01×10^{-8}) for genes that correlated with budding.

That these two independent methods of data analysis identified NPY among the several thousand genes present on the array suggested the relevance of NPY in the budding process. We also analyzed the expression of NPY in the developing embryonic kidney and found that it has high levels of expression at the initiation of UB formation (data not shown), which is consistent with its levels being elevated in the isolated UB. Given these results, further studies on NPY in WD budding were performed.

3.2.2 Expression and localization of NPY and its receptors

We first proceeded to verify the aforementioned results by QPCR. Consistent with the microarray, NPY was markedly upregulated in WDs budded in culture compared to either uncultured WDs or WDs cultured with a budding inhibitor (Figure 3.5A). In order to further characterize the possible role of NPY during WD budding, we sought to determine the presence of NPY, its homologs PYY and PP, and the cognate receptors Y1-Y5, within the developing kidney. We found that NPY was expressed in both the WD and the developing kidney while PYY was not present in the WD (Figure 3.5B). PP was not detected in the tissues tested. All NPY receptors were present in both the WD and the kidney (Figure 3.5C). These results further suggest that NPY and its receptors could regulate WD budding.

3.2.3 In vitro budding with GDNF

We went on to evaluate the role of NPY in WD budding *in vitro*. It has previously been shown that the WD isolated from mesonephric tubules can undergo robust budding in the presence of GDNF only with the addition of another growth factor such as FGF1 (Maeshima et al., 2007; Rosines et al., 2007). However, FGF1 is not highly expressed at this time, suggesting that the physiological growth factor supporting GDNF budding is something other than FGF1. Based on the microarray network and statistical analysis, as well as QPCR data, NPY seemed like a promising candidate for this role. The WDs have attached intermediate mesodermal cells (WD(+IM)). Addition of only NPY without other growth factors did not result in budding (Figure 3.6A), while addition of 50 nM NPY to WDs cultured with only GDNF (without an FGF) resulted in impressive budding of 90% of the WDs compared with minimal budding in only 10% of WDs that only had GDNF (alone) added to the culture system (Figure 3.6B-C). The length and area of the buds that formed in the presence of NPY were also markedly enlarged compared

to the buds that formed in the presence of GDNF alone (250% and 384%, respectively, Figure 3.6D). To determine if stimulation of the Y2 receptor would also facilitate budding, we added PYY, which acts mainly through the Y2 receptor, to cultured WDs. This had similar effects as NPY; however, PP, which acts mainly through the Y4 receptor, did not stimulate budding (Figure 3.6E). This raises the possibility that a redundant system exists which may compensate for the absence of any one component. Together, the microarray, network, statistical and functional data suggest that NPY is a key supporting growth factor for GDNF-dependent budding.

3.2.4 Role of NPY in GDNF-dependent budding

We then sought to determine which G protein coupled receptor NPY might be acting through. We stimulated budding without NPY by supplementation of FGF1 to GDNF to obtain budding of the WD(+IM) cultures. Addition of a peptide inhibitor to the Y1 receptor (PYX-1) or a chemical inhibitor (BIBP3226) resulted in budding inhibition while inhibitors of the Y2 receptor (BIIE 0246) or the Y5 receptor (L-152,804) did not inhibit budding (Figure 3.6F).

Thus, NPY stimulates GDNF-dependent budding in the WD(+IM) and blockade of its Y1 receptor by either a peptide or chemical inhibitor prevents this process. Since NPY is present in the thin layer of intermediate mesoderm (IM) surrounding the epithelial component of the WD, we sought to determine if this was a potential source of the NPY necessary for GDNF-dependent budding in the WD(+IM) system. We attempted to block expression of NPY via RNA interference. With control fluorescent siRNA, excellent penetration of the IM surrounding the WD was observed; penetration of the epithelial cells of the WD was variable (Figure 3.7A). We used a commercially available pool of 4 siRNAs targeted to rat NPY and added that to our culture system. An effect was seen in approximately half of the experiments. In these experiments, siRNA treatment of WD cultures targeting NPY showed decreased budding compared to control

siRNA targeting cyclophilin B or without treatment (Figure 3.7C-G). The number of buds decreased by 60% and the length of the buds that formed decreased by 30% (Figure 3.7E&F). The RNA expression of NPY decreased between 40 to 61% of the level in the control. In experiments where the level of NPY was only decreased to 61% there was no effect on budding (data not shown) whereas experiments in which NPY expression decreased to 40% showed decreased budding (Figure 3.7G), suggesting there may be a threshold where the effect of NPY reduction will have an effect. Based on the excellent penetration of the labeled siRNA into the IM but not the WD, we assume that the effect observed is due to >50% blockade of NPY expression in the IM.

3.2.5 NPY augments GDNF-induced budding but not GDNF-independent budding

The DNA array data described above suggested that GDNF stimulation leads to NPY expression. However, budding can be elicited without the presence of GDNF, suggesting an explanation for how rudimentary kidneys form in the absence of extant GDNF-ret signaling (Maeshima et al., 2007). Conceivably, NPY could be upregulated during budding in general or primarily as a response to GDNF signaling. Thus, it is important to determine whether NPY supports both GDNF-dependent and GDNF-independent budding or whether its role is specific to GDNF-dependent budding. To assess this, the expression of NPY in GDNF-dependent versus GDNF-independent budding was gauged. GDNF-dependent budding was obtained in vitro by utilizing GDNF plus an additional factor added to the culture medium, which could be an FGF (such as FGF1 or FGF7), or NPY (Figure 3.8A). GDNF-independent budding was elicited through the addition of FGF7 plus inhibition of activin A (via follistatin (FST) or a neutralizing anti-activin antibody) (Figure 3.8B) (Maeshima et al., 2007). NPY expression was increased in the GDNF-dependent condition whereas the buds formed via the GDNF-independent budding

mechanism did not exhibit increased NPY expression (Figure 3.8C). In contrast to the GDNF-dependent budding, addition of the NPY Y1, Y2 and Y5 receptor inhibitors did not inhibit formation of buds in WDs cultured in a GDNF-independent manner (data not shown). Furthermore, when NPY was added to WDs that were cultured without GDNF, this did not result in increased budding events (Figure 3.6A). These results suggest that the role of NPY is specific to GDNF-dependent budding.

3.2.6 Rescue of BMP4 inhibition of budding by NPY and Restoration of Akt

Phosphorylation

Because GDNF signals through a variety of pathways, we sought to determine which pathway NPY might be assisting. Prior studies suggest that NPY may act through the MAPK, MEK/ERK or PI3-kinase/Akt pathways (Anitha et al., 2006; Mannon and Raymond, 1998; Pierce et al., 2001). It has been previously shown that BMP4 inhibits GDNF-mediated budding of the WD both in vivo and in vitro (Tang et al., 2002), and it is believed that this balance is one of the important elements in limiting budding to a single site in vivo. However, the mechanism is not well understood. In our studies addition of BMP4 decreased budding and concomitantly localization of GFR α 1 to budding regions (c.f. Figure 3.9A & C) suggesting that BMP4 directly affects signaling of GDNF. Significantly, addition of BMP4 decreased expression of Ret in the WD (Figure 3.9G). This inhibition of both GDNF receptors by BMP4 may be the endogenous means by which budding is suppressed by BMP4.

At 100 ng/ml of BMP4, budding was almost completely inhibited (Figure 3.9C); however, addition of NPY resulted in restoration of budding and GFR α 1 localized zones of budding to levels similar to WDs cultured without BMP4 (Figure 3.9D). In order to determine which pathway NPY activated during rescue of budding, we performed a Western blot for

phosphorylated and total ERK and Akt of WDs cultured under conditions of BMP4 suppression of GDNF-dependent budding with or without 200 nM NPY (Figure 3.9E-F). WDs rescued with NPY showed elevated levels of phosphorylated Akt compared to those without NPY treatment; however, the relative amount of phosphorylated ERK (p44/42 MAPK) was not enhanced. These data suggests BMP4 acts to quench Akt signaling and that NPY rescues BMP4 inhibition via reactivation of the Akt pathway.

There were no reported kidney phenotypes for NPY mutant animals (Erickson et al., 1996); however, we decided to ascertain this. Analysis of NPY deficient mice showed no apparent kidney defects at E11, E18 or in adult mice (data not shown). This might be explained by the redundant network and overlapping functions in the NPY family, such as is the case where the Y2 receptor is upregulated in Y1 deficient mice (Wittmann et al., 2005). In the case of NPY deficiency, PYY could compensate for the missing neuropeptide. Also, NPY could be only one of many budding facilitators such as FGFs, Wnts and heregulin that become activated during budding.

3.2.7 NPY transcriptional program

We sought to determine what transcriptional programs were elicited by NPY. In order to do this we compared WD(+IM)s cultured with GDNF and NPY, GDNF and FGF1, or BMP4 with GDNF and FGF1 (Figure 3.10A). We obtained microarray expression data for these 3 conditions and again analyzed them utilizing NMF clustering, gene ontology and pathway analysis (Figure 3.10B). We noticed that many genes involved with kidney development were higher in the two budded WD samples compared to the BMP4-treated sample such as *Ret*, *Gfra1*, *Met* and various FGFs (Table 3).

Since NPY did not rescue WDs treated with activin A (data not shown) but did rescue WDs treated with BMP4, we wondered if there were differences in the transcriptional programs which would lead to why this was the case. In NMF analysis with activin A microarray data added to the previously analyzed data, the activin A and BMP4 samples partitioned together. When the number of metagenes was set to 4 one BMP4 and one activin A sample partitioned into one group and two BMP4 and two activin A samples partitioned into a second group (data not shown). NPY and FGF1 samples partitioned into their own metagenes, similar to the NMF analysis without activin A, indicating that these transcriptional profiles were distinct from the inhibited conditions and from each other.

Next, we compared the microarrays of the budded WDs with the inhibited conditions by utilizing fold-change analysis. Self-organizing maps were generated to view the data at a glance (Figure 3.11A). The unbudded, uncultured WDs had a pattern that appeared to be almost opposite to the two budded WDs, while the SOMs for BMP4 and activin A were very similar, corroborating the NMF data. We next selected genes that were two-fold higher in both budded conditions compared to either BMP4 or activin A treated WDs. We then subselected genes that were annotated by Gene Ontology and were categorized into “GO:4871: signal transducer activity” or “GO:30528: transcription regulator activity” (Figure 3.11B). We found 89 genes uniquely downregulated by BMP4, 44 genes uniquely downregulated by activin A, and 20 genes that were commonly downregulated. IPA networks were generated with these gene lists (Figure 3.11C-E). The network of the commonly downregulated genes was similar to previous networks that showed Ret and NPY as important budding regulators. In all three networks we noticed the presence of various signaling pathways which are also reported to be activated by Ret, such as ERK, p38 MAPK, PI3-kinase, etc. We decided to test which of these might be important for WD budding. To do this we added various signaling inhibitors to WDs cultured with GDNF and FGF1. We found that inhibition of p38 MAPK, MEK/ERK, JNK or PKC did not inhibit budding

in our WD culture system. However, blockade of various points in the PI3-kinase/Akt pathway inhibited budding (Figure 3.11F). Based on this data, we modified the previous IPA networks (Figure 3.3 and Figure 3.11) to exclude some of the signaling pathways that did not affect budding and then merged the networks. This refined network had several additional nodes added by the software, such as retinoic acid. Since retinoic acid was also previously implicated in renal development (Mendelsohn et al., 1999) we decided to test this in our in vitro system. Similar to FGF1 or NPY, all-trans retinoic acid augmented WD budding with GDNF (data not shown). We then performed ANOVA + pattern matching with all the microarray data and selected genes with a P value < 0.001. These genes were merged with the refined network and reanalyzed by IPA (Figure 3.12).

3.3 Discussion

Based on the data presented here, we propose a feed-forward mechanism of budding where GDNF signals through its receptor Ret to stimulate Akt (Figure 3.12). Activation by GDNF or downstream signaling leads to increased NPY expression (as well as other facilitatory factors such as FGFs) which in turn upregulates Ret expression, thus amplifying the signal by increasing the sensitivity to GDNF. A complicated underlying network of interconnected genes supports the budding process. The inhibitor, BMP4, on the other hand, may suppress budding by two mechanisms (1) downregulating Ret and GFR α 1 expression and/or localization, thus preventing amplification of signaling and budding from occurring and (2) blockade of the PI3-kinase/Akt signaling. Whether these two events are directly related or if one causes the other remains to be determined. The GDNF-independent budding mechanisms, presumably responsible for rudimentary kidney formation when GDNF signaling is disrupted, bypass GDNF-

Ret and stimulate the PI3-kinase/Akt pathways, leading to budding that is not affected by NPY, as shown in Figure 3.8B (Maeshima et al., 2007).

Formation of the ureteric bud (UB) via budding from the Wolffian duct (WD) is the key initiating step in kidney development. Failure of this step results in renal agenesis. The regulation of Ret by endogenous inhibitors of budding, such as BMP4 and activin A, may be the mechanism by which ectopic budding is regulated. Although GDNF appears to be the central modulator of UB formation, the downstream pathways and effector molecules that regulate epithelial outpouching remain undefined. Using a recently described in vitro model system of WD budding, we were able to study the effect of NPY and BMP4 on WD budding. In these in vitro experiments, the WD was separated from the mesonephros and gonadal ridge to isolate key morphogenetic processes involved in WD budding. In the data we presented, 10% of the WDs with a layer of IM (WD(+IM)) budded (minimally) with addition of only GDNF compared to approximately 100% that budded impressively with GDNF when the mesonephros and gonadal ridge were not removed, suggesting that these tissues influence the budding process (Maeshima et al., 2006; Tang et al., 2002). The PI3-kinase/Akt pathway was reported to be essential for bud formation (Tang et al., 2002). The PI3-kinase pathway appears to be activated in both the GDNF-dependent and GDNF-independent (FGF7) mechanisms suggesting common downstream pathways may be activated through separate initial signaling events (Maeshima et al., 2006; Tang et al., 2002). Although FGF7 is usually not expressed during early kidney development, we have found it and other FGFs upregulated in a few of the developing kidneys in vivo in the absence of the Ret receptor suggesting that this or other genes not typically present during normal kidney development may be responsible for the significant number of UBs that do form in the absence of GDNF signaling (Maeshima et al., 2007). This redundant mechanism may, in part, contribute to the robustness of kidney development.

We utilized a systems biological approach to analyze budded and unbudded tissue isolated from the developing rat kidney. Diverse tools such as NMF for pattern recognition, gene ontology filtering and pathway analysis were combined to narrow down the genes of interest into two primary gene networks. Not surprisingly, the first network included both GDNF receptors. The second grouping suggested that NPY was a worthy candidate for study. A second method of analyzing the data was to use ANOVA plus pattern matching to discern genes significant in the budding process. With this analysis, NPY was found to be the gene with the greatest correlation to budding.

Alternate methods of analysis generally resulted in Ret, GFR α 1 and NPY being selected as significant genes. If GO filtering were skipped and the genes were sent directly to IPA, 6 networks were generated. The first network (Cell Morphology, Cellular Growth and Proliferation) included the GDNF receptors Ret and GFR α 1. NPY was in the 5th network (Cellular Development, Nervous System Development and Function, Cancer). Some of the other networks included cell cycle, cell death, and cellular growth. If, on the other hand, the GO Signal Transduction list was further subdivided into signaling ligands (GO:5102 receptor binding), 17 genes remained and IPA generated only one network which contained NPY (along with several other genes known to be involved in early kidney development such as kit, neurturin and Wnt11). These receptor binding ligands may act to modulate the budding process in concert with GDNF-Ret.

The power of this approach to identify novel factors in developmental processes is highlighted here since knockout of NPY does not result in an overt kidney phenotype (Erickson et al., 1996), a finding which we have confirmed. However, as we describe here, NPY/PYY/PP and the Y1-Y5 receptors are likely to form a redundant, though crucial, system. The effect of NPY on WD budding is not likely to be an in vitro phenomenon since NPY is dynamically expressed in

the *in vivo* developing kidney. Furthermore, our data demonstrates that NPY rescues budding in BMP4 treated WDs. Thus, NPY modulates two of the key pathways known to regulate *in vivo* budding, and the *in vitro* model faithfully reproduces *in vivo* predictions. It has been suggested that endogenous BMP4 acts to suppress Ret expression along the cephalic portion of the WD *in vivo* thereby preventing the formation of ectopic buds; thus, NPY may assist GDNF in overcoming BMP4 suppression of budding in the WD. That NPY acts through the PI3-kinase/Akt pathway was suggested by the finding that addition of NPY restored phospho-Akt signaling in WDs exposed to BMP4. Stimulation of the PI3-kinase pathway has been shown to promote renal epithelial cell proliferation during tubular development and regeneration (Derman et al., 1995; Zhuang et al., 2007), thus it is plausible that NPY stimulation of the PI3-kinase pathway leads to the proliferation of epithelial cells required to initiate UB formation. This is supported by our data demonstrating that buds stimulated by NPY are quantitatively larger than their counterparts without NPY added. NPY has been shown to exert similar proliferative effects in both the central and enteric nervous systems (Anitha et al., 2006).

Our data suggests that the role of NPY in UB formation is to assist GDNF-mediated budding. GDNF has been shown to induce expression of NPY in enteric neurons; in a similar manner, GDNF induced bud formation in the WD leads to increased NPY expression. In contrast, buds formed through the “bypass” mechanism do not have such upregulation. It seems plausible that GDNF stimulation of NPY leads to a feed-forward effect where epithelial cell proliferation and morphogenesis is sustained by NPY once the process is initiated by GDNF. NPY, and other factors stimulated by GDNF, may directly or indirectly lead to increased Ret receptor expression, increasing the local responsiveness of the WD epithelia to GDNF. BMP4 suppression of budding along the caudal portion of the WD downregulates Ret expression; however, at the location of UB emergence, GDNF and NPY (and other factors such as Gremlin) may act synergistically to overcome BMP4 inhibition (Michos et al., 2004).

The results of this study suggest there is a core set of genes required for budding to occur. Although GDNF appears to be a central modulator of UB formation, we demonstrate that other factors such as NPY contribute to this process. Loss of these factors may not manifest as obvious kidney phenotypes when genetically perturbed, but they likely contribute to the robustness of the developmental processes and may play a role in the determination of nephron number and disease (Shah et al., 2004). The identification of these types of augmenting factors can only be achieved through an approach such as the one described in this study, since the *in vivo* knockout of these factors is unlikely to result in a readily detectable developmental phenotype. It will only be through the elucidation of these pathways that a comprehensive network for kidney development can be proposed. Whether or not GDNF-dependent and GDNF-independent bud formation is regulated via the same network remains to be determined.

3.4 Methods

3.4.1 Reagents

Recombinant human BMP4, FGF7, follistatin and rat GDNF were from R&D systems (Minneapolis, MN). Recombinant FGF1 was from Calbiochem (EMD, San Diego, CA). NPY, PYY, PP, NPY 3-36, and NPY 13-36 were from GenScript (Piscataway, NJ). PYX-1 and BIBP3226 were purchased from Bachem Bioscience (King of Prussia, PA). BIIE0246 was purchased from Tocris Biosciences (Ellisville, MO). DMEM/F12 was purchased from Gibco (Invitrogen, Carlsbad, CA). Fetal bovine serum (FBS) was from Biowhittaker (Walkersville, MD). Donor donkey serum was from Gemini Bio-Products (West Sacramento, CA). Fluorescein labeled Dolichos biflorus (horse gram) agglutinin was from Vector Labs (Burlingame, CA). Goat anti-GRF α 1 was from R&D Systems. Anti-ZO-1 and anti-E-Cadherin were from Zymed

(Invitrogen). Rabbit anti-phospho-Akt (Ser473), anti-total-Akt, anti-phospho-p44/42 MAPK (Thr202/Tyr204), and anti-p44/42 MAPK were from Cell Signaling Technology (Beverly, MA). Alexa Fluor 488 or 594 secondary antibodies were from Molecular Probes (Invitrogen). All signaling inhibitors were from Calbiochem. All other reagents were from Sigma.

3.4.2 Isolation and culture of the Wolffian duct

Wolffian duct (WD) cultures were performed as previously described (Maeshima et al., 2006). Briefly, embryos from time pregnant Sprague-Dawley rats (Harlan, Indianapolis, IN) at day 13 of gestation were utilized for all cultures. The WDs along with a thin layer of attached mesodermal mesenchymal cells were dissected using a stereomicroscope and fine forceps (FST, Foster City, CA). The WDs were placed on 0.4 μm pore sized Transwell filters (Costar, Cambridge, MA) in 12 or 24-well tissue culture dishes. Culture medium consisting of DMEM/F12, 10% FBS, and growth factors were added below the Transwell. The “standard” GDNF-dependent budding control consisted of 125 ng/ml GDNF with 125 ng/ml FGF1.

3.4.3 NPY knockout animal

NPY(-/-) mice were obtained from The Jackson Laboratory (Bar Harbor, Maine) strain name: 129S-Npy^{tm1Rpa}/J, stock number: 004545. The use and care of animals reported in this study conform to the procedures of the laboratory’s animal protocol approved by the Animal Subjects Program of the University of California, San Diego.

3.4.4 siRNA

ON-TARGETplus SMARTpool Rat NPY siRNA was purchased from Dharmacon (Thermo Fisher Scientific, Chicago, IL) with target sequences of: GAUGCUAGGUAACAAACGA, CCUUGUUGUCGUUGUAUUAU, GCAUUCUGGCUGAGGGGUA, and UCAUCACCAGACAGAGAU. Control siRNA targeted cyclophilin B, also known as peptidylprolyl isomerase B, had a sequence of 5'-GGAAAGACUGUCCAAAAA-3' (siGENOME D-001136-01-20, Dharmacon). siGLO Green was utilized as a fluorescent oligonucleotide control transfection indicator (D-001630-01-02, Dharmacon).

4 to 6 hours before transfection, WDs were placed on Transwell filters above culture medium (DMEM/F12+10%FBS). DharmaFECT IV (Dharmacon) was diluted to 3% in Opti-mem. siRNA was diluted to 1 μ M and siGLO was diluted to 100 nM in Opti-mem reduced serum media (Gibco). The mixtures were allowed to incubate separately for 5 minutes at room temperature. Afterwards, either the siRNA or the siGLO mixture was combined with the DharmaFECT mixture and gently mixed together at room temperature for 20 minutes. The final concentration of siRNA oligomers was 500 nM or 50 nM for siGLO transfection indicator. This mixture was then applied on top of the Transwell filter, directly in contact with the WD cultures. 125 ng/ml GDNF and FGF1 were added to the media underneath the Transwell and the culture was allowed to grow for 24 to 48 hours.

3.4.5 Immunohistochemistry

Cultured WDs were fixed with 4% PFA for 1-2 hours at room temperature, followed by incubation with the primary antibody in blocking solution overnight at 4°C. Three rinses in PBS with 0.1% Tween (PTW) was followed by incubation with the secondary antibody in blocking

solution with 10% donkey serum overnight at 4°C. The samples were then thoroughly rinsed with PTW and view with a confocal microscope (Nikon D-Eclipse C1).

3.4.6 Western blot

Samples were lysed in buffer containing 100 mM NaCl, 1% Triton-X 100, 0.5% sodium dodecyl sulfate, 20 mM EDTA, 10 mM HEPES and 0.5% sodium deoxycholate with Sigma protease inhibitor cocktail (1:10), 20 mM DTT, and 10 mM Na₃VO₄. Protein concentration was determined by BCA analysis (PIERCE, Rockford, IL). 20 µg of protein from each sample was run on SDS-PAGE using NuPAGE Novex Bis-Tris Gels (4-12%) (Invitrogen) and transferred to a nitrocellulose membrane. The membrane was blocked with 2% milk (w/v), 1% Triton X-100, 0.01M EDTA in 0.04M Tris HCl pH 7.5, incubated with primary antibody for 1 hour, washed with Tris-buffered saline with 0.1% Tween-20 (TBST), and incubated with a peroxidase-labeled secondary antibody for 1 hour. After rinsing with TBST, the membrane was exposed to HyBlot CL autoradiography film (DENVILLE, Metuchen, NJ) using Supersignal West Pico Chemiluminescent Substrate (PIERCE, Rockford, IL).

3.4.7 RT-PCR

RNA was isolated from WDs or kidneys using the RNeasy micro kit (Qiagen, Valencia, CA) and converted to cDNA using SuperScript III First-Strand Synthesis System for RT-PCR (Invitrogen). Amplification of cDNA by PCR was performed using the HotStartTaq Master Mix kit (Qiagen). The primers utilized are NPY (NM_012614) forward: 5'-GGCCAGATACTACTCCGCTCTGCG-3' reverse: 5'-TTCACAGGATGAGATGAGATGTG-3' (Chottova Dvorakova et al., 2008), PYY (NM_001034080) forward: 5'-

CTCTGTTCTCCAAACTGCTC-3' reverse: 5'-ACCAAACATGCAAGTGAAGTC-3', PP (NM_012626) forward: 5'-CATACTACTGCCTCTCCCTG -3' reverse: 5'-GTTTCGTATTGAGCCCTCTG-3', NPY Y1 receptor (X95507) forward: 5'-AAATGTATCACTTGCGGCGTTCA-3' reverse: 5'-GCGACCACGATGGAGAGCAG-3' (Jackerott and Larsson, 1997), Y2 receptor (NM_023968) forward: 5'-CCCGGATCTGGAGTAAGCTAAA-3' reverse: 5'-GTGGAGCACATCGCAATAATGT-3' (Chottova Dvorakova et al., 2008), Y4 receptor (NM_031581) forward: 5'-TTGCAGTTCTCTGGCTGCCCTG-3' reverse: 5'-CTTGCTACCCATCCTCATAGAT-3', Y5 receptor (NM_012869) forward: 5'-CCAGGCAAAAACCCCGAGCAC-3', reverse: 5'-GGCAGTGGATAAGGGCTCTCA-3', and β -actin (NM_031144) forward: 5'-TCATCACTATCGGCAATGAGC-3' reverse 5'- CTCCTTCTGCATCCTGTCAGC-3'. The PCR conditions were 15 minutes at 95°C followed by 35 cycles of 45 seconds at 94°C, 45 seconds at 60°C, and 1 minute at 72°C, and concluding with 10 minutes at 72°C.

3.4.8 Real-time PCR

All primers were designed with PerlPrimer (Marshall, 2004). The primers used are Gapdh forward 5'-ATGATTCTACCCACGGCAAG-3', reverse 5'-CTGGAAGATGGTGATGGGTT-3'; NPY forward 5'-GACATGGCCAGATACTACTC-3' reverse 5'-ATCTCTTGCCATATCTCTGTC-3'; Ret forward 5'-CCCTATATGTAAATGACACGGA-3', reverse 5'-CTTCTTCTGCAATGTATGTCCC-3'; and cyclophilin B forward 5'-CAATATGAAGGTGCTCTTCG-3', reverse 5'-CAAAGTATACCTTGACTGTGAC-3'. 5 μ L of PowerSybr Green master mix (Applied Biosystems), 1 μ M primers, water, and cDNA for a total of 10 μ L was run on an Applied Biosystems 7500 Fast Real-Time PCR machine. The program was set to 50°C for 2 minutes and

95°C for 10 minutes with 40 cycles of 95°C for 15 seconds and 60°C for 1 minute, and concluded with a dissociation step.

3.4.9 Microarray analysis

RNA from the various tissues was isolated with the Abion RNAqueous Micro Kit (Applied Biosystems) following the manufacturer's protocol. The purified RNA was processed by the UCSD Microarray Core facility and hybridized to the Rat Genome 230 2.0 Array (Affymetrix). Data normalization and fold-change analysis was performed with Genespring GX (Agilent). Briefly, the data was normalized to unity per chip and per gene.

NMF was performed using the GenePattern (Broad Institute, MIT) server and client software (Brunet et al., 2004; Reich et al., 2006). The data was preprocessed to remove genes that did not vary by 8-fold or 800, which reduced the data set from 31,000 to 2007 genes. The number of metagenes was set to 4 and the rest of NMF variables were kept at the default values. We selected four metagenes based on the maximum cophenetic coefficient score after performing NMF-consensus clustering with our data (i.e. it was the largest value that also had a cophenetic coefficient of 1.0).

ANOVA and pattern matching (Pavlidis, 2003; Pavlidis and Noble, 2001) was performed with data normalized with Genespring GX. The pattern was set as budding or non-budding. The budding sample was the isolated ureteric bud. The two non-budding samples were the two uncultured, unbudded WDs (iWD and WD(+IM)). The test type was set to parametric test, without assuming equal variances. The false discovery rate was varied between 0.001 and 0.00001. No multiple testing correction or post hoc tests were performed. The software reported the P-value for each gene.

Acknowledgements

The authors thank Kevin Bush and Wei Wu for helpful advice. Yohan Choi was supported by a Training Grant from the NIH (T-32, HL007261). S.K.N. is supported by National Institute of Diabetes and Digestive and Kidney Diseases grants RO1-DK57286 and RO1-DK65831.

Chapter 3, in full, is currently being prepared for submission for publication. Choi, Yohan; Tee, James B.; Gallegos, Thomas F.; Shah, Mita M.; Oishi, Hideto; Sakurai, Hiroyuki; Kitamura, Shinji; Nigam, Sanjay K. The dissertation author was the primary investigator and author of this paper.

3.5 Figures

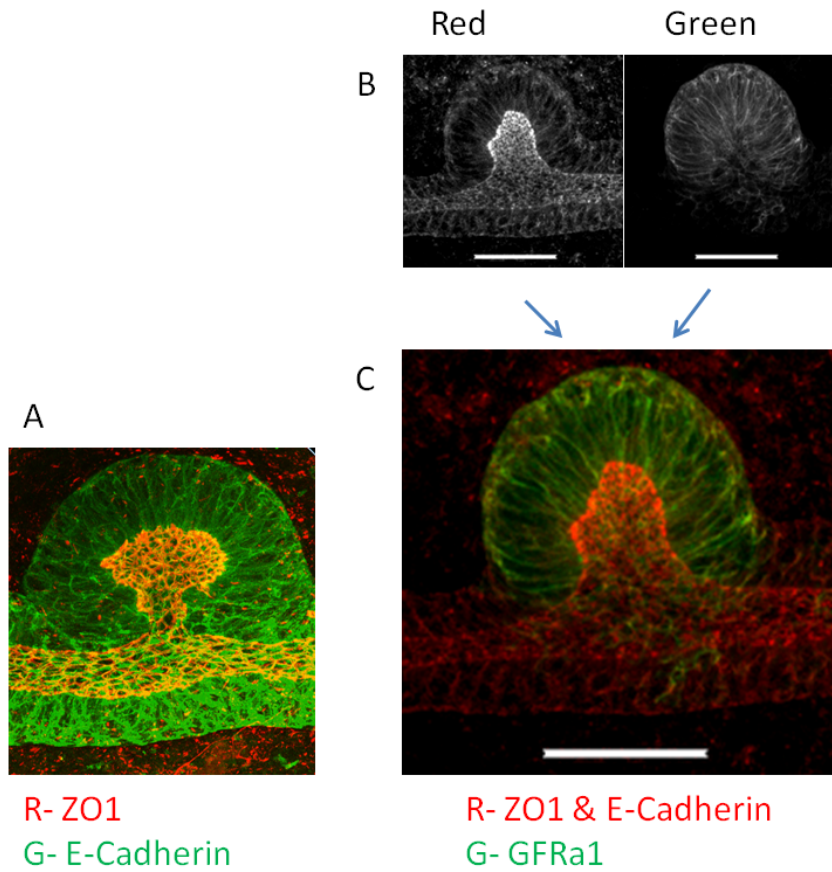


Figure 3.1: WD budding

(A) Budded WD stained for the epithelial marker E-Cadherin (green) and the tight junction protein ZO-1 (red), which indicates the apical surface. (B-C) Budded WD stained for GFR α 1 (green) and both ZO-1 & E-Cadherin (red). 50 μ m scale bar.

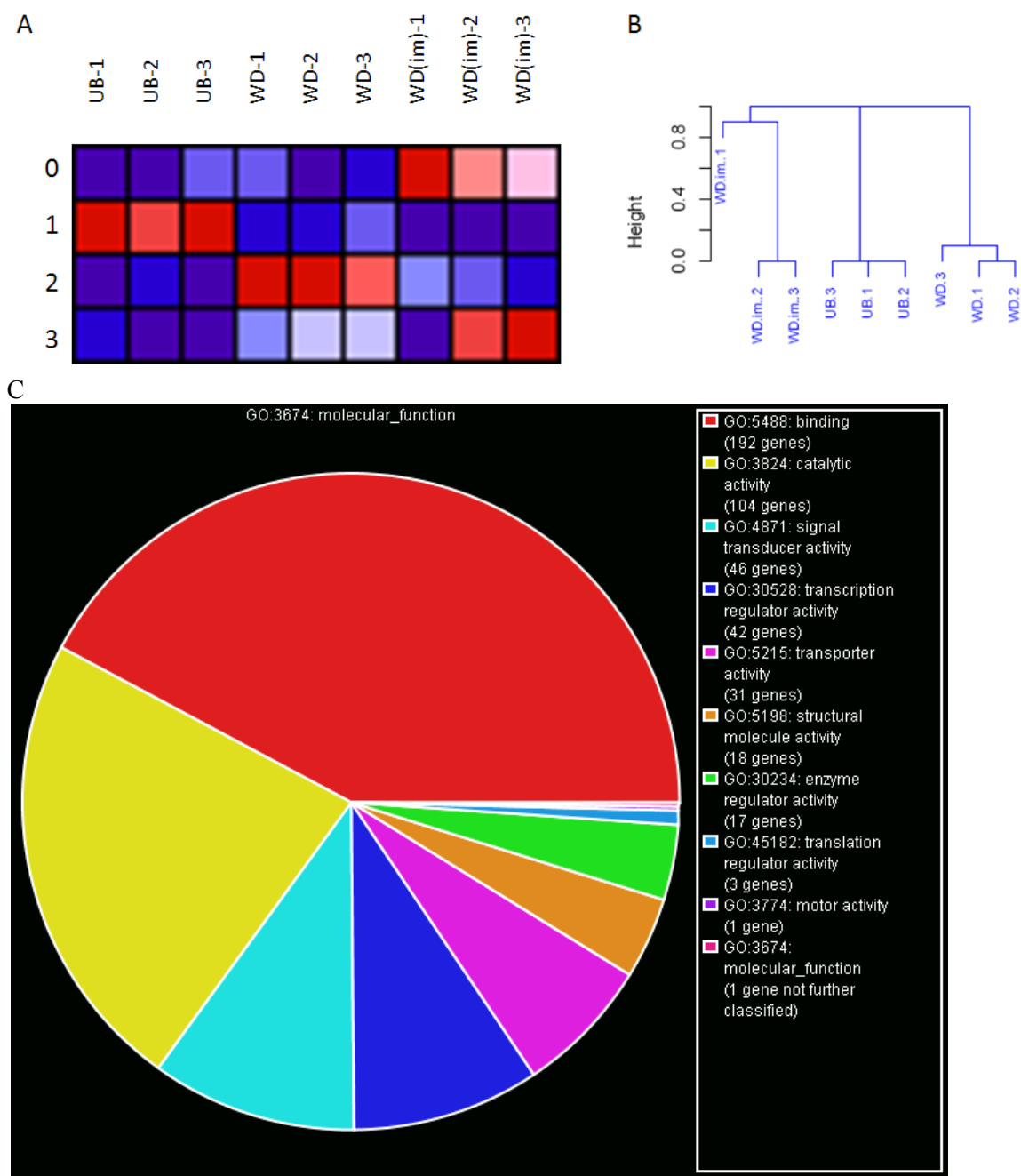


Figure 3.2: Microarray analysis

(A) Nonnegative Matrix Factorization (NMF) was applied to the microarray data that was preprocessed to include genes that changed at least 8-fold and by 800 units. The data was factored into 4 metagenes. UB: isolated ureteric bud, WD: isolated Wolffian duct, WD(im): Wolffian duct with intermediate mesoderm. (B) Ordered linkage tree of samples. (C) Gene Ontology classification of genes enriched in the ureteric bud.

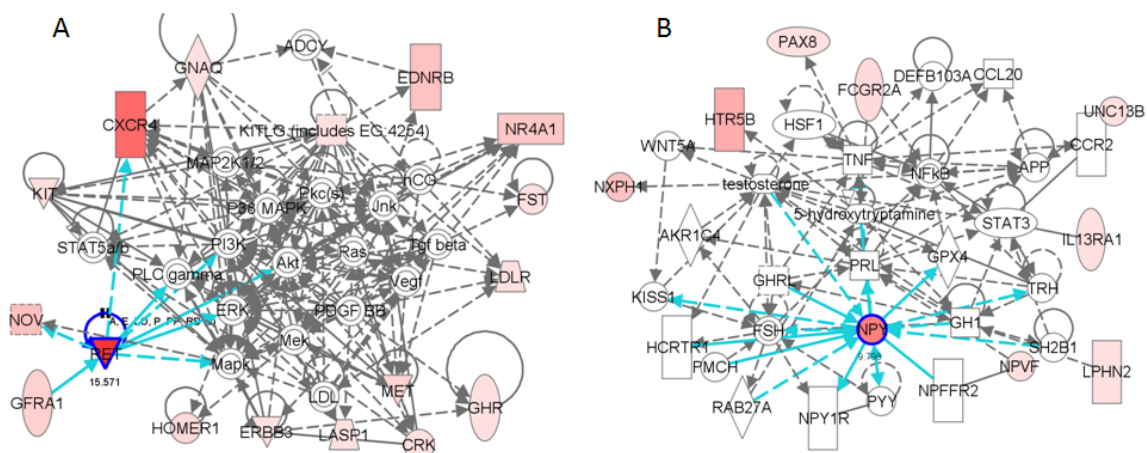


Figure 3.3: Ingenuity Pathway Analysis (IPA) of microarray data generated several genetic networks.

(A) Network with Ret classified as “Cellular Development” and “Nervous System Development and Function”. (B) Network with NPY as a connection hub classified by IPA as “Behavior, Digestive System Development & Function” and “Cell Signaling.” See Table 1.

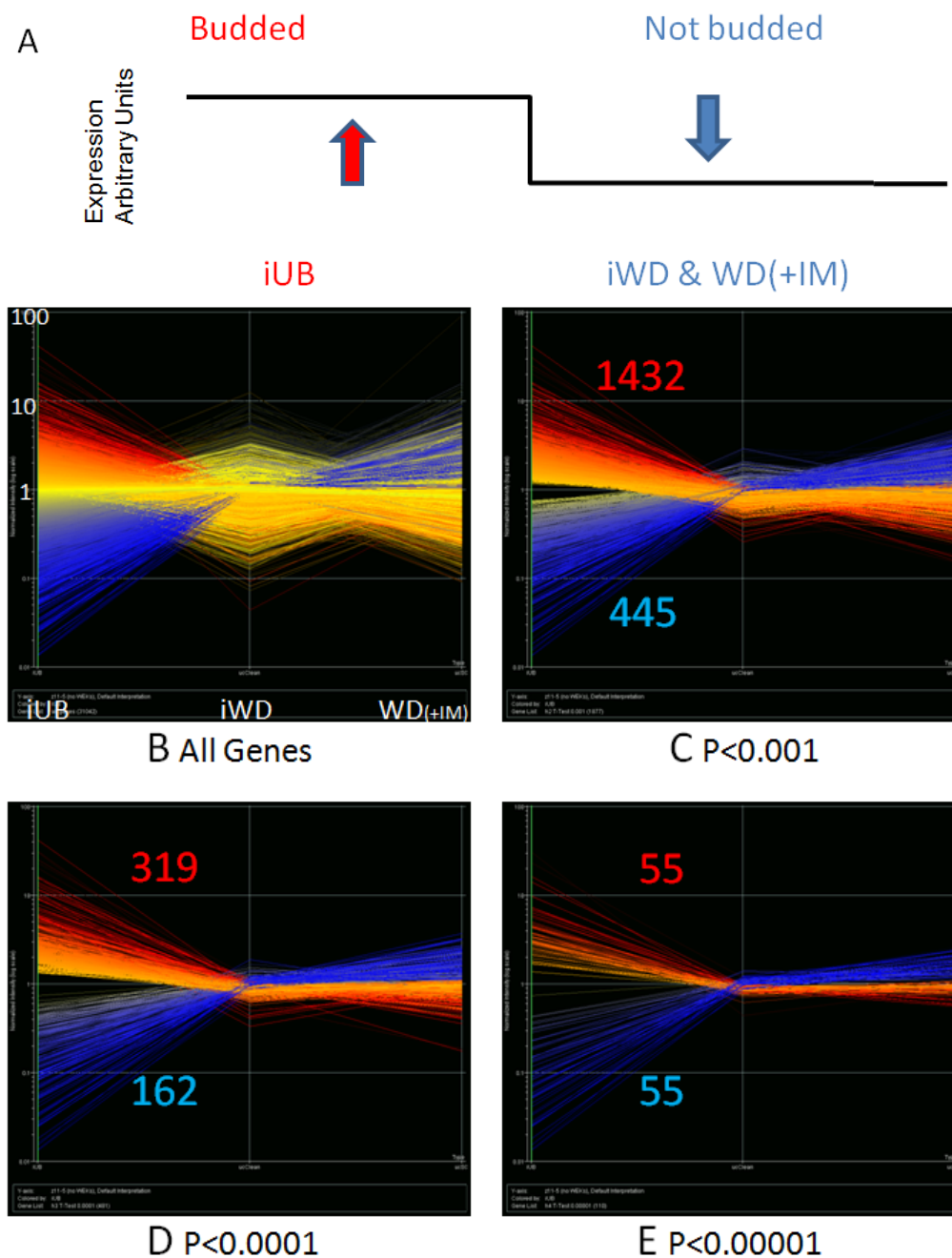


Figure 3.4: ANOVA and pattern matching

(A) Pattern set for ANOVA analysis. iUB –isolated ureteric bud, iWB – isolated Wolffian duct, WD(+IM) – Wolffian duct with mesodermal cells. (B) Line graph showing all genes. Y-axis is normalized expression and the X-axis are the samples: iUB, iWD and WD(+IM). (C-E) Line graphs corresponding to budding (red) or non-budding (blue) for (C) $P < 0.001$ 1877 genes: 1432 upregulated in budding, 445 downregulated in budding, (D) $P < 0.0001$ 481 genes: 319 up, 162 down, (E) $P < 0.00001$ 110 genes: 55 up, 55 down. Graphs display normalized log intensity on the Y-axis for iUB. iWD and WD(+IM) are plotted along the X-axis.

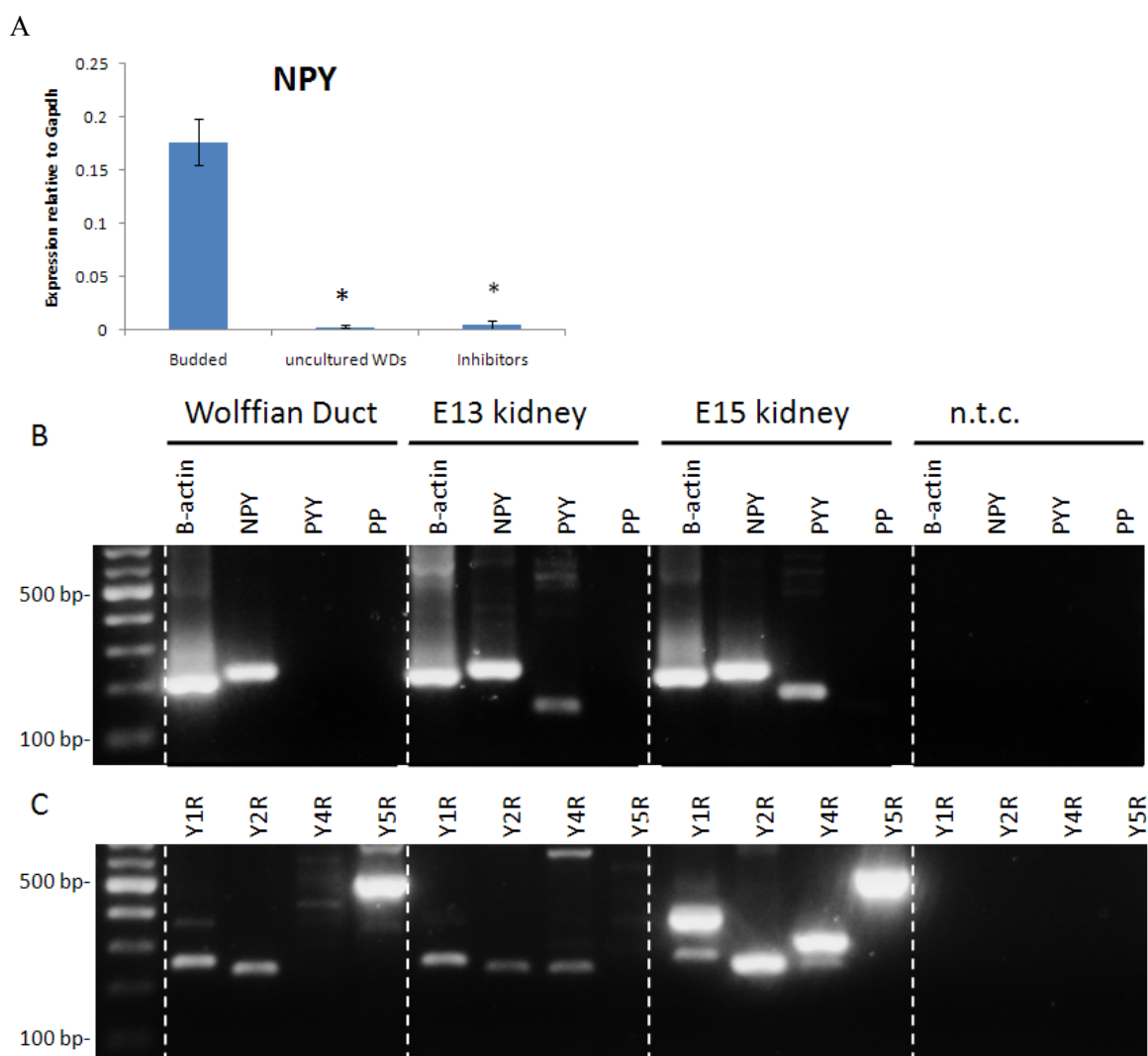


Figure 3.5: NPY expression

(A) Comparison of NPY expression relative to Gapdh in WDs cultured with GDNF and FGF1 (Budded) with uncultured unbudded WDs and WDs cultured with GDNF and FGF1 with BMP4, Activin A, or Akt inhibitor IV. * $P < 0.05$. (B) RT-PCR of NPY: 234 bp, PYY: 141 bp and PP: 142 bp in the WD, E13 & E15 kidneys, and no template control (n.t.c.). (C) NPY receptors Y1: 258 bp, Y2: 235 bp, Y4: 292 bp, and Y5: 524 bp.

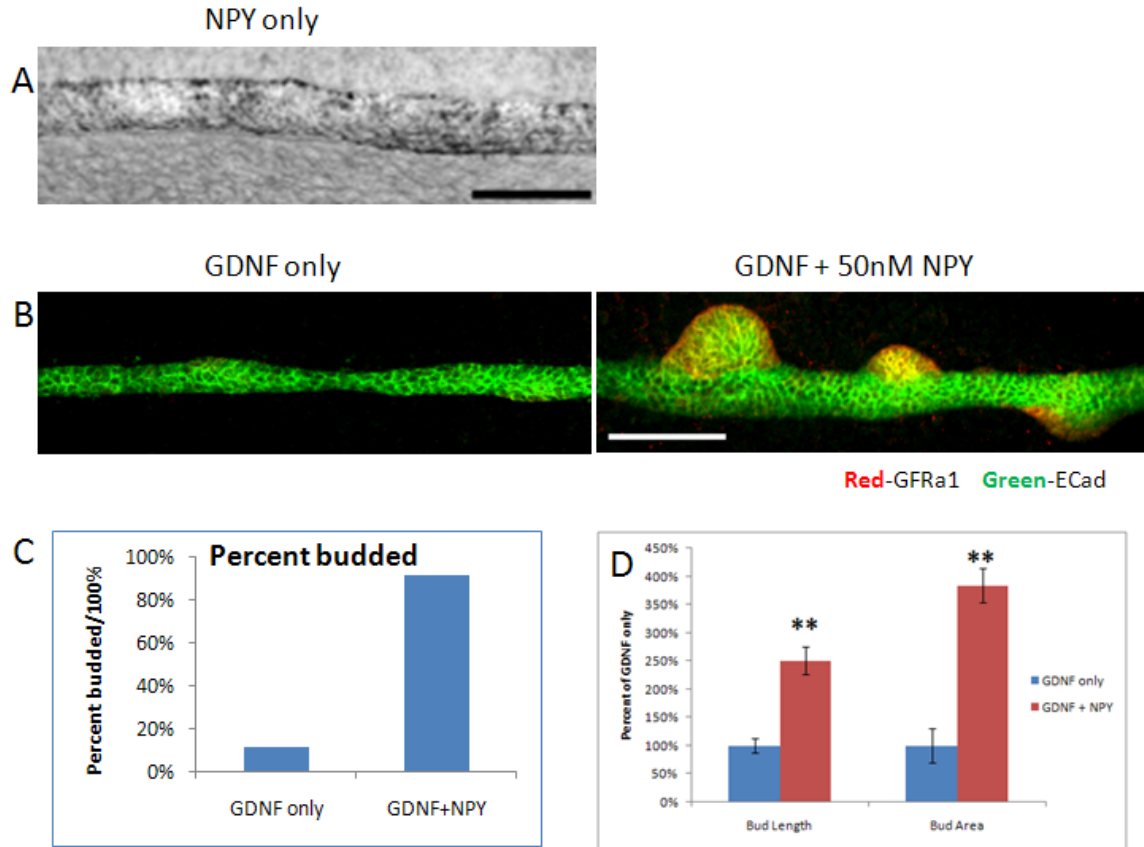


Figure 3.6: NPY augments bud formation in vitro.

(A) Addition of only NPY did not induce budding in the WD. Scale bar 100 μ m. (B-C) Addition of concentrations ranging from 50nM to 2 μ M of NPY to WDs cultured with 125 ng/ml GDNF resulted in 90% budding (right) compared to 10% budding without added NPY (left). Confocal images (top row) Red: GFR α 1, Green: E-Cadherin Scale bar: 100 μ m; Fluorescent images (lower row) show Dolichus biflorus (green) and GFR α 1 (red). (D) Quantification of length and area increase with addition of NPY (compared to those WDs exposed to just GDNF that did form a bud). ** P < 0.01 (E) Effect of Y-receptor inhibitors on budding. (F) Effect of NPY analogs on budding.

E

<u>Analog</u>	<u>Receptor(s) stimulated</u>	<u>Effect</u>
PYY	Y2	Budding
PP	Y4	No budding

F

<u>Receptor</u>	<u>Inhibitor</u>	<u>Effect</u>
Y1	BIBP3226	Inhibition at >10uM
	PYX-1	Inhibition at >10uM
Y2	BIIE 0246	No inhibition
Y5	L152,804	No inhibition

Figure 3.6 Continued

(E) Effect of Y-receptor inhibitors on budding. (F) Effect of NPY analogs on budding.

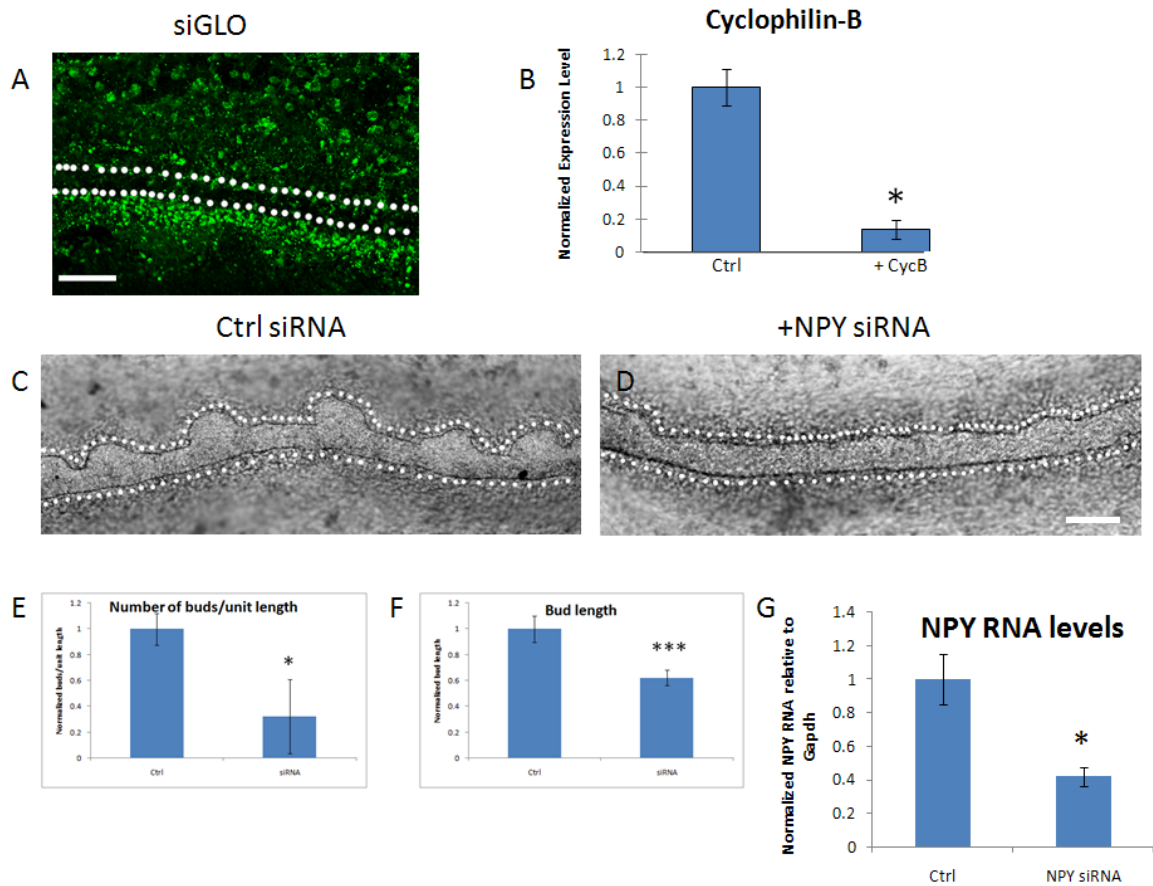


Figure 3.7: siRNA

(A) siGLO added for 24 hours showed penetration into the intermediate mesoderm and slightly inside the WD epithelium (dotted lines). (B) siRNA directed against Cyclophilin B showed a decrease to approximately 20% of controls without siRNA. WDs were cultured (D) with and (C) without siRNA directed towards NPY. (E) The number of buds per unit length decreased with NPY siRNA as did the (F) length of the bud. (G) Experiments that showed a decrease in budding had a reduction of NPY mRNA to approximately 40% of controls. * $P < 0.05$, *** $P < 0.001$. 100 μ m scale bar

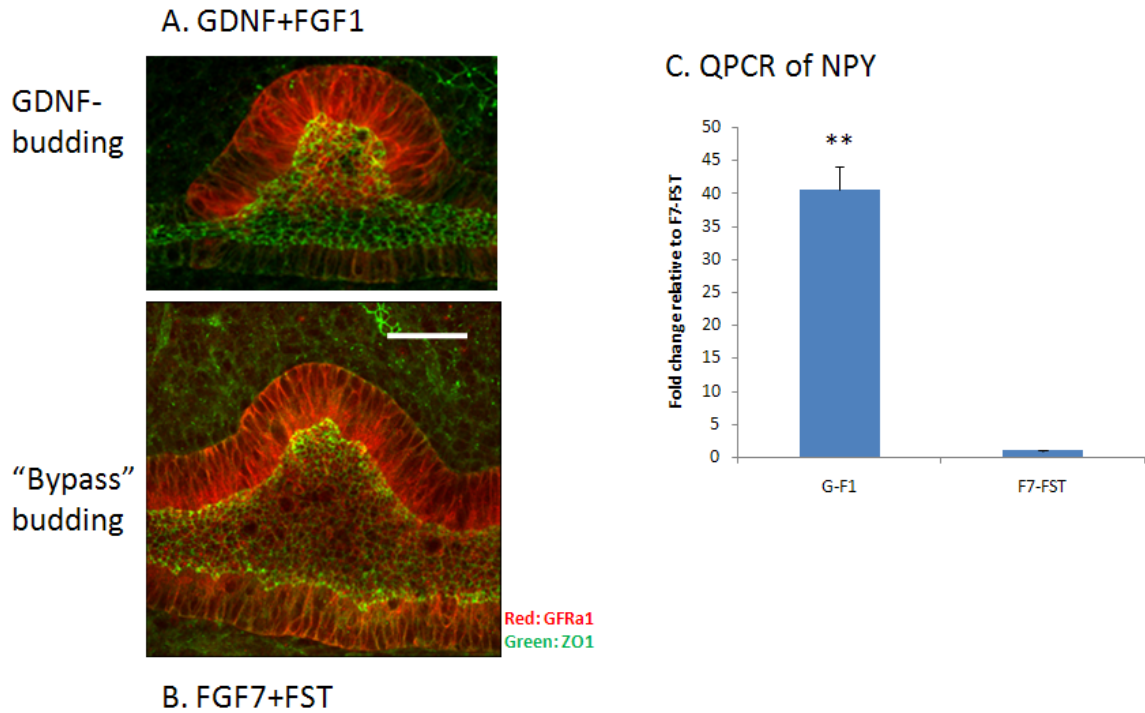


Figure 3.8: Budding in GDNF dependent (A) and independent (B) pathways.

(A) GDNF + FGF1 (B) FGF7 + follistatin (FST) (E). Red is GFR α 1. Green is ZO-1 (bright spots) and E-cadherin. Scale bar 50 μ m. (C) Relative expression of NPY in budded WDs cultured with or without GDNF. NPY expression in GDNF-dependent and independent budding induced to bud with GDNF+FGF1 or FGF7+FST normalized to WDs cultured with FGF7+FST using the Delta-Delta Ct method. ** P<0.01.

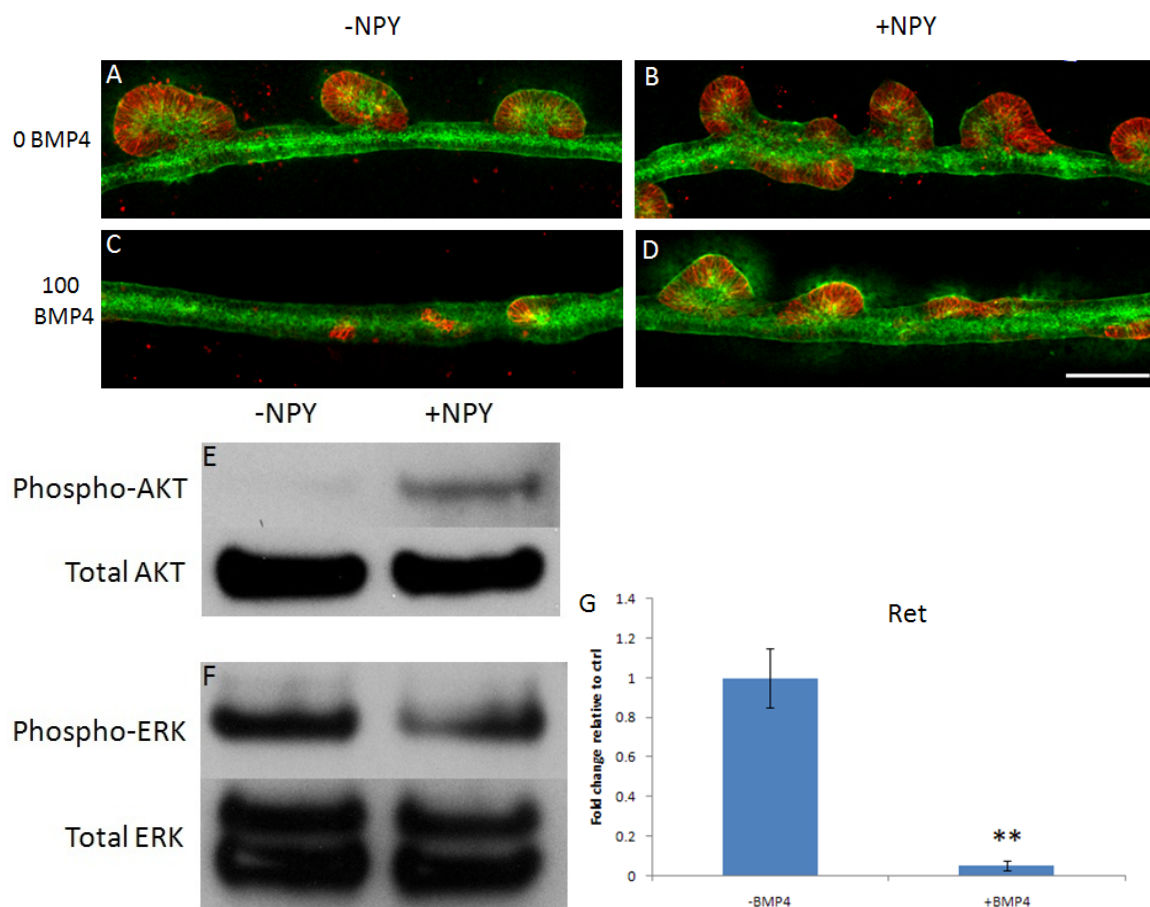


Figure 3.9: NPY rescue of BMP4 inhibition

WDs cultured with 125 ng/ml of GDNF and FGF1 without NPY (left side: A & C) with 0 (A & B) or 100 (C & D) ng/ml BMP4 added. WD with 200 nM NPY added (right side: B & D). A-D: Red: GFRα1. Green: DB. Scale bar: 100 μM. (E) Western Blot of Phospho-Akt (Ser473) and total Akt and (F) Phospho-ERK (p44/42 at Thr202/Tyr204) and total ERK in WDs treated with 100 ng/ml BMP4 without NPY (left, inhibited) or with 200 nM NPY (right, budded) treated WDs. (G) Relative expression of Ret in WDs without and with BMP4 treatment. ** P<0.01

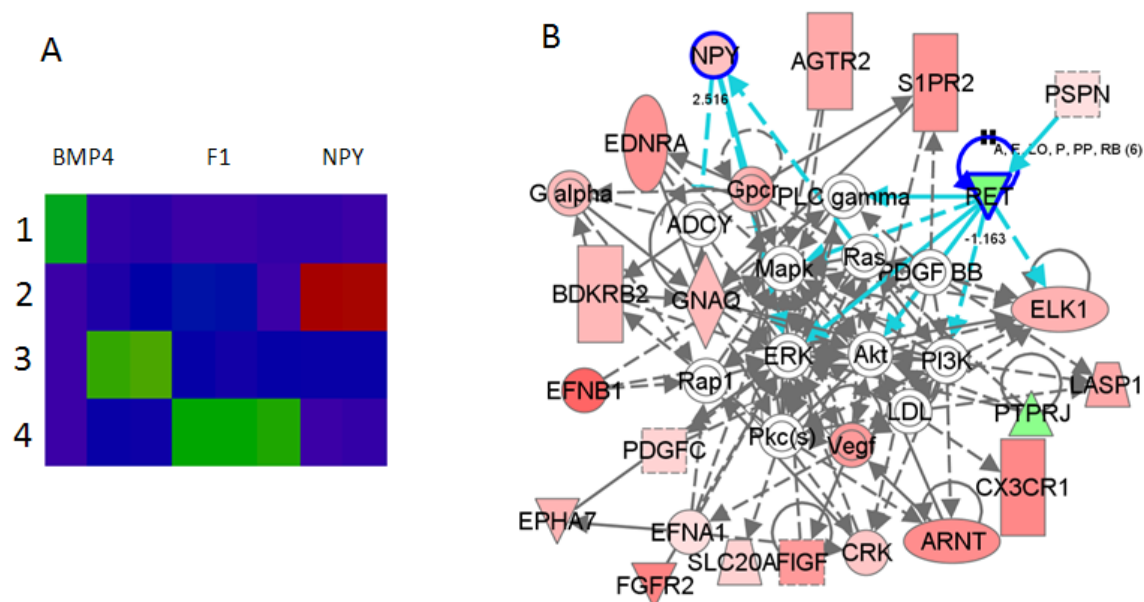


Figure 3.10: NPY transcriptional network

(A) WDs cultured with (1) GDNF + NPY (NPY), (2) GDNF + FGF1 (F1), or (3) GDNF + FGF1 + BMP4 (BMP4). NMF with 4 metagenes separated into two clusters for the BMP4-treated WDs and clusters for FGF1 and NPY. The genes within the FGF1 and NPY-enriched metagenes (e.g. metagenes 2 and 4) were filtered to include only those that were annotated with GO “Signal Transduction” or “Transcriptional Regulation.” These genes were then grouped by IPA. (B) A sample IPA network is shown.

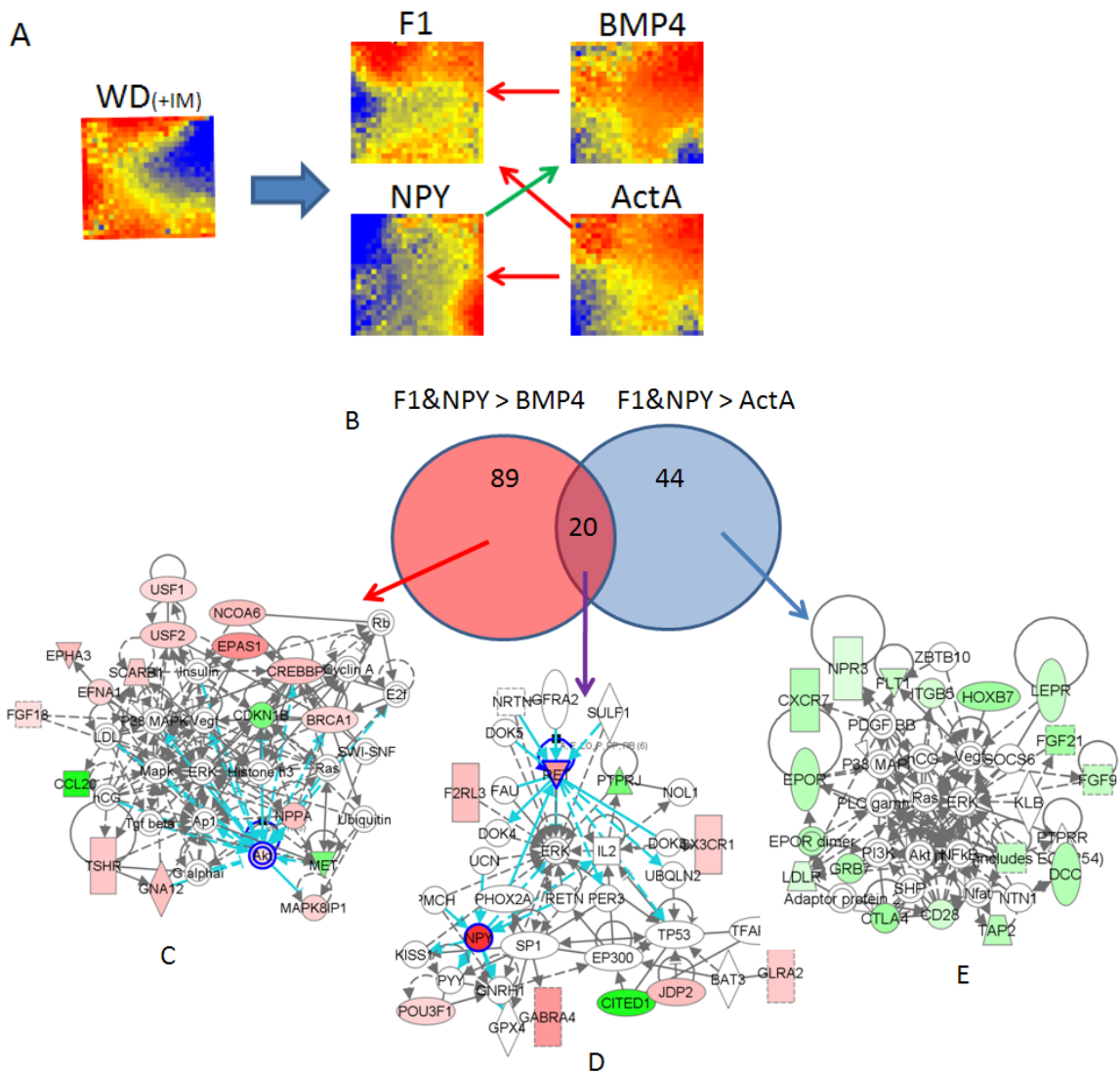


Figure 3.11: Comparison of FGF1 and NPY vs. BMP4 and activin A.

(A) SOM for microarrays of WD(+IM): untreated WDs; F1: WDs cultured with GDNF and FGF1; NPY: WDs cultured with GDNF + NPY; BMP4: WDs cultured with GDNF, FGF1 and BMP4; ActA: WDs cultured with GDNF, FGF1 and activin A. Activin A inhibits budding in either FGF1 or NPY cultured WDs while BMP4 inhibits budding only in FGF1-treated WDs (red arrows). NPY rescues budding inhibition of BMP4 (green arrow). (B) Comparison of FGF1 and NPY arrays with those of WDs treated with BMP4 or activin A. 89 unique genes were two-fold higher in FGF1 and NPY treated WDs compared to BMP4. 44 unique genes were two-fold higher in FGF1 and NPY treated WDs compared to activin A. 20 genes were commonly downregulated by both BMP4 and activin A. (C) IPA network for genes downregulated by BMP4. (D) IPA network for genes downregulated by both BMP4 and activin A. (E) IPA network of genes downregulated by activin A (colored by activin A).

F	Signaling Pathway	Compound(s)	Effect on budding
	p38 MAPK	PD169316 SB203580	No inhibition
	MEK/ERK	PD98059 MEK inhibitor II	No inhibition
	JNK	JNK inhibitor II & III	No inhibition
	PKC	Calphostin C	No inhibition
	PI3-kinase	LY294002	Inhibition
	Akt	Akt inhibitor IV	Inhibition
	IKK	IKK-2 inhibitor IV	Inhibition

Figure 3.11 continued

(F) Result of blockade of various signaling pathways on WDs cultured with GDNF and FGF1.

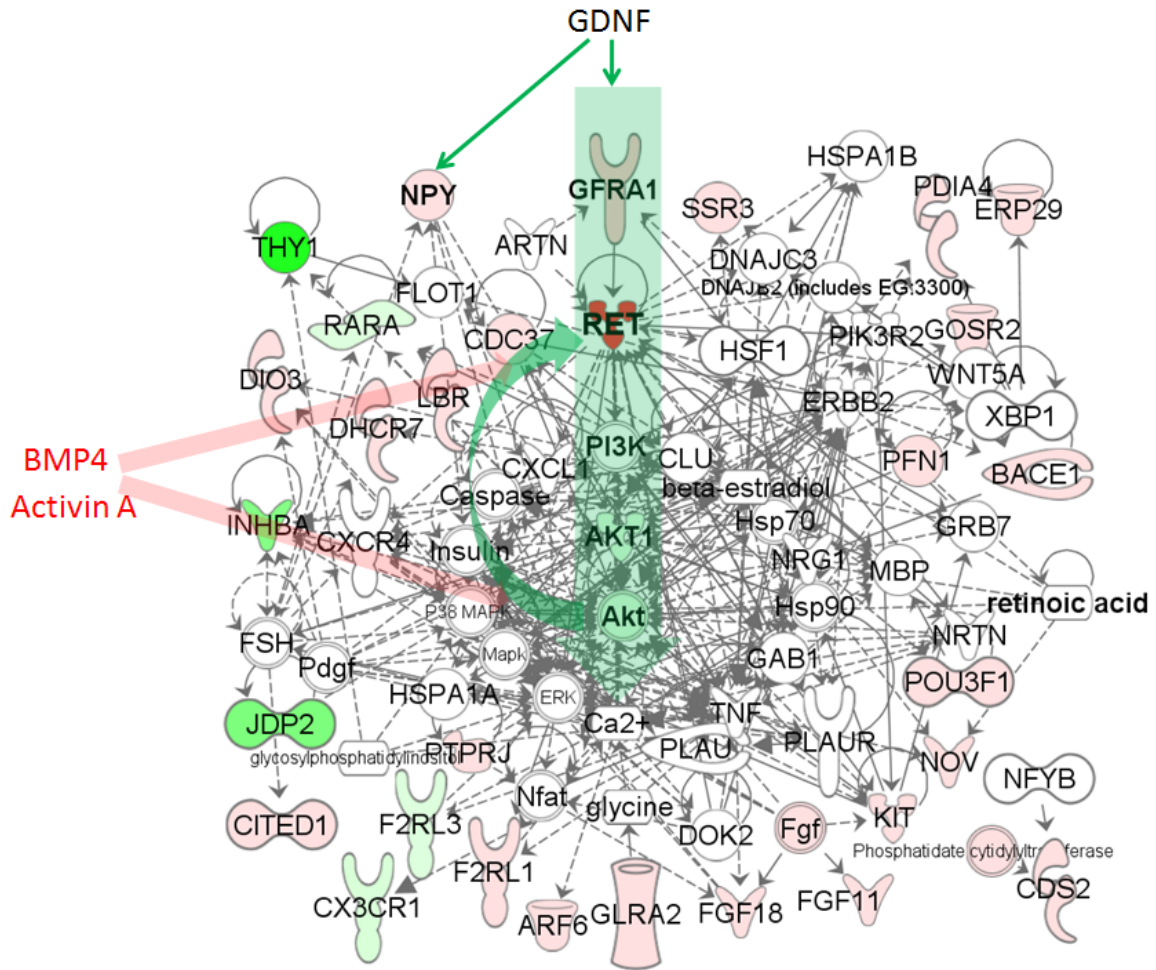


Figure 3.12: Budding signaling diagram

Feed-forward budding with GDNF signaling through its receptor Ret. This leads to increase in NPY expression and upregulation in Ret expression, amplifying the signal. The inhibitors BMP4 and activin A, on the other hand, work to suppress Ret expression, preventing signaling and budding. FGFs and retinoic acid support budding. Ret also stimulates other signaling pathways that are either redundant or do not directly affect budding. A complicated underlying network supports this budding process.

Table 3.1: IPA networks

Molecules/Genes	Score	Top Functions
Crk, Cxcr4, Ednrb, Erbb3, Fst, Gfra1, Ghr, Gnaq, Homer1, Kit, Kitlg, Lasp1, Ldlr, Met, Nov, Nr4a1, Ret	43	Cellular Development, Hair and Skin Development, Nervous system Development and Function
Fcgr2a, Htr5b, Il13ra1, Lphn2, Npvf, Npy, Nxph1, Pax8, Unc13b	19	Behavior, Digestive System Development and Function, Cell Signaling

Table 3.2: ANOVA & pattern matching selected genes enriched in the isolated ureteric bud

Probe Name	P-value	Common	Description
1387154_at	2.01E-08	NPY02; RATNPY	neuropeptide Y
1370177_at	1.41E-07	Taa1; Tage4	poliovirus receptor ets variant gene 4 (E1A enhancer binding protein, E1AF) (predicted)
1380168_at	1.54E-07	Etv4; Pea3	
1367869_at	4.04E-07	MGC93253	oxidation resistance 1 formyltetrahydrofolate synthetase domain containing 1 (predicted)
1390141_at	5.76E-07	Fthfsdc1_predicted	
1392064_at	6.55E-07	Dlx1_predicted	distal-less homeobox 1 membrane protein, palmitoylated 6 (MAGUK p55 subfamily member 6) (predicted)
1380062_at	9.94E-07	Mpp6_predicted	UI-R-CU0-bus-a-01-0-UI.s1 UI-R-CU0 Rattus norvegicus cDNA clone
1381545_at	1.22E-06		
1373625_at	1.24E-06	Shmt; mShmt	serine hydroxymethyl transferase 1 (soluble)
1384828_at	1.75E-06	Kif7_predicted	kinesin family member 7 (predicted)
1380749_at	2.09E-06	Sh2d4a	SH2 domain containing 4A
1373653_at	2.58E-06	Papd1_predicted	PAP associated domain containing 1 (predicted) v-kit Hardy-Zuckerman 4 feline sarcoma viral oncogene homolog
1386540_at	2.60E-06	Kit	
1384950_at	2.61E-06	MGC94512	phosphatidylinositol 4-kinase type-II beta
1388485_at	2.79E-06	BRAK; chemokine	chemokine (C-X-C motif) ligand 14
1368032_at	4.14E-06	Nopp140	nucleolar and coiled-body phosphoprotein 1
1369473_at	4.63E-06	Pgm1	phosphoglucomutase 1
1368674_at	4.68E-06	Pygl	liver glycogen phosphorylase
1370162_at	5.02E-06	Pp4r1	protein phosphatase 4, regulatory subunit 1
1374947_at	5.41E-06	Bcar3_predicted	breast cancer anti-estrogen resistance 3 (predicted)
1373379_at	5.79E-06	Irak1_predicted	Interleukin-1 receptor-associated kinase 1 (predicted)
1374748_at	6.20E-06	Shmt; mShmt	serine hydroxymethyl transferase 1 (soluble)
1368931_at	6.22E-06	SH3P13; Sh3d2c1	SH3 domain protein 2 C1
1368943_at	6.37E-06	Rnase4	ribonuclease, RNase A family 4
1368290_at	6.58E-06	MGC93040	cysteine rich protein 61
1376711_at	6.61E-06	Cldn11	claudin 11 G protein-coupled receptor, family C, group 5, member B (predicted)
1373336_at	7.00E-06	Gprc5b_predicted	
1395555_at	7.12E-06	p28	golgi SNAP receptor complex member 1
1372088_at	7.63E-06	Rnf25	ring finger protein 25
1389367_at	7.74E-06	Schip1_predicted	schwannomin interacting protein 1
1368174_at	7.79E-06	LOC497816	hypothetical gene supported by NM_019371
1374105_at	7.79E-06	Hig1	hypoxia induced gene 1
1377631_at	9.49E-06	Col9a3_predicted	procollagen, type IX, alpha 3 (predicted)
1368305_at	9.81E-06	Mch2; MGC93335	caspase 6
1393101_at	9.88E-06	Fbx110_predicted	F-box and leucine-rich repeat protein 10
	1.16E-05	Ret	Ret

Table 3.3 NPY Transcriptional Program (selected genes enriched in budded WDs)

Fgf3
Fgf11
Fgf12
Fgf18
Fgfr4
Gfra1
Npy
Ngf gamma
Hgfr (Met)
Neuregulin 2
Ret
Retinoic acid receptor
Wnt11

Supplemental Table 3.4 Genes in IPA networks for Figure 3.11**Fig11C**

<u>Symbol</u>	<u>Synonym(s)</u>
Akt	Akt protein, Pkb
Ap1	Ap1 protein
BRCA1	BRCA1
CCL20	CHEMOKINE EXUDUS 1
CDKN1B	CYCLIN-DEPENDENT KINASE INHIBITOR P27
CREBBP	CREB BINDING PROTEIN
Cyclin A	Cyclin A protein, Cyclin A(t)
E2f	
EFNA1	EPHRIN A1
EPAS1	Hif1alpha related factor
EPHA3	AW492086
ERK	Erk protein
FGF18	
G alpha1	G protein ai ALPHA SUBUNIT OF THE G12 FAMILY OF HETEROTRIMERIC G PROTEINS
GNA12	
hCG	CG, Chorionic Gonadotropin
Histone	
h3	Histone H3 protein
Insulin	C-peptide
LDL	low density lipoprotein
Mapk	Map Kinase
MAPK8IP1	JNK-INTERACTING PROTEIN 1
MET	C-MET, HGFR
NCOA6	AIB3, HOX1.1, HOXA7
NPPA	ATRIAL NATRIURETIC FACTOR
P38 MAPK	p38, P38 MAPK protein
Ras	p21 Ras, p21 Ras protein, Ras protein
Rb	pRb, Rb Tumor Suppressor
SCARB1	Scavenger receptor class b1
SWI-SNF	Swi/Snf
Tgf beta	LAP, Tgfb
TSHR	THYROTROPIN RECEPTOR
Ubiquitin	Polyubiquitin
USF1	
USF2	
Vegf	

Supplemental Table 3.4 continued**Fig11D**

<u>Symbol</u>	<u>Synonym(s)</u>
BAT3	SCYTHE
CITED1	MSG1
CX3CR1	Fractalkine receptor
DOK3	AI450713
DOK4	FLJ10488
DOK5	2700055C10Rik, C20orf180, MGC16926
EP300	A430090G16
ERK	Erk protein
F2RL3	PAR4
FAU	Finkel-biskis-reilly murine sarcoma virus ubiquitously expressed
GABRA4	
GFRA2	Gdnfr beta
GLRA2	GLR
GNRH1	GNRH
GPX4	1700027O09Rik
IL2	INTERLEUKIN-2
JDP2	JUNDM2
KISS1	Eseptin
NOL1	120kDa
NPY	NEUROPEPTIDE Y
NRTN	NEURTURIN
PER3	2810049O06RIK
PHOX2A	ARIX
PMCH	Melanin Concentrating Hormone
POU3F1	
PTPRJ	AI450271
PYY	GHYY
RET	C-RET
RETN	ADSF
SP1	Trans-acting transcription factor 1
SULF1	AI467640
TFAP2C	AA409384
TP53	bb1
UBQLN2	ubiquitin 2
UCN	UROCORTIN

Supplemental Table 3.4 continued**Fig11E**

<u>Symbol</u>	<u>Synonym(s)</u>
Adaptor protein 2	AP2
Akt	Akt protein
CD28	CD28 ANTIGEN
CTLA4	CD152
CXCR7	AW541270
DCC	C030036D22RIK
EPOR	EP-R
EPOR dimer	
ERK	Erk protein
FGF21	
FGF9	GAF
FLT1	AI323757
GRB7	KIAA4028
hCG	Chorionic Gonadotropin
HOXB7	HOMEBOX C1
ITGB5	INTEGRIN BETA 5
KITLG (includes EG:4254)	C-KIT LIGAND
KLB	AV071179
LDLR	FH
LEPR	LEPTIN RECEPTOR
Nfat	nfat gene
NFkB	NF-KAPPA B
NPR3	Natriuretic Peptide Receptor C
NTN1	AI561871
P38 MAPK	p38
PDGF BB	Pdgfb dimer
PI3K	Pi 3-kinase
PLC gamma	Phospholipase C gamma
PTPRR	DKFZp781C1038
Ras	p21 Ras
SHP	
SOCS6	1500012M23RIK
TAP2	ABC18
Vegf	
ZBTB10	4832414A18

Supplemental Table 3.5: Genes in IPA network in Figure 3.12

Akt	Fgf	NFYB
AKT1	FGF11	NOV
ARF6	FGF18	NPY
ARTN	FLOT1	NRG1
BACE1	FSH	NRTN
beta-estradiol	GAB1	P38 MAPK
Ca ²⁺	GFRA1	Pdgf
Caspase	GLRA2	PDIA4
CDC37	glycine	PFN1
CDS2	glycosylphosphatidylinositol	Phosphatidate cytidyltransferase
CITED1	GOSR2	PI3K
CLU	GRB7	PIK3R2
CX3CR1	HSF1	PLAU
CXCL1	Hsp70	PLAUR
CXCR4	Hsp90	POU3F1
DHCR7	HSPA1A	PTPRJ
DIO3	HSPA1B	RARA
DNAJB2 (includes EG:3300)	INHBA	RET
DNAJC3	Insulin	retinoic acid
DOK2	JDP2	SSR3
ERBB2	KIT	THY1
ERK	LBR	TNF
ERP29	Mapk	WNT5A
F2RL1	MBP	XBP1
F2RL3	Nfat	

CHAPTER 4

Differential Signaling between GDNF-independent and GDNF-dependent Ureteric Bud Formation Occurs with Overlapping Genetic Networks

Abstract

GDNF signaling through its receptor Ret is the major initiating factor in the budding of the ureteric bud from the Wolffian duct. However, mice deficient in GDNF or its cognate receptors $GFR\alpha 1$ and Ret can still form a ureteric bud and a rudimentary kidney in the absence of GDNF/Ret signaling. Whether this ureteric bud is formed via distinct or overlapping transcriptional networks is not currently known. To address this question, we performed microarray expression analysis on both Ret-deficient and wild-type metanephroi and found Fosb and Jun higher in the mutant kidneys compared to the wild-type. We also found several FGFs expressed higher in some of the mutant kidneys. Cross-species analysis led to the question of whether GDNF-dependent and GDNF-independent budding were regulated by different signaling pathways. To test this, we utilized an in vitro WD culture system and found several differences in the response to budding between GDNF-dependent and GDNF-independent bud formation. GDNF-independent budding was sensitive to inhibition of JNK signaling whereas GDNF dependent budding was not. Conversely GDNF-independent budding was not sensitive to PI3-kinase inhibition or exposure to BMP4 or a PKA activator. Both budding mechanisms were inhibited when Akt or Src were blocked suggesting that there were overlapping budding pathways. We compared both GDNF-independent and GDNF-dependent budding against an

unbudded Wolffian duct and found expression of several cytokines, suggesting that these cytokines mediate a common, core budding network which is blocked by Src or Akt inhibition.

4.1 Introduction

Development of the metanephric kidney begins with the budding of the Wolffian duct (WD) to form the ureteric bud (UB). The UB grows into an adjacent region of intermediate mesoderm known as the metanephric mesenchyme (MM). After invading the MM the UB undergoes repeated dichotomous branching events to form the collecting system: 30,000 to 40,000 collecting ducts in rats. During the development of the collecting system the UB induces the MM to undergo a mesenchymal-to-epithelial transformation, which eventually forms the glomerulus through the distal tubule of the nephron. Thus, a reciprocal interaction between the UB and MM causes the growth of the kidney: the MM induces the UB to grow and branch while the UB causes the MM to condense and become an epithelial tube (Saxon, 1987).

Importance of GDNF: Glial cell-derived neurotrophic factor (GDNF), a member of the TGF- β superfamily, is believed to be the main soluble factor that induces the Wolffian duct to form the UB. GDNF signals through the Ret receptor tyrosine kinase and the GPI-linked co-receptor GFR α 1 (Sariola and Saarma 2003). The proper regulation of GDNF is important in the formation of a single UB.

GDNF deletion: *Gdnf* knockout mice are characterized by kidney agenesis, dysgenesis, or hypogenesis (Moore, Klein et al. 1996; Pichel, Shen et al. 1996; Sanchez, Silos-Santiago et al. 1996). Mice lacking either the GDNF receptor GFR α 1 (Cacalano, Farinas et al. 1998) or the co-receptor Ret (Schuchardt, D'Agati et al. 1994; Schuchardt, D'Agati et al. 1996) also do not usually form kidneys. Other mice showed kidney agenesis via reduction of GDNF from knocking out upstream mediators of GDNF expression, such as *Eya1*, *Pax2*, *Gdf11*, etc (reviewed in (Brodbeck

and Englert 2004)). Some knockout mice have no UB formation, but have normal expression of *Gdnf*, at least in early stages of budding. *Six1* and *Wt1* are examples of such genes. The mechanism of action is not known. Although the mRNA levels of *Gdnf* are normal in these animals, these genes could affect the protein levels (Kreidberg, Sariola et al. 1993; Xu, Zheng et al. 2003).

Increased GDNF expression/sensitivity: Transgenic misexpression of GDNF throughout the WD in vivo (Shakya, Jho et al. 2005) or application of GDNF-soaked beads next to the WD in organ culture (Sainio, Suvanto et al. 1997) cause multiple, ectopic UBs to emerge. Mice lacking *Sprouty1* have multiple ureters and kidneys. *Sprouty1* appears to limit the sensitivity of the WD to GDNF (Basson, Akbulut et al. 2005). Similarly, *Slit2/Robo2* knockout mice also have multiple ureters. Mice lacking *FoxC1* are characterized by duplex kidneys and double ureters; which can be explained by an increased expression of *Gdnf* and *Eya1* (Kume, Deng et al. 2000). Both *Slit2/Robo2* and *FoxC1* have been shown to restrict the GDNF expressed region.

WD budding is modulated through functionally antagonizing GDNF action by other members of the TGF- β superfamily: BMP4 and activin. BMP4, expressed in the mesenchyme surrounding the WD, may act to decrease the WD's sensitivity to GDNF. Mice lacking BMP4 die before kidney development, but heterozygotes sometimes have duplicated ureters (Miyazaki, Oshima et al. 2000). Consistent with this, BMP4 has been shown to block the effect of GDNF in organ culture (Brophy, Ostrom et al. 2001). Although mice lacking activin-A (Matzuk, Kumar et al. 1995) or activin receptors (Oh and Li 1997) have normal kidneys, recent experiments suggest that it is an endogenous inhibitor of UB outgrowth from the WD (Maeshima, Vaughn et al. 2006). Activins are involved in organogenesis and tissue remodeling (Chang, Brown et al. 2002). Follistatin binds to activins and related ligands, blocking their activity (Chang, Brown et al. 2002). Activin A was shown to inhibit branching morphogenesis of the UB, while addition of follistatin to the culture was found to restore branching (Bush, Sakurai et al. 2004).

Signaling: Ret, like other receptor tyrosine kinases, can activate various signaling pathways including RAS/extracellular signal-regulated kinase (ERK), phosphatidylinositol 3-kinase (PI3-kinase)/Akt, p38 mitogen activated protein kinase (MAPK), and c-Jun N-terminal kinase (JNK) pathways (reviewed in (Takahashi 2001)). Of these, it is not currently known which pathways are critical in budding. Although GDNF signaling is very important for budding of the WD, it may not be the only signaling molecule. Our recent data suggest that fibroblast growth factors (FGF) may also be involved in budding. FGFs are involved in cell growth, chemotaxis, cell migration, differentiation, cell survival, and apoptosis (Bottcher and Niehrs 2005). FGFs bind to and activate receptor tyrosine kinases, FGF Receptors (FGFR), which signal through Ras/MAPK, PLC γ /Ca²⁺, and PI3-kinase/Akt (reviewed in (Bottcher and Niehrs 2005)); this is almost identical to the downstream molecules activated by Ret. On the inhibitor side, BMP4 and activin signal through the Smad pathway. Sprouty1, which prevents the formation of supernumerary budding (i.e. inhibits budding), was originally identified as an antagonist of FGF signaling (Hacohen, Kramer et al. 1998). Taken together, it is likely that interaction of receptor tyrosine kinases and Smad and/or Sprouty determines bud formation from the WD.

GDNF bypass: The main reason for examining intracellular signaling pathways is because of the existence of a “GDNF bypass” for budding. A significant percentage (20-50%, (Schuchardt, D'Agati et al. 1994; Moore, Klein et al. 1996)) of GDNF, Ret, and GFR α 1 knockout mice continue to form a ureteric bud and the reasons for this are currently unclear. We hypothesized that a UB might be stimulated to form from the WD without GDNF if the same sets of signaling pathways (e.g. PI3-kinase which is activated in Ret signaling) are activated by a combination of different growth factors (Maeshima, Sakurai et al. 2007).

4.2 Results

4.2.1 Ret mutant and wild-type kidneys

E12.5 Ret mutant and wild-type kidneys were stained for epithelial markers (ZO-1 and E-cadherin) as well as for the GDNF co-receptor GFR α 1 (Figure 4.1). The Ret mutant kidney had formed a bud with GFR α 1 expression; however, it did not branch. The wild-type kidney of the littermate control had undergone two rounds of branching (4 tips). When E11.5 kidneys from Ret(-/-) and Ret(+/-) were cultured in vitro, the Ret(-/-) kidneys did not undergo iterative branching or mesenchymal-to-epithelial transformation (Figure 4.2)(Schuchardt, D'Agati et al. 1996).

4.2.3 Microarray analysis of kidneys with and without Ret

Genomic DNA was used to genotype Ret mutant and wild-type pups. The number of Ret (-/-) embryos was approximately 16% (16 out of 101 pups), which is somewhat less than the Mendelian 25%, suggesting that some knockout embryos were absorbed in utero. In our limited test, approximately 57% of the Ret(-/-) embryos formed visible kidneys at day 11.5, which is similar to what was previously published (Schuchardt, D'Agati et al. 1994; Schuchardt, D'Agati et al. 1996). Three biological replicates of Ret(-/-) and Ret (+/+) kidneys were hybridized to the Affymetrix Mouse Genome 430 2.0 Array.

Microarray samples were clustered via non-negative matrix factorization (NMF) to compare samples (data not shown). NMF has been used in extracting facial features from pictures and contextual text mining (Lee and Seung 1999). NMF is a method utilized to extract relevant biological correlations in gene expression data (Brunet, Tamayo et al. 2004). Analysis of the data by separation into two metagenes did not give the expected result of wild-type in one group and knockout in the other, probably due to variation in age/development of the kidneys.

This may indicate that the natural variation of maturing kidneys is greater than the variation between wild-type and knockout kidneys, suggesting that budding occurs through a common genetic network.

However, there must be some distinctions between these kidneys since the initial stimulus for budding for the Ret mutants presumably bypasses GDNF signaling. Differential expression analysis was performed to determine enrichment of genes in either the Ret mutant kidneys or the wild-type kidneys (Figure 4.3). There were 1,466 genes that were expressed 2-fold or higher in the Ret(-/-) kidneys and that did not have absent flags in all replicates. Various FGFs were enriched in the knockout kidneys (Table 1). The gene that was expressed highest in the knockout relative to the wild-type was Fosb, a leucine zipper protein that can dimerize with JUN family members to form the AP-1 transcription factor. Table 1 shows a list of selective genes that were upregulated in the knockout kidney compared to wild-type. Of the genes expressed higher in the ret mutant, 180 were annotated with a gene ontology of “development.” The interactions between these genes were analyzed using Ingenuity Pathway Analysis (IPA). Automated analysis generated 9 networks of interactions between these genes. A sample network with the Jun oncogene as a “hub” molecule is shown (Figure 4.4A).

As expected, Ret was upregulated in the wild-type kidneys compared to the Ret(-/-) kidneys. Other genes enriched in the wild-type kidneys were Adam 22, Lim 8, as well as several FGF family members (Table 2). Networks generated by IPA for genes higher in wild-type kidneys were divided into 10 groups. One network that included Ret and had a “hub” centered around PI3-kinase is shown (Figure 4.4B).

4.2.4 Cross-species comparison of GDNF-dependent and independent budding

Comparison of Mouse and Rat microarray data was performed in order to find conserved genes that were differentially expressed between GDNF-dependent and GDNF-independent kidney formation (Figure 4.5). Rat E13 Wolffian ducts (WD) were induced to bud with GDNF and FGF1 for the GDNF-dependent condition. We previously reported WD budding with FGF7 and follistatin or anti-activin A (Maeshima, Sakurai et al. 2007). We had discovered that FGF7 as well as other FGFs were expressed in the metanephroi that developed in the Ret mutants even though they are not normally expressed in wild-type metanephroi of littermates, which is consistent with the current data. Although follistatin was expressed in the E11 metanephroi, it was not differentially expressed between the mutants and wild-types, suggesting that some other factor or factors were responsible for the UB formation in the absence of Ret signaling. We previously found that heregulin-alpha (HRG) induced GDNF-independent growth in ureteric bud epithelia so decided to test if the WD would also respond to HRG (Sakurai, Bush et al. 2005). Addition of HRG alone did not induce budding in our WD culture system; however, addition of FGF7 with HRG induced very robust budding. Therefore, for the rat GDNF-independent condition, the WDs were induced to bud with FGF7 and HRG. Rat microarray data from Affymetrix Rat genome 230 2.0 array was converted via homology tables to compare with the Mouse 430 2.0 microarray. A T-Test analysis indicated 502 genes that correlated with GDNF-dependent budding and 263 genes that correlated with GDNF-independent samples. These gene lists were grouped into networks by IPA (data not shown). Akt, p38 MAPK, PI3-kinase, and other pathways were suggested by IPA to play a role in budding/kidney development.

4.2.5 In vitro culture

Since Fosb was the highest upregulated gene in the knockout metanephroi and since the various signaling pathway molecules were mapped on the IPA networks when comparing mouse kidneys and rat WDs, we decided to investigate JNK and well as other signaling pathways in GDNF-dependent and independent budding. In order to perturb signaling we utilized an in vitro culture system to determine the effect of signaling inhibition on budding. WDs were isolated from E13 rat embryos as previously described (Maeshima, Vaughn et al. 2006; Rosines, Sampogna et al. 2007). WDs were induced to bud in vitro with or without GDNF (Figure 4.6). Budding with GDNF was accomplished by adding GDNF plus FGF1. GDNF alone did not usually lead to budding (Maeshima, Vaughn et al. 2006). Budding without GDNF was accomplished by addition of FGF7 plus an additional factor: anti-activin or follistatin (Maeshima, Sakurai et al. 2007) or HRG. Neither FGF7 alone nor addition of just follistatin or HRG elicited budding. A combination of two growth factors was required in this culture system.

4.2.6 GFR α 1 localization

Localization of GFR α 1 was limited to the budding areas in WDs treated with GDNF; however, those treated with FGF7 expressed GFR α 1 all along the WD. The buds produced by either method were capable of inducing MM and undergoing iterative branching morphogenesis (Maeshima, Sakurai et al. 2007). However, Ret knockout kidneys did not show GFR α 1 expression in all areas of the UB (Figure 4.1).

4.2.7 Inhibitor Studies

GDNF-dependent and independent budding had some similarities and differences in how they reacted to various inhibitors of budding (Figure 4.7). Blockade of PI3-kinase inhibited

budding for GDNF-dependent budding but not for GDNF-independent budding; however, Akt pathway inhibition resulted in lack of budding for both conditions, suggesting that the GDNF-independent budding mechanisms activate Akt via pathways independent of PI3-kinase. Inhibition of MEK/ERK or p38 MAPK did not inhibit budding for either condition. Blocking JNK with JNK inhibitor II blocked budding in FGF7-follistatin induced bypass budding but not GDNF-induced budding, suggesting that the JNK pathway is important for GDNF-independent budding but not for the GDNF-dependent budding process. In contrast to JNK inhibition, addition of BMP4 or the PKA agonist dibutyryl-cAMP blocked GDNF-dependent budding but not GDNF-independent budding. Inhibition of SRC with PP2 inhibited budding in both conditions.

4.2 8 Common budding genes

Since the NMF showed that the Ret mutant and wild-type samples were very similar, we questioned if there were genes or networks of genes common to both GDNF-dependent and GDNF-independent budding. Since there were approximately 29,000 genes that varied less than 2-fold we needed a comparison to reduce the number of genes to a manageable amount. We decided to compare both mouse and rat GDNF-dependent and independent samples with an uncultured, unbudded rat WD(+IM) sample (Figure 4.8A). T-Test analysis found 590 genes that correlated with the budded conditions that had a P value less than 0.01. 337 of these genes correlated positively with the budded conditions. In order to find genes that were involved with signaling, this set of genes was further subselected to include genes that were annotated by GO:4871 signal transducer activity or GO:30528 transcription regulator activity, which resulted in 74 genes (Table 3). These genes were then sent to IPA to determine network connections between these genes (Figure 4.8B). Several cytokines were central “hub” molecules, such as interleukin 6 (IL6) and tumor necrosis factor (TNF). We hypothesize that the GDNF-dependent

and GDNF-independent networks feed into this common budding network rather than existing as two discrete entities.

4.3 Discussion

This research began with the question of why animals without *Ret*, *Gdnf*, or *Gfra1* still form a ureteric bud and rudimentary kidneys 20%-50% of the time. To address this question we performed mRNA microarray expression analysis comparing wild type kidneys with those that were deficient in *Ret*. The first finding was that the *Ret* mutant kidneys were very much similar in gene expression to the wild-type kidneys. Our replicate data did not cluster separately between wild-type and mutant kidneys when NMF analysis was performed with two metagenes, strongly pointing to a common transcriptional budding network. Fold-change analysis also indicated that the samples were more similar than different, with 80% of the genes varying less than two-fold (Figure 4.3). The replicate samples did not completely cluster together; this was most likely due to the slight age differences between the animals due to imprecise timing of metanephroi collection. That this created more transcriptional changes than did the difference between mutant and wild-type metanephroi also hints to a common network of genes in budding.

However, although the number of genes that changed were low in comparison with the total number of genes, we were able to discern genes that were significantly expressed higher in most of the *Ret* deficient metanephroi. One example is FGF7, which is normally not detected until later in the formation of the kidney. In kidneys that were formed in the *Ret*-deficient animals FGF7 as well as other FGFs such as FGF17 were expressed. The expression of various FGFs may be the organism's compensatory mechanism of activating signaling pathways to form the ureteric bud despite the absence of *Ret* signaling. The analysis of these two conditions

resulted in several gene networks indicating the involvement of *Fosb* and possibly *Jun* in the GDNF-independent budding mechanism.

Cell cultures lacking *Ret* were found to activate cMet upon stimulation with high levels of GDNF (Popsueva, Poteryaev et al. 2003). This may partially explain formation of budding in *Ret* mutant animals since GDNF and $GFR\alpha 1$ are still present; however, it does not explain the formation of kidneys in *Gdnf* or *Gfra1* knockouts. Another method of eliciting budding may be the activation of the JNK signaling pathway. Although we don't know what directly stimulates JNK, it could be various FGFs that become activated in the absence of *Ret* signaling. We detected *Fosb* as the most highly differentially expressed gene in the *Ret*($-/-$) metanephroi. When we inhibited JNK signaling in vitro without GDNF, inhibition of budding occurred whereas no inhibition of budding was seen in cultures with GDNF. This suggests that the JNK signaling pathway is superfluous in GDNF-dependent budding but becomes necessary in the absence of GDNF. This redundancy might explain some of the robustness of kidney development. There were other genes expressed higher in *Ret* mutants such as *Stat5b*, a transcription factor that may be associated with retinoic acid receptor binding. *Akap13*, which may function to coordinate Rho signaling as well as PKA, might be partially upregulated in knockout kidneys. These represent just two of many genes that become activated in the absence of *Ret* signaling.

Cross-species analysis of in vivo mouse metanephroi with in vitro rat cultured WDs was performed to refine the budding networks between GDNF-dependent and independent bud formation. Since there is no mutant rat deficient in *Ret*, we utilized our WD culture system to induce budding without GDNF to simulate a GDNF-independent bud. This analysis suggested that there may be differences in signaling pathways between GDNF-dependent and independent bud formation.

We were able to test JNK signaling as well as various other signaling pathways in the GDNF-dependent and independent formation of the WD by utilizing an in vitro culture system. We were able to elicit budding with or without GDNF by addition of a combination of growth factors. GDNF alone was not sufficient to form a bud in the WD cultured without mesonephric tubules or gonadal ridge. Addition of an FGF, such as FGF1 or FGF7 facilitated the budding process. Besides FGF, addition of NPY (Choi, Tee, et al, in preparation) with GDNF allowed budding to occur. GDNF-independent budding was accomplished by addition of FGF7 plus another factor. That a signal growth factor was not sufficient to elicit budding may be due to the many levels of regulation of budding. There may be a feedback inhibition loop by endogenous activin A (Maeshima, Sakurai et al. 2007). This inhibition can be overcome via addition of neutralizing antibodies or follistatin. Another method of overcoming endogenous budding inhibition is the addition of heregulin-alpha, which was found to induce GDNF-independent growth in ureteric buds (Sakurai, Bush et al. 2005).

This culture system allowed us to confirm that PI3-kinase activation was essential for GDNF-dependent budding whereas Akt activation was essential for both GDNF-dependent and independent budding. This suggests that Akt is activated via PI3-kinase-independent mechanisms in the absence of GDNF stimulation. We also found that inhibition of MEK did not alter budding in either condition. However, the MEK pathway is probably important in the iterative branching program of the UB as MEK inhibition was shown to decrease branching in vitro (Watanabe and Costantini 2004). It is interesting that addition of BMP4 did not block budding in WDs cultured with FGF7 and follistatin. BMP4 is thought to be one of the major endogenous inhibitors of budding. However, based on our in vitro work it appears to only negatively regulate GDNF-dependent budding.

Although the initiating factor(s) for budding is different between the Ret mutant and wild-type, there may be a core set of genes that regulate budding, whether it is GDNF-dependent

or independent. The Akt pathway can be activated by GDNF or FGFs. Therefore in the absence of Ret, expression of several FGFs can compensate for the lack of Ret signaling. The small differences between the Ret mutant kidneys and the wild-type kidneys are consistent with this. In other words, the differences account for the disparate budding initiation methods; while the bulk of the similar genes are part of a common budding network. There may be various cytokines, such as interleukins and TNF, which play a role in budding of the WD. In this study we utilized FGF7 and follistatin or FGF7 and heregulin-alpha. However, we don't know what endogenous factors are produced to induce budding in the absence of Ret signaling. Further investigation is warranted.

4.4 Methods

4.4.1 Reagents

Akt inhibitor IV, JNK inhibitor II, PD98059, MEK inhibitor II, LY294002, IKK-2 inhibitor IV, PP2, PP3, dibutyryl-cAMP, and recombinant rat FGF1 were from CalBiochem (EMD, San Diego, CA). Recombinant rat GDNF, FGF7, heregulin-alpha, follistatin, and goat anti-GFR α 1 were from R&D Systems (Mineapolis, MN). Fetal bovine serum (FBS) was from Biowhittaker (Walkersville, MD). DMEM/F12 was from Gibco (Invitrogen, Carlsbad, CA). Mouse anti-ZO-1 and mouse anti-E-Cadherin were from Zymed (Invitrogen). Alexa Fluor 488 or 594 secondary antibodies were from Molecular Probes (Invitrogen). Donor Donkey Serum was from Gemini Bio-Products (West Sacramento, CA). All other reagents were from Sigma.

4.4.2 Isolation and culture of Wolffian ducts

Wolffian ducts were dissected with a thin layer of intermediate mesenchyme from E13.5 Sprague-Dawley rats (Harlan, Indianapolis, IN) as previously described (Rosines, Sampogna et al. 2007). WDs were placed on top of Transwell filters (Costar, Cambridge, MA) with a 0.4 μ m pore size. Culture medium was composed of DMEM/F12, 10% FBS and growth factors.

MEK/ERK was inhibited with addition of 20 μ M PD98059 or up to 100 μ M MEK inhibitor II. JNK was blocked with 5 to 10 μ M JNK inhibitor II, and PKC was blocked with 1 μ M Calphostin C. PI3-kinase was inhibited with 10-20 μ M LY294002, Akt was inhibited with 5 μ M Akt inhibitor I, IV, or VIII, and IKK was blocked with IKK-2 inhibitor IV. Src was blocked by PP2 and PKA was stimulated by dibutyl-cAMP.

4.4.3 Ret mutant kidneys

Genotyping of Ret mutant embryos was performed as previously described (Schuchardt, D'Agati et al. 1994). Kidneys were visually inspected for the presence of a ureteric bud before processing for microarray analysis.

4.4.4 Microarray

Mouse wild-type or mutant kidneys were lysed and RNA was extracted with the Qiagen RNEasy Micro kit (Qiagen). The UCSD genechip core processed the mouse RNA using the NuGEN Ovation kit to amplify the RNA before hybridization to the GeneChip Mouse Genome 430 2.0 microarray (Affymetrix). Rat RNA was hybridized to the GeneChip Rat Genome 230 2.0 microarray.

GeneSpring GX 7.3.1 (Silicon Genetics) was used to analyze fold-change data. Data was preprocessed by converting any value less than 0.01 to 0.01. Data was normalized per chip to the

50th percentile. Data was normalized per gene to the median. Conversion of Rat 230 2.0 to Mouse 430 2.0 was done using both the homology table supplied on the Affymetrix web site as well as the Resourcer database (Tsai, Sultana et al. 2001). Approximately 62% of the probe sets on the rat array was converted to a homologous probe set on the mouse array; however, since there are approximately 30% more probe sets in the mouse array that translated to approximately 29% of translated rat probes having a value on the mouse array. Network analysis was performed using the Ingenuity Pathway Analysis (IPA, Ingenuity Systems, Redwood City, CA) plugin for GeneSpring.

4.4.5 Immunohistochemistry

Cultures were fixed in 4% PFA for 1 hour at room temperature before rinsing in PBS with 0.1% Tween-20 (PTW). Primary antibodies were applied overnight in blocking solution (PTW with 1% BSA) at 4°C. Three rinses in PTW were performed and then the cultures were incubated in secondary antibody with 10% donkey serum in blocking solution overnight at 4 °C. Samples were then rinsed with PTW and viewed with a confocal microscope (Nikon D-Eclipse C1).

Acknowledgements

The authors thank Frank Costantini (Columbia University Medical Center, NY) for supplying the Ret heterozygous mice. The authors thank Kevin Bush and Wei Wu for helpful suggestions; Mita Shah, Ankur Dnyanmote and James Tee for critical reading; and Duke A. Vaughn for preliminary work with GDNF-independent WD budding. Yohan Choi was supported

by a Training Grant from the NIH (T-32, HL007261). S.K.N. is supported by National Institute of Diabetes and Digestive and Kidney Diseases grants RO1-DK57286 and RO1-DK65831.

Chapter 4, in part, is currently being prepared for submission for publication. Choi, Yohan; DeCambre, Marvalyn; Ito, Chiharu; Nigam, Sanjay K. The dissertation author was the primary investigator and author of this paper.

4.5 Figures

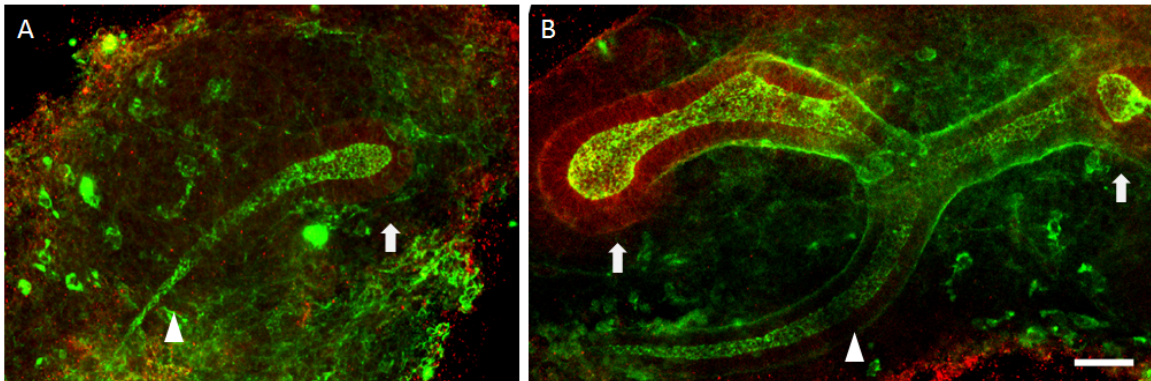


Figure 4.1: Mouse *Ret*(*-/-*) and WT kidneys

GFR α 1 expression in (A) *Ret* KO E12.5 mouse kidney with unbranched UB and (B) wild-type E12.5 mouse kidney with 2 rounds of branching. GFR α 1 (red) is localized to the UB tips (arrows). The ureter (arrow heads) does not express GFR α 1. Green shows E-cadherin and ZO-1. 50 μ m scale bar.

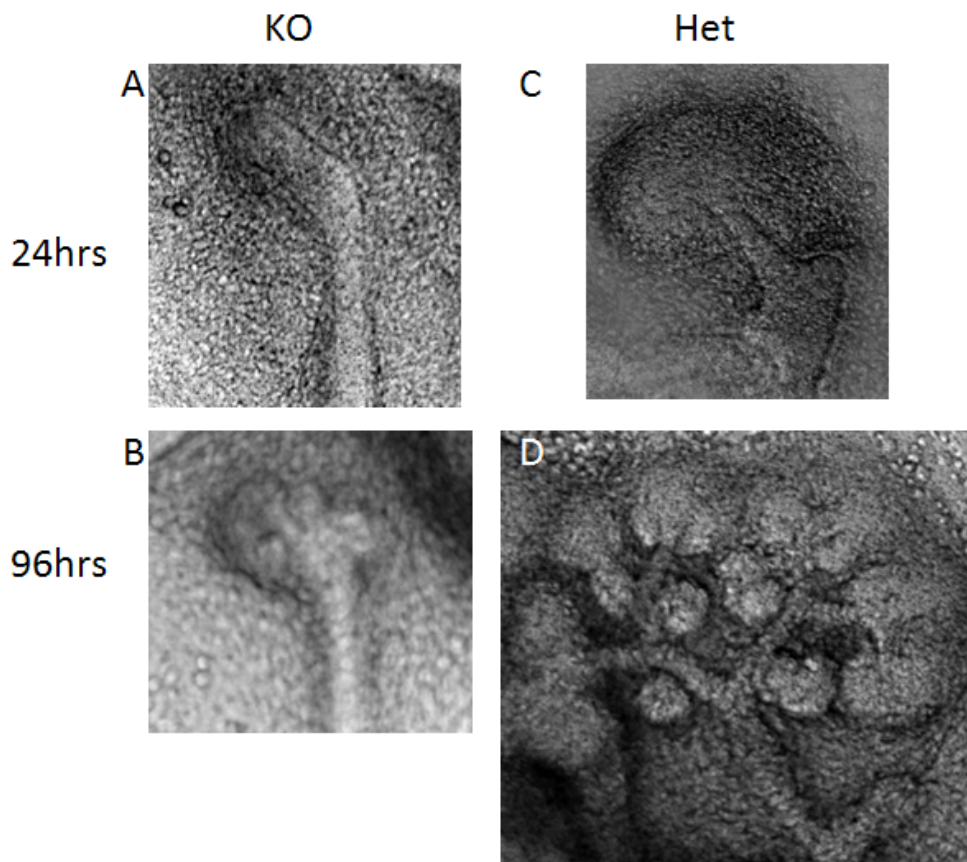


Figure 4.2: Kidney cultures

E11.5 kidneys were cultured on top of Transwell filters with DMEM/F12 with 10% FBS for 4 days. (A) & (B) Ret (-/-) kidneys did not grow in culture. (C) & (D) Ret (+/-) kidneys underwent iterative branching morphogenesis and formation of nephrons.

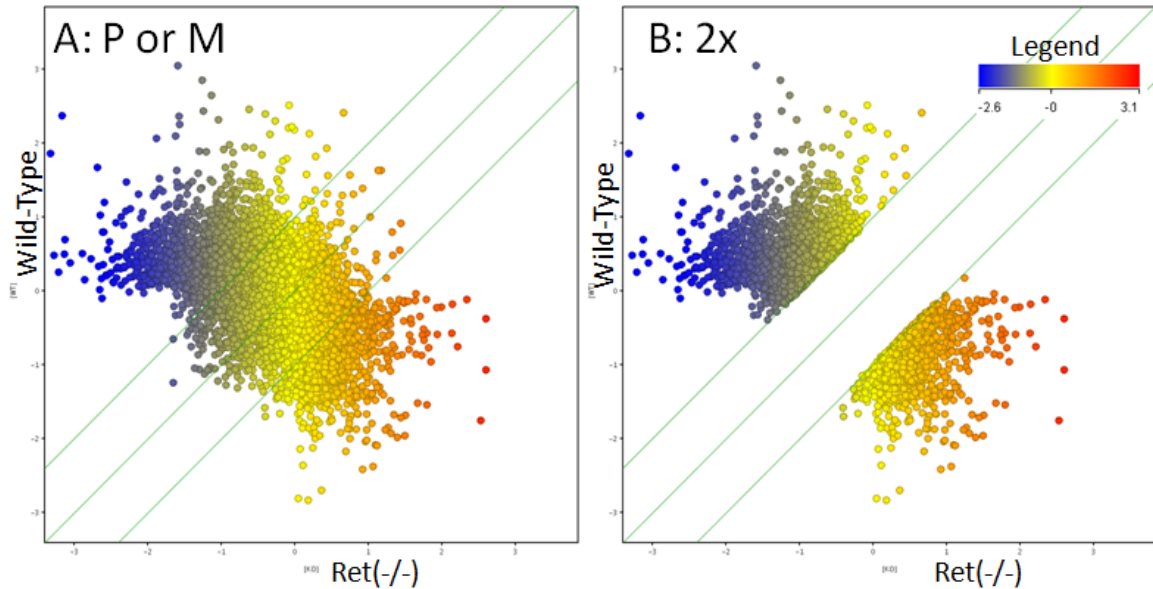


Figure 4.3: Scatter plots.

Comparison between microarray data for Ret(-/-) and Ret(+/+) kidneys. (A) 33,035 of 45,101 probe sets that had a P or M flag in at least one of the six biological replicates. X-axis is the Ret(-/-) and the y-axis is the wild-type kidney. The scatter plot are colored according to expression on the Ret(-/-) arrays. (B) 1466 genes were upregulated 2-fold or greater in the Ret(-/-) kidneys and 1811 were upregulated 2-fold or greater in the wild-type kidneys.

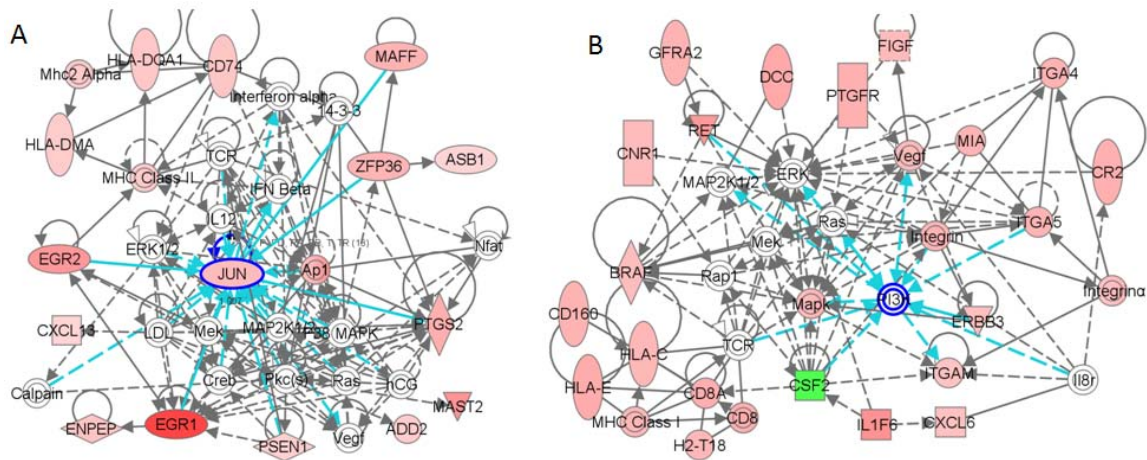


Figure 4.4: Ingenuity Pathway Analysis (IPA) networks.

Genes were selected that were differentially expressed by 2-fold or higher and that contained the Gene Ontology annotation of Development. (A) Genes expressed higher in the Ret mutant kidneys were processed by IPA into 9 networks, of which one is shown. Jun is highlighted, showing the interactions with various neighbors. (B) Genes expressed higher in the wild-type kidney were processed by IPA into 10 networks. One network that included Ret is shown. PI3-kinase is highlighted.

A

Signaling Pathway	Compound(s)	Effect on GDNF budding	Effect on "bypass"
p38 MAPK	PD169316 SB203580	No inhibition	No inhibition
MEK/ERK	PD98059 MEK inhibitor II	No inhibition	No inhibition
JNK	JNK inhibitor II & III	No inhibition	Inhibition
PKC	Calphostin C	No inhibition	No inhibition
PI3-kinase	LY294002	Inhibition	No inhibition
Akt	Akt inhibitor IV	Inhibition	Inhibition
BMP	BMP4	Inhibition	No inhibition
Activin	Activin A	Inhibition	--
Src	Herbimycin A PP2	Inhibition	Inhibition
PKA	dibutyryl cAMP	Inhibition	No inhibition


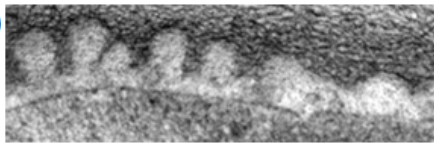
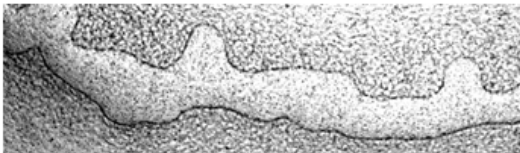
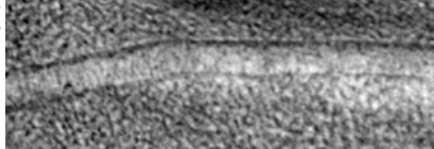
	Ctrl		+ JNK inhibitor
+GDNF	<p>B</p> 	+	<p>D</p> 
-GDNF	<p>C</p> 	+	<p>E</p> 

Figure 4.7: GDNF-dependent and independent budding

Effect of various signaling pathway inhibitors in GDNF-dependent and GDNF-independent budding. (A) Budding or no budding in GDNF-dependent (3rd column) or independent budding (4th column) as a function of inhibition of the p38 MAPK, PI3-kinase (LY294002), Akt pathway (Akt inhibitor IV), MEK pathway (MEK inhibitor II), JNK pathway (JNK inhibitor II), addition of BMP4, the SRC inhibitor PP2, or PKA activator dibutyryl cAMP. (B) Sample GDNF-dependent budding without inhibitor added. (C) Sample GDNF-independent budding without inhibitor added. (D) Sample GDNF-dependent budding with JNK inhibitor II. (E) Sample GDNF-independent budding with JNK inhibitor II.

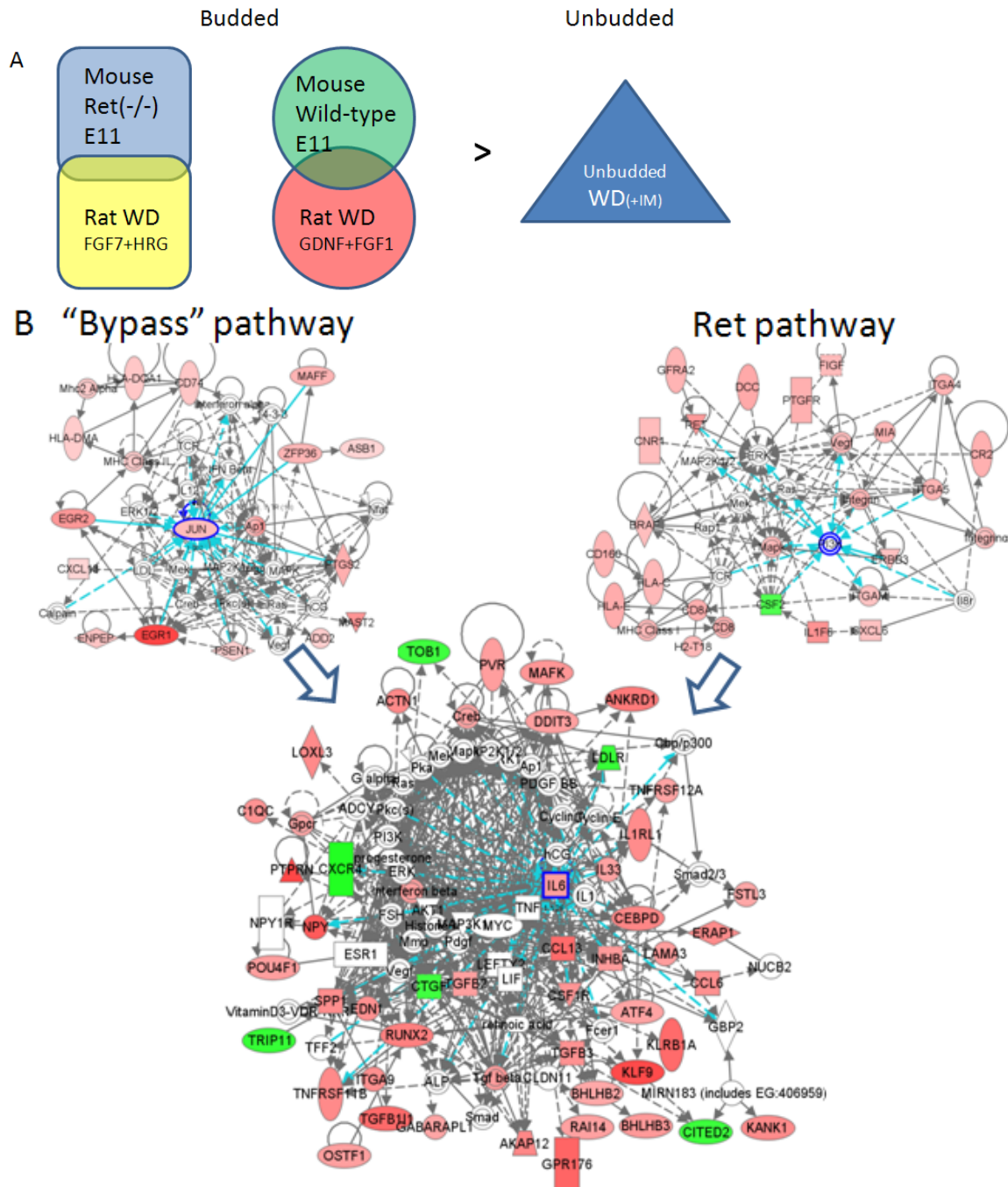


Figure 4.8: Budding network

(A) Comparison of wild-type and Ret mutant mouse metanephroi and rat WDs induced to bud in vitro with uncultured unbudded WD(+IM) were made to determine common budding genes. (B) Both the Ret pathway and “Bypass” pathways feed into a common budding network, which then leads to WD budding.

Table 4.1: Genes upregulated in Ret(-/-) kidneys

Affy Probe	Fold-change	Name	
1438405_at	4.68	Fgf7, Kgf	fibroblast growth factor 7
1418376_at	3.90	Fgf15	fibroblast growth factor 15 (*)
1421523_at	3.71	Fgf17	fibroblast growth factor 17
1420085_at	3.70	Fgf4, KS3, Hstf-1	fibroblast growth factor 4 (*)
1449826_a_at	2.56	Fgf2, Fgfb	fibroblast growth factor 2 (*)
1422134_at	25.93	Fosb	FBJ osteosarcoma oncogene B
1420178_at	21.19		Signal transducer and activator of transcription 5B (Stat5b)
1439697_at	15.47	AI255955; AV239853; IL-1RAcP; IL-1R AcP; 6430709H04Rik	interleukin 1 receptor accessory protein
1445160_at	14.49	Nav3	neuron navigator 3
1457644_s_at	13.79	Cxcl1	chemokine (C-X-C motif) ligand 1
1424733_at	13.34	P2Y14; Gpr105; A330108O13Rik	purinergic receptor P2Y, G-protein coupled, 14
1422606_at	12.65	Cors; CTRP3; Corcs; CORS-26; AI315029; 2310005P21Rik	C1q and tumor necrosis factor related protein 3
1441852_x_at	11.83		autophagy-related 16-like 1 (yeast)
1421114_a_at	11.5	Dspg3; PG-Lb; SLRR3B	dermatan sulphate proteoglycan 3
1417853_at	11.32	Cacc	chloride channel calcium activated 1 ; chloride channel calcium activated 2
1456829_at	10.99	Pnma3	paraneoplastic antigen MA3

(*) "A" flag in both conditions

Table 4.2: Genes upregulated in Ret(+/+) kidneys compared to Ret (-/-)

Affy Probe	Fold-change	Name	
1445645_at	58.07		A disintegrin and metallopeptidase domain 22 (Adam22), transcript variant beta, mRNA
1436359_at	42.79	Ret	Ret proto-oncogene (Ret), mRNA
1426438_at	35.93	Dby; D1Pas1-rs1; 8030469F12Rik	DEAD (Asp-Glu-Ala-Asp) box polypeptide 3, Y-linked
1427300_at	33.78	L3; Lhx7	LIM homeobox protein 8
1443442_at	30.97		expressed sequence AU022084
1449838_at	30.24	Aeg2; CRS3; SGP28; CRISP-3	cysteine-rich secretory protein 3
1459742_at	23.91		15 days embryo brain cDNA, RIKEN full-length enriched library, clone:G630032A08 product:unclassifiable, full insert sequence
1418476_at	18.88	CLF-1; CRLM3; NR6.1	cytokine receptor-like factor 1
1440655_at	17.04		SH3-domain GRB2-like (endophilin) interacting protein 1 (Sgip1), mRNA
1453264_at	13.59	MARVD3; Mrvldc3; AI642133; 1810006A16Rik	MARVEL (membrane-associating) domain containing 3
1448756_at	12.72	p14; Cagb; GAGB; L1Ag; BEE22; MRP14; 60B8Ag; AW546964	S100 calcium binding protein A9 (calgranulin B)
1417171_at	12.54	Emt; Tsk; Tcsk	IL2-inducible T-cell kinase
1457945_at	12.47		Eukaryotic translation initiation factor 2, subunit 3, structural gene Y-linked (Eif2s3y), mRNA
1418847_at	11.74	AII; AU022422	arginase type II
1445143_at	11.46	Vash1	vasohibin 1
1447396_at	8.986		Fibroblast growth factor 1, mRNA (cDNA clone MGC:46904 IMAGE:5137246) (*)
1427582_at	5.767	Fgf-6	fibroblast growth factor 6 (*)
1438924_x_at	4.828	Fibp	Fibroblast growth factor (acidic) intracellular binding protein, mRNA (cDNA clone MGC:25555 IMAGE:3969355)
1451693_a_at	3.387	Fhfl; AV114868	fibroblast growth factor 12
1440270_at	2.706	Fgf12	fibroblast growth factor 12
1450440_at	2.017	AU042498	glial cell line derived neurotrophic factor family receptor alpha 1

(*) "A" flag in both conditions

Table 4.3: Genes common to GDNF-dependent and independent budding

Affy Probe	Common	Description
1427385_s_at	Actn1a; 3110023F10Rik	actinin, alpha 1
1419706_a_at	Srsc5; AI317366	A kinase (PRKA) anchor protein (gravin) 12
1432466_a_at	AI255918	apolipoprotein E
1449289_a_at	Ly-m11; beta2-m	beta-2 microglobulin
1424123_at	CCT; MGC19050	cDNA sequence BC011209
1420380_at	JE; CF; AI323594	chemokine (C-C motif) ligand 2
1417266_at	c10; MRP-1; Scya6 SR-PSOX;	chemokine (C-C motif) ligand 6
1418718_at	0910001K24Rik	chemokine (C-X-C motif) ligand 16
1448710_at	murine CXCR-4	chemokine (C-X-C motif) receptor 4
1419872_at	Csf1r	colony stimulating factor 1 receptor
1449401_at	C1qg; C1qc; AI385742	complement component 1, q subcomponent, gamma
1416953_at	Ccn2; Hcs24; Fisp12; fisp- 12	polypeptide
1419398_a_at	Dp1; AU022809; AW495741	connective tissue growth factor
1451924_a_at	ET-1; preproET	deleted in polyposis 1
1425574_at	Hek; AW492086	endothelin 1
1455426_at	Hek; AW492086	Eph receptor A3
1435476_a_at	Fcgr2b	Eph receptor A3
1433833_at	Fad104; 1600019O04Rik	Fc receptor, IgG, low affinity IIb
1422803_at	Flrg; E030038F23Rik	fibronectin type III domain containing 3B
1416418_at	GEC1; 9130422N19Rik	follistatin-like 3
1442116_at	Gpr176	gamma-aminobutyric acid (GABA(A)) receptor-associated protein-like 1
1422542_at	Gpr34	gene model 1012, (NCBI)
1421947_at	2010305F15Rik	G protein-coupled receptor 34
1455089_at	2010305F15Rik	guanine nucleotide binding protein (G protein), gamma 12
1418349_at	DTS; MGC107656	Guanine nucleotide binding protein (G protein), gamma 12 (Gng12), mRNA
1422053_at	Inhba	heparin-binding EGF-like growth factor
1420860_at	(alpha)92610002H11Rik	inhibin beta-A
1425145_at	T1; Fit-1; T1/ST2; St2-rs1	integrin alpha 9
1450297_at	Il-6	interleukin 1 receptor-like 1
1450296_at	Ly55a; NKR-P1 2	interleukin 6
1427512_a_at	[a]3B; Lama3B	killer cell lectin-like receptor subfamily B member 1A
1424408_at	PINCH2	laminin, alpha 3
1421821_at	Hlb301	LIM and senescent cell antigen like domains 2
1418269_at	Lor2; Loxl2	low density lipoprotein receptor
1419272_at	Myd88	lysyl oxidase-like 3
		myeloid differentiation primary response gene 88

Table 4.3 continued

1419127_at	0710005A05Rik	neuropeptide Y
1419534_at	LOX-1; SR-EI; Scare1	oxidized low density lipoprotein (lectin-like) receptor 1
1423903_at	PVS; 3830421F03Rik IA-2; mIA-A; KIAA4064;	poliovirus receptor
1416588_at	mKIAA4064	protein tyrosine phosphatase, receptor type, N
1417601_at	BL34	regulator of G-protein signaling 1
1416200_at	Il-33;	RIKEN cDNA 9230117N10 gene
1421375_a_at	2A9; OP; AI790405;	S100 calcium binding protein A6 (calcyclin)
1449254_at	minopontin	secreted phosphoprotein 1
1417763_at	SSR; 2510001K09Rik AA408197;	signal sequence receptor, alpha
1420915_at	2010005J02Rik	signal transducer and activator of transcription 1
1424272_at	Aprf;	signal transducer and activator of transcription 3
1421533_at	Cat1; 4831426K01Rik	solute carrier family 7 (cationic amino acid transporter, y+ system), member 1
1435251_at	mKIAA0713 AI450776;	sorting nexin 13
1427407_s_at	6030460N08Rik	thyroid hormone receptor interactor 11
1423250_a_at		transforming growth factor, beta 2
1417455_at	Tgfb-3; MGC118722 Hic5; ARA55; TSC-5;	transforming growth factor, beta 3
1418136_at	hic-5	transforming growth factor beta 1 induced transcript 1
1418309_at	Opg; TR1; OCIF	tumor necrosis factor receptor superfamily, member 11b (osteoprotegerin)
1418571_at	AI255180	tumor necrosis factor receptor superfamily, member 12a
1416942_at	Arts1; ERAAP; PILSA; PILSAP	type 1 tumor necrosis factor receptor shedding aminopeptidase regulator

CHAPTER 5

Conclusion

5.1 Supplemental data

The following experiments supplement the studies presented in Chapters 3 and 4 in order to define the role of NPY in isolated WD budding and isolated ureteric bud branching. NPY is expressed in both the WD epithelium and the mesenchyme surrounding the WD. Similarly, it is expressed in both the UB and the MM (Figure 5.1). However, it is not clear whether the effect of NPY on budding is autocrine or paracrine in nature or both. To circumvent the problem of NPY expression in the MM, isolated WD and iUB culture systems were employed.

5.1.1 NPY in isolated WD cultures.

As mentioned in Chapter 2 the WD can be cultured in a 3D matrix without attached mesenchymal cells. Culture with GDNF alone is not sufficient to elicit budding in the iWD system. Addition of GDNF plus NPY will stimulate budding when mesenchymal cells are attached (Chapter 3); however, it does not elicit budding in the WD system devoid of mesodermal cells (Figure 5.2). This suggests that NPY stimulates production of another (as yet unidentified) compound in the mesenchymal cells which in turn augment the WD budding program. The nature of this compound remains to be determined.

The WD(+IM) culture system will respond to NPY; however, the iWD system does not. The difference between these culture systems (besides the Matrigel matrix) is the layer of

intermediate mesoderm cells. NPY may act to release some other factor that is produced in this layer of cells, which then upregulates Ret expression, leading to a feed-forward stimulation of budding (Figure 5.3). Based on previous studies, it is possible that this stimulated factor could be an FGF or another secreted growth factor such as one of the BMPs, or a budding inhibitor deactivator, such as follistatin (Bush, Sakurai et al. 2004; Maeshima, Sakurai et al. 2007).

5.1.2 NPY added to isolated UB culture.

Chapter 2 discussed the WD culture in detail. This culture system is useful for studying budding in vitro. In order to study branching morphogenesis we utilize another in vitro culture system: isolated ureteric bud (iUB) in a 3D matrix. This culture system is very similar to the iWD culture system mentioned in Chapter 2. In fact, the iWD culture system was derived from the iUB system. UBs are isolated from E13 metanephroi, removing all the attached metanephric mesenchyme (MM). The T-shaped UBs are then suspended in a 3D matrix consisting of Matrigel and grown in culture with BSN conditioned medium with GDNF and FGF1 (Qiao, Sakurai et al. 1999). After several days in culture, branching morphogenesis can be seen.

NPY added to iUB culture resulted in greater numbers of branches compared to those without NPY (Figure 5.4). This suggests the NPY has a direct effect on the UB epithelium in branching morphogenesis, unlike the initial budding event.

5.1.3 Genetic mouse knockouts

Throughout the course of this research a number of target genes were uncovered which had a role in WD budding. To explore the potential function of these genes in vivo, knockout mice were obtained. We obtained genetic mutations for two of the genes that appeared in Table

2.1 (Ret and NPY) to ascertain their developmental defects, if any. A third gene, Engrailed, was one of the uncharacterized genes in the list. The developmental defects of Ret mutants are well characterized and there are no reported kidney defects in NPY mutants. However, it was hypothesized that a double heterozygous knockout might have a kidney defect due to reduced levels of the gene product.

Generation of knockout mice is a costly and time consuming process. Typically, the 129/Sv genomic library is screened for the gene or locus of interest. A DNA construct is produced using DNA from the genomic locus that flanks the DNA to be inserted. This is so normal function of the gene will be disrupted by either introduction of a stop codon, truncation of the mRNA sequence, or both. The DNA construct is inserted into mouse embryonic stem cells where homologous recombination will insert the constructed DNA, replacing a portion of the original DNA. Growth in selective media identifies ES cells that have taken up the construct. These ES cells are injected into a 3.5 day old embryo, which is then transplanted into the uterus of a surrogate mother, giving rise to chimeric mice. 8 weeks after birth, the male pups containing tissue from the modified ES cells are mated to wild-type females. The offspring are then tested to see if they carry the genetic modification (Ledermann 2000; Crawley 2007).

5.1.4 Ret knockout mice

Ret heterozygous mice were obtained from Dr. Frank Costantini (Columbia University Medical Center, NY). Genomic DNA was used to genotype Ret mutant and wild-type pups. The number of Ret (-/-) embryos was approximately 16% (16 out of 101 pups), which is somewhat less than the Mendelian 25%, suggesting that some knockout embryos were absorbed in utero (Figure 5.5). As previously described, the number of Ret(-/-) animals that formed kidneys varied

between 20-50% (Schuchardt, D'Agati et al. 1994; Schuchardt, D'Agati et al. 1996). In our limited test, approximately 57% of the Ret(-/-) embryos formed visible kidneys at day 11.5.

5.1.5 NPY knockout mice

NPY(-/-) mice were obtained from Jackson labs (strain name: 129S-Npy^{tm1Rpa}/J, stock number: 004545). A targeting vector was used to disrupt exon 2 of the Npy gene. No gene product (mRNA or protein) was detected by Northern or Western blot analysis of brain or adrenal gland tissue. These mice had no reported kidney phenotype, which was confirmed by examination of embryos or adult animals.

NPY(-/-) male mice were mated with Ret(+/-) females. The Npy(+/-)Ret(+/-) pups had normal kidneys at days E11 and E18 indistinguishable from Npy(+/-)Ret(+/+) littermates. Whether or not there are late-stage kidney defects in these mutant animals remains to be determined.

5.1.6 Engrailed K/O

Engrailed was found upregulated in the budded WD and iUB compared to the unbudded WDs and inhibited WD conditions (Chapter 2). It was previously found to be upregulated in the UB compared to the MM (Schwab, Patterson et al. 2003). The microarray data was confirmed by Q-PCR of budded WDs compared to uncultured or inhibited WDs (Figure 5.6). We sought to determine if the mouse knockout of Engrailed had a kidney phenotype.

Engrailed is a homeodomain protein that binds to a consensus sequence. It was found to regulate boundaries in developing brain (Davidson, Graham et al. 1988). Mice express two homologues: En1 and En2. En2 has greater sequence homology with rat Engrailed.

We have begun collaboration with Dr. Alexandra Joyner (NYU School of Medicine, NY) who has several En1 and En2 mutant mice. En1-lacZ staining from E11.5 embryos showed En1 was expressed on the ventral surface of the embryo but was not expressed in the urogenital system (private communication from G. Orvis). The Joyner lab also has a mutant mouse that expresses GFP with En2 (En2-GFP). The localization of GFP in the kidney region of these mice is currently under investigation. An En1/En2 double knockout is being bred by the Joyner lab to determine if there is a kidney phenotype.

5.2 Summary of findings

We used an in vitro assay to study WD budding. We looked at various signaling pathways stimulated by the receptor tyrosine kinase Ret and found that the WD responds to various signaling pathway inhibitors. Blocking p38 MAPK, MEK/ERK, JNK or PKC did not inhibit budding of the WD. However, inhibiting the PI3-kinase/Akt pathway did block budding.

NPY was found to be correlated to budding WDs. In vitro stimulation of budding with NPY showed that it could replace FGF when administered with GDNF to induce budding of the WD. Inhibition of the NPY Y1 receptor inhibited budding. We also found that addition of NPY reversed budding inhibition from BMP4 and restored phospho-Akt.

Based on the WD(+IM) and iWD experiments with GDNF and NPY, it appears that the effect of NPY on budding is indirect. There could be another factor stimulated by NPY that is released by the mesenchymal cells that causes the WD to bud. This is similar to how Vitamin A

activates receptors on stromal cells, which then release an unknown compound which upregulates Ret expression (Mendelsohn, Batourina et al. 1999). Also consistent with this are the siRNA experiments targeting NPY (discussed in Chapter 3). The inhibitory effect on budding was probably due to NPY reduction in the mesenchymal cells as siRNA was not able to disrupt genes in the WD epithelium (data not shown). However, NPY appears to have an effect directly on the branching epithelial tissues, as demonstrated by the increase in branching morphogenesis in the iUB experiments.

Although GDNF is a major component of UB formation, the WD can still form a bud in the absence of GDNF or its receptors. We can simulate this in vitro by addition of FGF7 and follistatin or FGF7 and heregulin-alpha (HRG) without any GDNF added. We found that these WDs responded differently to signaling pathway inhibitors compared to WDs cultured with GDNF. Specifically, the GDNF-independent WDs were sensitive to JNK inhibition but were not sensitive to PI3-kinase inhibition. We believe that there is a core budding network of genes that become activated in budding. This network has some differences in its initiation but the bulk of the network is identical.

5.3 Future directions

NPY appears to augment the budding process by recruiting a second factor that acts either directly or indirectly to facilitate budding and/or increase Ret expression. The identity of this compound has not yet been ascertained. Whether it is the same or different compound that is stimulated by activation of the retinoic acid receptor would be interesting to determine.

We mated NPY mutants with Ret mutants to see if there would be a kidney defect due to a “dosing effect” from having only one Ret allele. As reported, there were no differences seen;

however, there may be late stage defects in adult kidneys that were not observed. We are currently observing adult mice [NPY(-/-) and NPY(+/-)Ret(+/-)] to determine if there are differences in kidney size, number of branches or kidney function compared to wild-type mice.

Initial systems biology approaches were undertaken to attempt to make transcriptional networks from the microarray data (Chapters 3 and 4). These networks can be improved or modified by utilizing different approaches, such as integrating single value decomposition and robust regression to refine the network (Yeung, Tegner et al. 2002; Tegner, Yeung et al. 2003). After this, the network must be tested to see if it is valid. QPCR screening of the genes in the network will be the first step to validate the changing expression of the genes in various budded and unbudded states. Genetic perturbation of single points on the network can be accomplished by siRNA, which would further validate this model. However, if the budding network is robust, as we believe it to be, disruption of budding at points other than major “hubs” may require multiple genetic perturbations. This may lead to a type of layered network where disruption at major nodes (or hubs) of the network would indicate inhibition of budding but blocking minor connecting genes on the network would have minor effects (or effects only under certain conditions). The microarray data for various budding inhibitors presented in Chapter 2 can be incorporated to refine or augment this network. The value of this budding transcriptional network may be in its ability to predict the behavior of a tissue engineered WD in order to optimize growth and development.

The transcriptional network is most likely an overlay of many subnetworks all interacting to give the “overall” network that is captured by the microarray. Some cells at the budding tip may be actively proliferating while adjacent cells that remain unbudded are not proliferating (either quiescent or actively suppressed). Also, there is crosstalk between the mesenchyme and epithelium, with each mutually influencing the growth and development of the other. As the bud grows, portions of it may differentiate into a “stalk” type of cell. All these separate steps are

“lumped” together into the microarray. It is not likely that individual components can be easily extricated from this symphony of communicating cells by a purely mathematical approach. However, correlations between the iUB and iWD against the WD(+IM) and the E13 WEK may be able to separate out the epithelial signals from the mesenchymal signals. NMF applied to these 4 sets of microarrays partitions the data into epithelial arrays in one metagene and arrays with mesenchyme in another metagene (data not shown). Also, it may be useful to obtain RNA from just the budded portion of the WDs and compare it to the unbudded section from the same tissue (via laser-capture microdissection). QPCR of these RNA samples would then be utilized to separate the growth signal from a stop signal. This can be done at various time points to get a better overview of how the network is changing with time (e.g. 12, 24, 36 and 48 hours after culture).

In this study we focused on the initial budding event. However, as previously mentioned iterative branching of the UB may involve similar or the same pathways as budding, suggesting that the same set of genes will be activated. Although there are currently only a few microarray data points collected (2 in vivo branched conditions: iUB and E13 WEK vs. 4 in vitro budded samples: GDNF+FGF1, GDNF+FGF7, GDNF+NPY and FGF7+HRG), preliminary analysis indicates some differences between budding and branching. Also, early experiments implicate a role for NPY in UB branching. Recently, we were able to induce the WD to undergo limited branching morphogenesis in our culture system (without having to utilize a 3D matrix or conditioned media, Figure 2.12). This system may offer a promising platform in which to study the similarities and differences between budding and branching. RNA interference against candidate genes, such as Gap43, may help to screen candidate genes. Increasing our knowledge of the initial budding event may possibly lead to advances in tissue engineering or regenerative medicine for kidney replacement or regrowth.

5.4 Figures

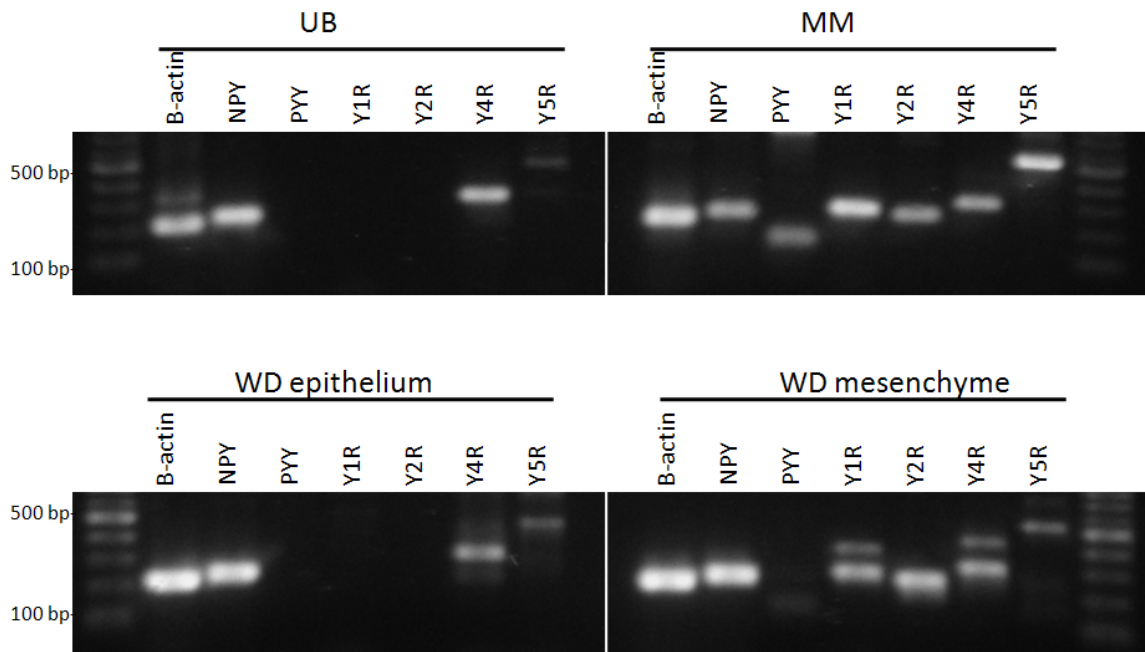


Figure 5.1: RT-PCR of NPY and its receptors

RT-PCR of NPY and its receptors in E13 rat UB, MM, WD, and intermediate mesoderm adjacent to the WD. NPY is present in both epithelial and mesenchymal tissue; however, the mesenchymal tissues express greater variety of NPY receptors.



Figure 5.2: Isolated WD (iWD) cultured with 125 ng/ml GDNF and 1 μ M NPY

All mesenchymal cells were separated from the WD epithelium. The WD was suspended in a 3D-ECM gel composed of a mixture of 50% Matrigel and 50% DMEM/F12. The WD was cultured in DMEM/F12 with 10% FBS with 125 ng/ml GDNF and 1 μ M NPY and allowed to grow for 5 days. Scale bar 100 μ m.

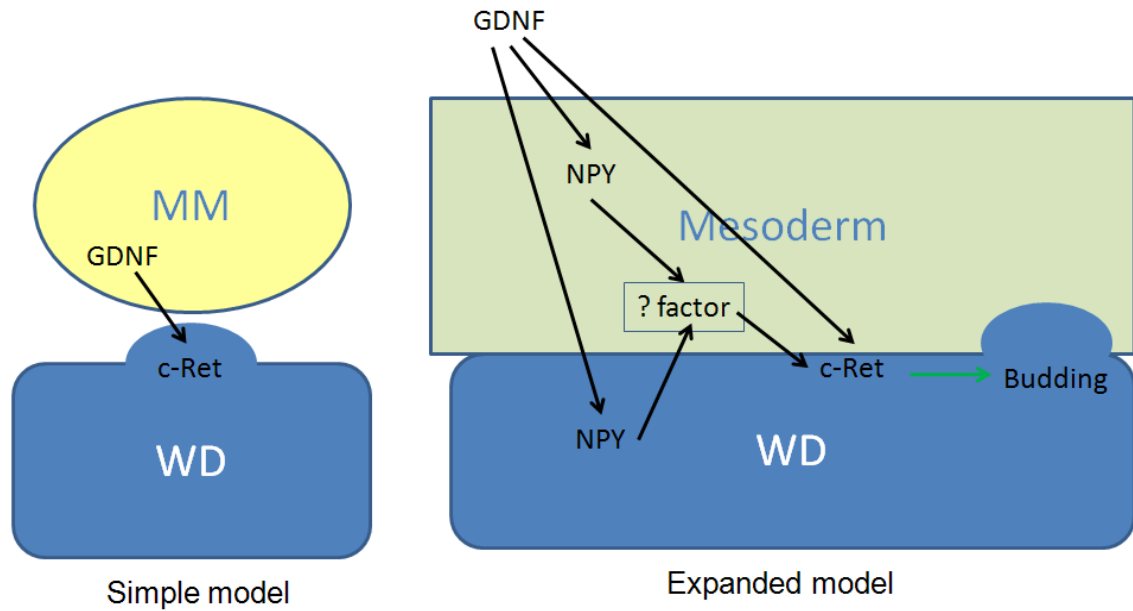


Figure 5.3: NPY budding model

The simple budding model of metanephric kidney development has GDNF released from the MM travelling to the WD where it binds to its receptors $GFR\alpha 1$ and Ret to induce emergence of the UB; however, the studies presented here raise the possibility that there may be other factors either from the MM, the adjacent intermediate mesoderm or the WD/UB itself that support or facilitate budding, such as NPY. NPY is stimulated by GDNF and may release an unidentified factor that will upregulate Ret expression, leading to budding.

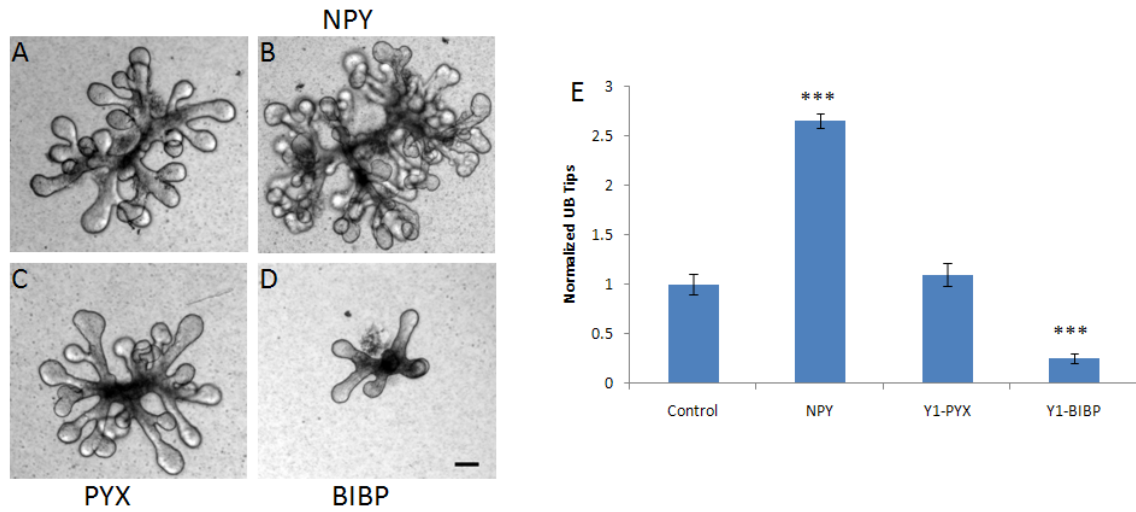


Figure 5.4: NPY increases UB branching.

(A) UB cultured for 5 days at 37°C with BSN-CM supplemented with 125 ng/ml GDNF, 125 ng/ml FGF1 and 10% FBS in Matrigel. (B) With 10 μ M NPY added. (C) With the Y1 receptor inhibitor PYX (10 μ M). (D) With the Y1 inhibitor BIBP (10 μ M), 100 μ m scale bar. (E) Quantification of number of UB tips. N = 6. Error bars represent standard error of the mean. *** P<0.001.

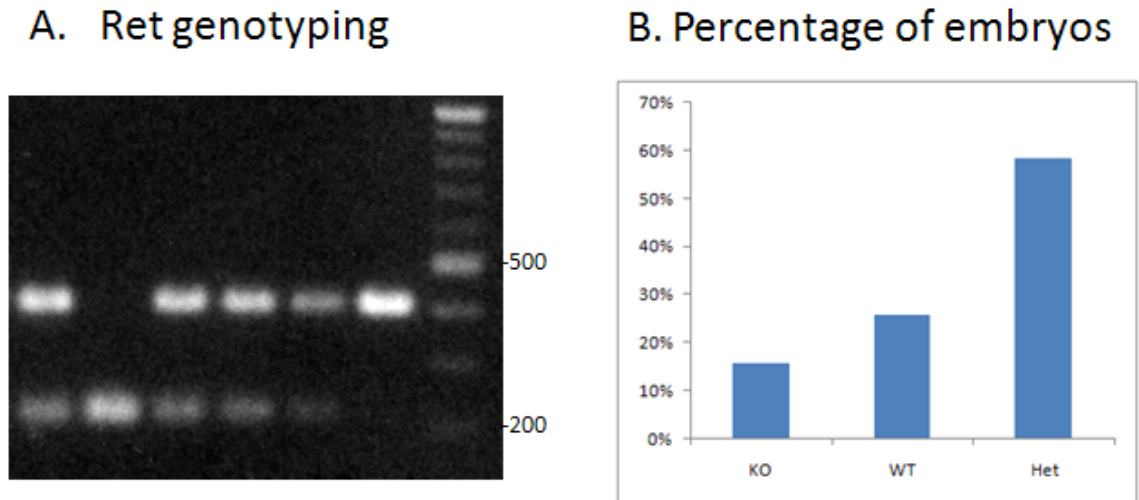


Figure 5.5: Ret KO

(A) Ret genotyping. Genotyping was performed as previously described (Schuchardt, D'Agati et al. 1994). Knockout alleles were at 416 bp and wild-type alleles were at 221 bp. Heterozygous animals showed both. (B) Ret(-/-) animals represented approximately 16% of pups, wild-type Ret(+/+) pups were 26% of the total, and heterozygous was 59%.

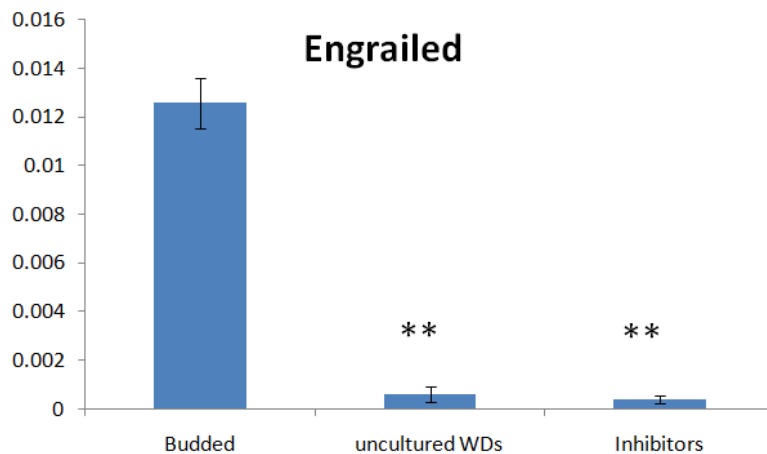


Figure 5.6: Engrailed QPCR

Expression of Engrailed relative to GAPDH. Budded WDs were cultured for 2 to 3 days with 125 ng/ml GDNF and FGF1. Uncultured WDs were isolated from E13 embryos and included a layer of intermediate mesoderm. “Inhibitors” were WDs cultured with GDNF and FGF1 with BMP4, Akt inhibitor IV, or Activin A added. ** P<0.01

SUPPLEMENTAL FIGURES

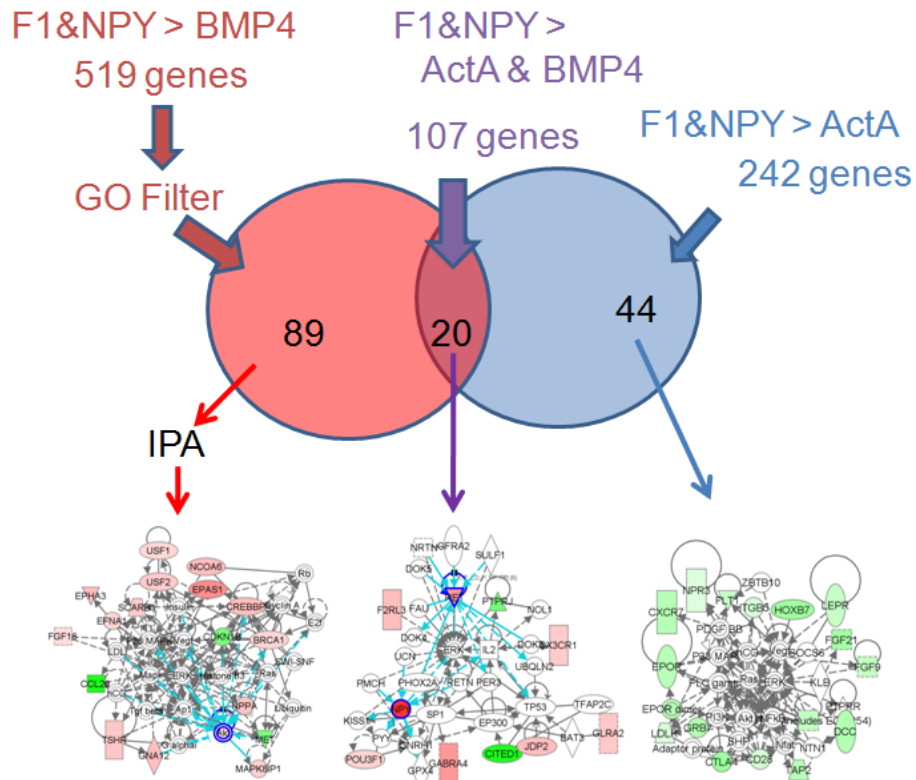


Figure 6.1: Expanded schematic of Fig. 3.11 B-E

Genes from budded WDs cultured with GDNF+FGF1 (F1) or GDNF+NPY (NPY) were compared against unbudded WDs cultured with GDNF+FGF1+BMP4 (BMP4) and GDNF+FGF1+Activin A (ActA) in order to generate gene lists. 519 genes were two-fold or greater in expression in both F1 and NPY samples compared to BMP4 samples. 89 genes in this set had the Gene Ontology (GO) label of “signal transduction” or “transcriptional regulation.” This filtered list of genes was then analyzed by IPA to generate a gene network diagram (Fig 3.11C). Similarly 107 unique genes were two-fold higher in the F1 and NPY samples compared to both the ActA and BMP4 samples. GO filtering resulted in 20 annotated genes, which produced the IPA network shown (Fig 3.11D). Lastly 242 unique genes were expressed two-fold higher in the F1 and NPY samples compared to the ActA samples. GO filtering reduced this to 44 genes. The IPA-generated network is shown (Fig 3.11E)

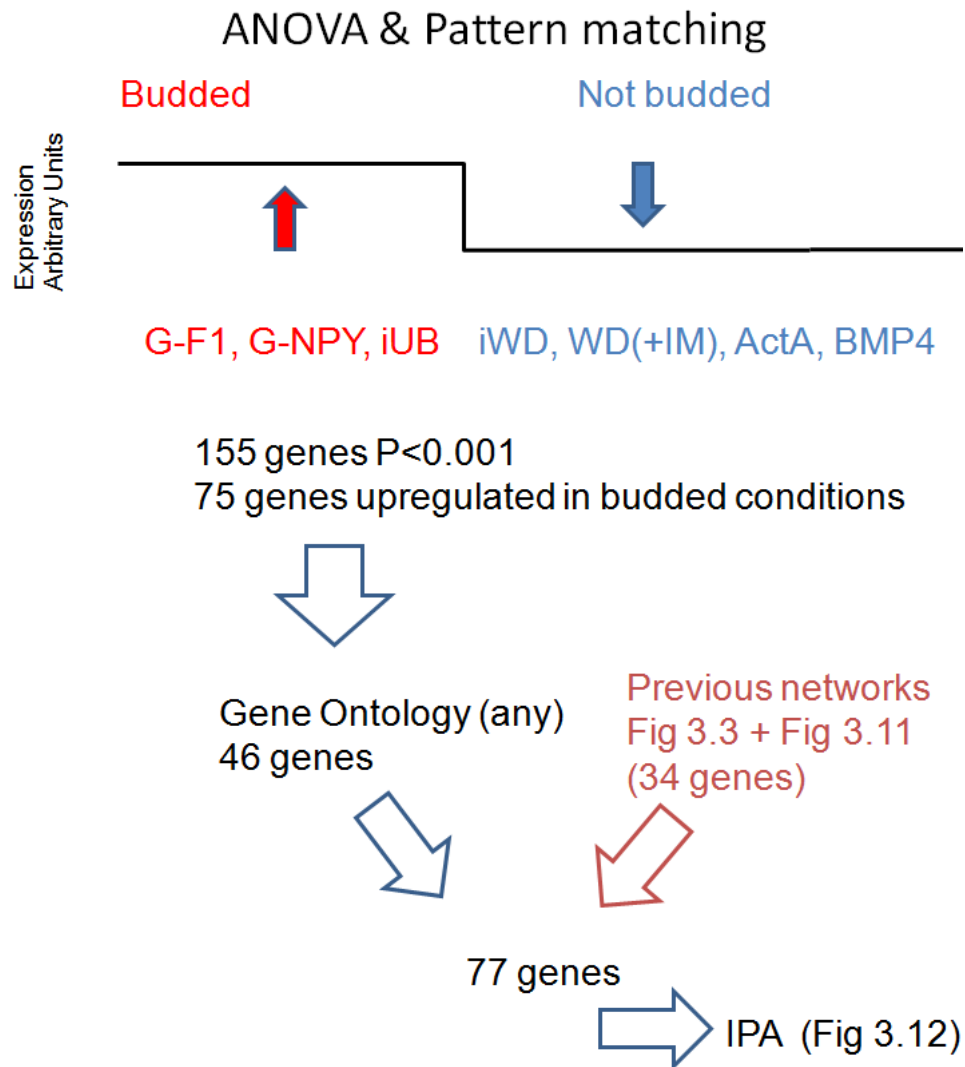


Figure 6.2: Schematic for generation of Fig 3.12

ANOVA + Pattern matching was applied to the 7 microarrays generating a list of 155 genes that had a P-value less than 0.001. Of these 75 were upregulated in the budded conditions (i.e. positive budding correlation). Gene Ontology filtering was used to select only annotated genes, which resulted in 46 genes remaining. This set was combined with genes from previous IPA networks (shown in Fig 3.3 and Fig 3.11) to obtain a set of 77 genes, which was then analyzed by IPA to generate the network shown.

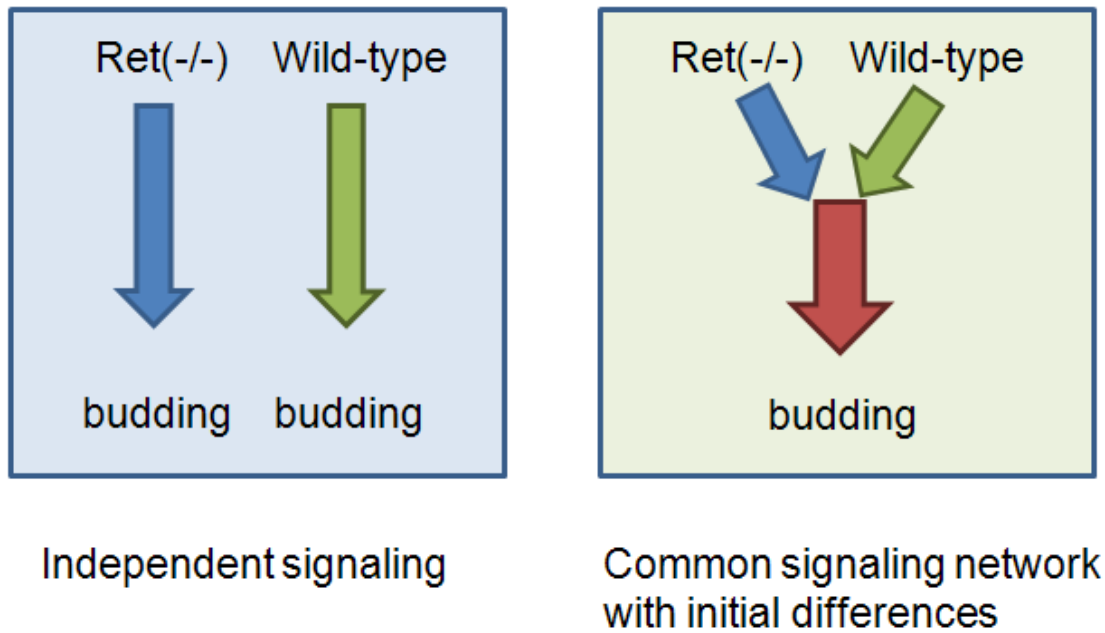


Figure 6.3: GDNF-dependent and independent budding networks

Two models for budding networks. (Left) Independent signaling. This model proposes that the kidneys formed by the *Ret*($-/-$) mutants utilize a completely different transcriptional network to induce budding compared to the wild-type animals. (Right) Common signaling network. This model recognizes that the initial budding trigger may have some differences; however, the bulk of the transcriptional network is overlapping between the mutant and wild-type kidneys.

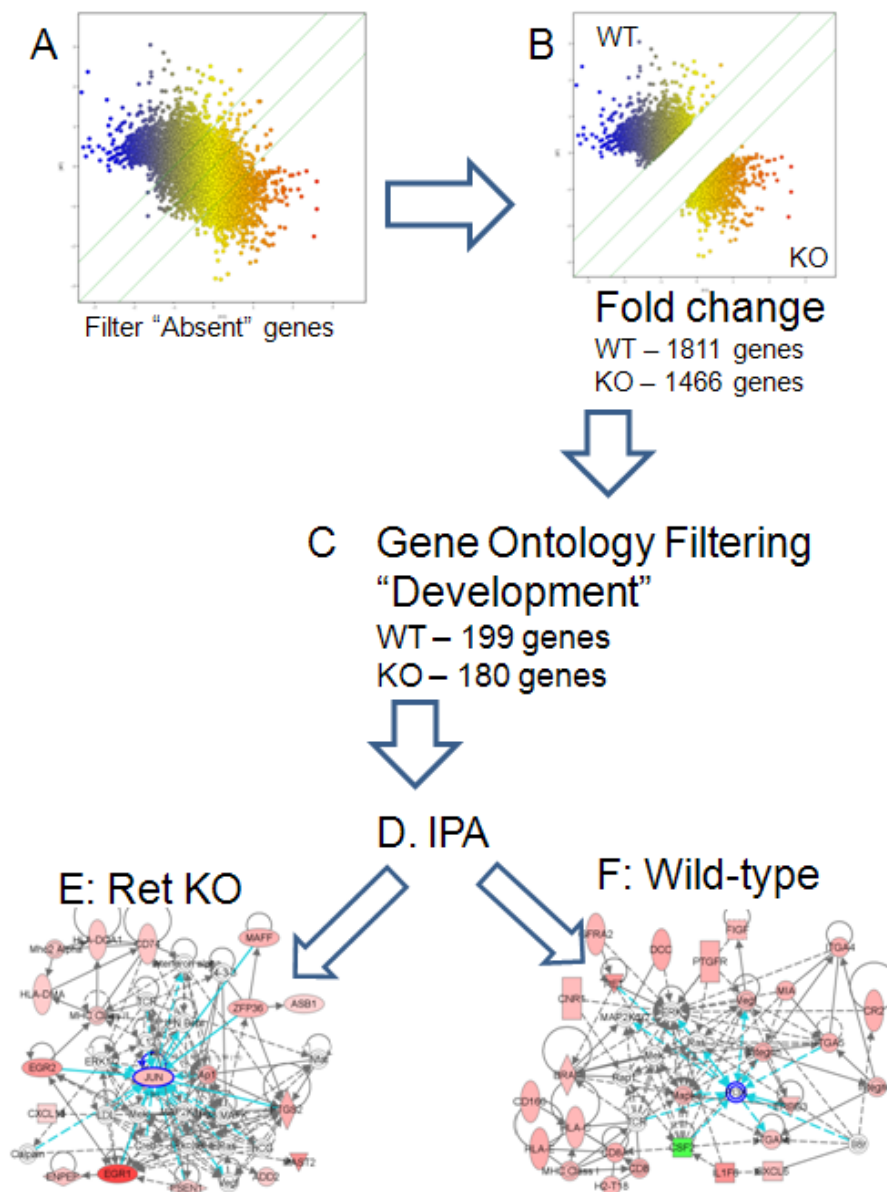


Figure 6.4: Schematic for generating IPA networks (Fig 4.4)

(A) Genes with all "Absent" flags were removed resulting in 33,035 of 45,101 probe sets. (B) Fold change analysis showed 1,811 genes were upregulated by two-fold or more in the wild-type kidneys and 1,466 genes were upregulated in the Ret(-/-) kidneys. (C) The gene lists were filtered to include only those genes that were annotated with the Gene Ontology label of "Development." This resulted in 199 genes and 180 genes for the wild-type and Ret mutant, respectively. (D) These two gene lists were sent to Ingenuity Pathway Analysis (IPA) to generate networks of genes. (E) Sample Ret knockout network (Figure 4.4A). (F) Sample wild-type kidney network (Figure 4.4B).

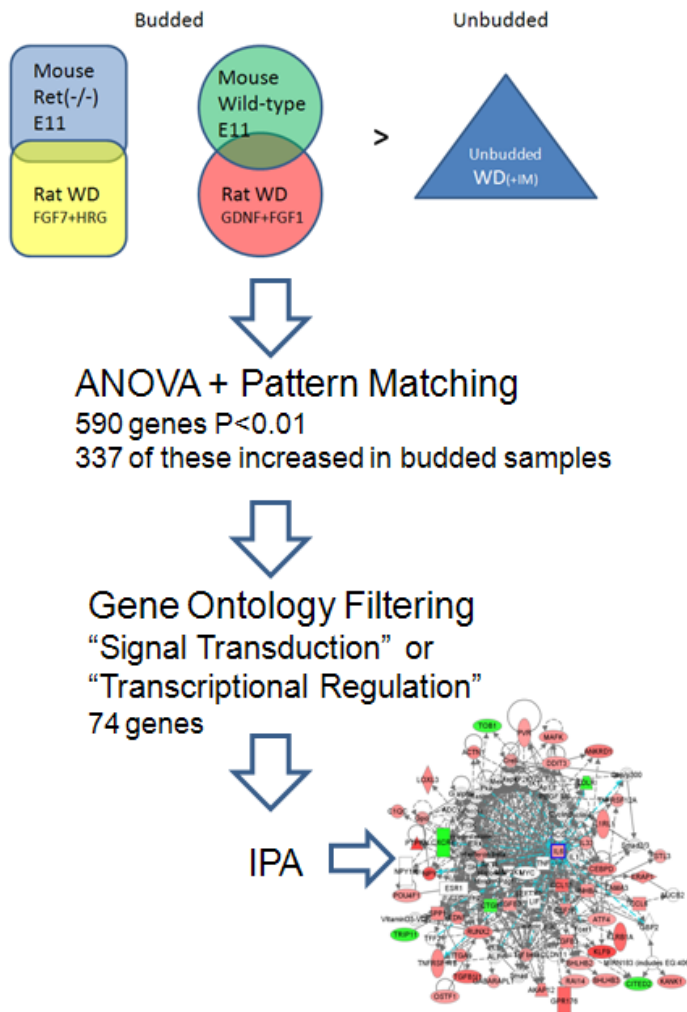


Figure 6.5: Generation of the “Common budding network” (Fig 4.8)

Mouse and rat microarray samples were compared to an unbudded rat WD as described in Chapter 4.2.8. ANOVA + Pattern matching resulted in 590 genes that had a P-value less than 0.01. Of these 337 correlated positively with budding (i.e. they increased in the budded samples). Next Gene Ontology filtering was applied using the categories “Signal Transduction” and “Transcriptional Regulation.” This resulted in 74 genes, which were sent to IPA. IPA generated 3 networks, which were combined to give the final diagram (Figure 4.8).

REFERENCES

- Allen, Y. S., T. E. Adrian, et al. (1983). "Neuropeptide Y distribution in the rat brain." Science **221**(4613): 877-9.
- Anitha, M., B. Chandrasekharan, et al. (2006). "Glial-derived neurotrophic factor modulates enteric neuronal survival and proliferation through neuropeptide Y." Gastroenterology **131**(4): 1164-78.
- Bald, M., M. Gerigk, et al. (1997). "Elevated plasma concentrations of neuropeptide Y in children and adults with chronic and terminal renal failure." Am J Kidney Dis **30**(1): 23-7.
- Bard, J. B. (2002). "Growth and death in the developing mammalian kidney: signals, receptors and conversations." Bioessays **24**(1): 72-82.
- Bard, J. B., A. Gordon, et al. (2001). "Early nephron formation in the developing mouse kidney." J Anat **199**(Pt 4): 385-92.
- Barnea, A., G. Cho, et al. (1995). "Brain-derived neurotrophic factor induces functional expression and phenotypic differentiation of cultured fetal neuropeptide Y-producing neurons." J Neurosci Res **42**(5): 638-47.
- Barreto-Estrada, J. L., W. E. Medina-Ortiz, et al. (2003). "The morphological and biochemical response of avian embryonic sympathoadrenal cells to nerve growth factor is developmentally regulated." Brain Res Dev Brain Res **144**(1): 1-8.
- Basson, M. A., S. Akbulut, et al. (2005). "Sprouty1 is a critical regulator of GDNF/RET-mediated kidney induction." Dev Cell **8**(2): 229-39.
- Basson, M. A., J. Watson-Johnson, et al. (2006). "Branching morphogenesis of the ureteric epithelium during kidney development is coordinated by the opposing functions of GDNF and Sprouty1." Dev Biol **299**(2): 466-77.
- Bates, C. M. (2007). "Role of fibroblast growth factor receptor signaling in kidney development." Pediatr Nephrol **22**(3): 343-9.
- Batourina, E., S. Gim, et al. (2001). "Vitamin A controls epithelial/mesenchymal interactions through Ret expression." Nat Genet **27**(1): 74-8.
- Berne, R. M. and M. N. Levy (2000). Principles of physiology. St. Louis, Mosby.
- Bischoff, A., W. Erdbrugger, et al. (1996). "Neuropeptide Y-enhanced diuresis and natriuresis in anaesthetized rats is independent of renal blood flow reduction." J Physiol **495** (Pt 2): 525-34.
- Bischoff, A. and M. C. Michel (1998). "Renal effects of neuropeptide Y." Pflugers Arch **435**(4): 443-53.

- Bottcher, R. T. and C. Niehrs (2005). "Fibroblast growth factor signaling during early vertebrate development." Endocr Rev **26**(1): 63-77.
- Boyle, S. and M. de Caestecker (2006). "Role of transcriptional networks in coordinating early events during kidney development." Am J Physiol Renal Physiol **291**(1): F1-8.
- Brodbeck, S. and C. Englert (2004). "Genetic determination of nephrogenesis: the Pax/Eya/Six gene network." Pediatr Nephrol **19**(3): 249-55.
- Brophy, P. D., L. Ostrom, et al. (2001). "Regulation of ureteric bud outgrowth by Pax2-dependent activation of the glial derived neurotrophic factor gene." Development **128**(23): 4747-56.
- Brunet, J. P., P. Tamayo, et al. (2004). "Metagenes and molecular pattern discovery using matrix factorization." Proc Natl Acad Sci U S A **101**(12): 4164-9.
- Bullock, S. L., J. M. Fletcher, et al. (1998). "Renal agenesis in mice homozygous for a gene trap mutation in the gene encoding heparan sulfate 2-sulfotransferase." Genes Dev **12**(12): 1894-906.
- Burkhoff, A., D. L. Linemeyer, et al. (1998). "Distribution of a novel hypothalamic neuropeptide Y receptor gene and its absence in rat." Brain Res Mol Brain Res **53**(1-2): 311-6.
- Bush, K. T., H. Sakurai, et al. (2004). "TGF-beta superfamily members modulate growth, branching, shaping, and patterning of the ureteric bud." Dev Biol **266**(2): 285-98.
- Cacalano, G., I. Farinas, et al. (1998). "GFRalpha1 is an essential receptor component for GDNF in the developing nervous system and kidney." Neuron **21**(1): 53-62.
- Cantley, L. G., E. J. Barros, et al. (1994). "Regulation of mitogenesis, motogenesis, and tubulogenesis by hepatocyte growth factor in renal collecting duct cells." Am J Physiol **267**(2 Pt 2): F271-80.
- Castoria, G., A. Migliaccio, et al. (2001). "PI3-kinase in concert with Src promotes the S-phase entry of oestradiol-stimulated MCF-7 cells." Embo J **20**(21): 6050-9.
- Cecka, J. M. (2005). "The OPTN/UNOS Renal Transplant Registry." Clin Transpl: 1-16.
- Chevendra, V. and L. C. Weaver (1992). "Distributions of neuropeptide Y, vasoactive intestinal peptide and somatostatin in populations of postganglionic neurons innervating the rat kidney, spleen and intestine." Neuroscience **50**(3): 727-43.
- Colmers, W. F. and Q. J. Pittman (1989). "Presynaptic inhibition by neuropeptide Y and baclofen in hippocampus: insensitivity to pertussis toxin treatment." Brain Res **498**(1): 99-104.
- Costantini, F. and R. Shakya (2006). "GDNF/Ret signaling and the development of the kidney." Bioessays **28**(2): 117-27.
- Crawley, J. N. (2007). What's wrong with my mouse? behavioral phenotyping of transgenic and knockout mice. Hoboken, John Wiley.

- Cullen-McEwen, L. A., J. Drago, et al. (2001). "Nephron endowment in glial cell line-derived neurotrophic factor (GDNF) heterozygous mice." Kidney Int **60**(1): 31-6.
- Dahl, U., A. Sjodin, et al. (2002). "Genetic dissection of cadherin function during nephrogenesis." Mol Cell Biol **22**(5): 1474-87.
- Davidson, D., E. Graham, et al. (1988). "A gene with sequence similarity to Drosophila engrailed is expressed during the development of the neural tube and vertebrae in the mouse." Development **104**(2): 305-16.
- Davies, J. A. and J. B. Bard (1998). "The development of the kidney." Curr Top Dev Biol **39**: 245-301.
- Devarajan, K. (2008). "Nonnegative matrix factorization: an analytical and interpretive tool in computational biology." PLoS Comput Biol **4**(7): e1000029.
- Erickson, J. C., K. E. Clegg, et al. (1996). "Sensitivity to leptin and susceptibility to seizures of mice lacking neuropeptide Y." Nature **381**(6581): 415-21.
- Esquela, A. F. and S. J. Lee (2003). "Regulation of metanephric kidney development by growth/differentiation factor 11." Dev Biol **257**(2): 356-70.
- Ewald, D. A., P. C. Sternweis, et al. (1988). "Guanine nucleotide-binding protein Go-induced coupling of neuropeptide Y receptors to Ca²⁺ channels in sensory neurons." Proc Natl Acad Sci U S A **85**(10): 3633-7.
- Foucart, S. and H. Majewski (1989). "Inhibition of noradrenaline release by neuropeptide Y in mouse atria does not involve inhibition of adenylate cyclase or a pertussis toxin-susceptible G protein." Naunyn Schmiedebergs Arch Pharmacol **340**(6): 658-65.
- Gray, H. and W. H. Lewis (1918). *Anatomy of the human body*. Philadelphia; New York, Lea & Febiger.
- Grieshammer, U., M. Le, et al. (2004). "SLIT2-mediated ROBO2 signaling restricts kidney induction to a single site." Dev Cell **6**(5): 709-17.
- Grote, D., A. Souabni, et al. (2006). "Pax 2/8-regulated Gata 3 expression is necessary for morphogenesis and guidance of the nephric duct in the developing kidney." Development **133**(1): 53-61.
- Hack, C. J. (2004). "Integrated transcriptome and proteome data: the challenges ahead." Brief Funct Genomic Proteomic **3**(3): 212-9.
- Hackenthal, E., K. Aktories, et al. (1987). "Neuropeptide Y inhibits renin release by a pertussis toxin-sensitive mechanism." Am J Physiol **252**(3 Pt 2): F543-50.
- Hansel, D. E., B. A. Eipper, et al. (2001). "Neuropeptide Y functions as a neuroproliferative factor." Nature **410**(6831): 940-4.

- Hatini, V., S. O. Huh, et al. (1996). "Essential role of stromal mesenchyme in kidney morphogenesis revealed by targeted disruption of Winged Helix transcription factor BF-2." Genes Dev **10**(12): 1467-78.
- Held, P. J., F. Brunner, et al. (1990). "Five-year survival for end-stage renal disease patients in the United States, Europe, and Japan, 1982 to 1987." Am J Kidney Dis **15**(5): 451-7.
- Hida, M., S. Omori, et al. (2002). "ERK and p38 MAP kinase are required for rat renal development." Kidney Int **61**(4): 1252-62.
- Keller, G., G. Zimmer, et al. (2003). "Nephron number in patients with primary hypertension." N Engl J Med **348**(2): 101-8.
- Kim, H. J. and D. Bar-Sagi (2004). "Modulation of signalling by Sprouty: a developing story." Nat Rev Mol Cell Biol **5**(6): 441-50.
- Klein, G., M. Langegger, et al. (1988). "Neural cell adhesion molecules during embryonic induction and development of the kidney." Development **102**(4): 749-61.
- Klin, M., M. Waluga, et al. (1998). "Plasma catecholamines, neuropeptide Y and leucine-enkephalin in uremic patients before and after dialysis during rest and handgrip." Boll Chim Farm **137**(8): 306-13.
- Kobayashi, A., K. M. Kwan, et al. (2005). "Distinct and sequential tissue-specific activities of the LIM-class homeobox gene *Lim1* for tubular morphogenesis during kidney development." Development **132**(12): 2809-23.
- Kreidberg, J. A., H. Sariola, et al. (1993). "WT-1 is required for early kidney development." Cell **74**(4): 679-91.
- Kume, T., K. Deng, et al. (2000). "Murine forkhead/winged helix genes *Foxc1* (*Mf1*) and *Foxc2* (*Mfh1*) are required for the early organogenesis of the kidney and urinary tract." Development **127**(7): 1387-95.
- Ledermann, B. (2000). "Embryonic stem cells and gene targeting." Exp Physiol **85**(6): 603-13.
- Liu, W. M., R. Mei, et al. (2002). "Analysis of high density expression microarrays with signed-rank call algorithms." Bioinformatics **18**(12): 1593-9.
- Maeshima, A., H. Sakurai, et al. (2007). "Glial cell-derived neurotrophic factor independent ureteric bud outgrowth from the Wolffian duct." J Am Soc Nephrol **18**(12): 3147-55.
- Maeshima, A., D. A. Vaughn, et al. (2006). "Activin A is an endogenous inhibitor of ureteric bud outgrowth from the Wolffian duct." Dev Biol **295**(2): 473-85.
- Mah, S. P., H. Saueressig, et al. (2000). "Kidney development in cadherin-6 mutants: delayed mesenchyme-to-epithelial conversion and loss of nephrons." Dev Biol **223**(1): 38-53.

- Majumdar, A., S. Vainio, et al. (2003). "Wnt11 and Ret/Gdnf pathways cooperate in regulating ureteric branching during metanephric kidney development." Development **130**(14): 3175-85.
- Mannon, P. J. and J. M. Mele (2000). "Peptide YY Y1 receptor activates mitogen-activated protein kinase and proliferation in gut epithelial cells via the epidermal growth factor receptor." Biochem J **350 Pt 3**: 655-61.
- Mannon, P. J. and J. R. Raymond (1998). "The neuropeptide Y/peptide YY Y1 receptor is coupled to MAP kinase via PKC and Ras in CHO cells." Biochem Biophys Res Commun **246**(1): 91-4.
- Matsumoto, M., T. Nomura, et al. (1996). "Inactivation of a novel neuropeptide Y/peptide YY receptor gene in primate species." J Biol Chem **271**(44): 27217-20.
- McDonald, J. K. (1988). "NPY and related substances." Crit Rev Neurobiol **4**(1): 97-135.
- Mendelsohn, C., E. Batourina, et al. (1999). "Stromal cells mediate retinoid-dependent functions essential for renal development." Development **126**(6): 1139-48.
- Meyer, T. N., C. Schwesinger, et al. (2004). "Spatiotemporal regulation of morphogenetic molecules during in vitro branching of the isolated ureteric bud: toward a model of branching through budding in the developing kidney." Dev Biol **275**(1): 44-67.
- Michel, M. C., A. Beck-Sickinger, et al. (1998). "XVI. International Union of Pharmacology recommendations for the nomenclature of neuropeptide Y, peptide YY, and pancreatic polypeptide receptors." Pharmacol Rev **50**(1): 143-50.
- Michel, M. C. and W. Rascher (1995). "Neuropeptide Y: a possible role in hypertension?" J Hypertens **13**(4): 385-95.
- Michos, O., L. Panman, et al. (2004). "Gremlin-mediated BMP antagonism induces the epithelial-mesenchymal feedback signaling controlling metanephric kidney and limb organogenesis." Development **131**(14): 3401-10.
- Millar, B. C., T. Weis, et al. (1991). "Positive and negative contractile effects of neuropeptide Y on ventricular cardiomyocytes." Am J Physiol **261**(6 Pt 2): H1727-33.
- Miner, J. H. and C. Li (2000). "Defective glomerulogenesis in the absence of laminin alpha5 demonstrates a developmental role for the kidney glomerular basement membrane." Dev Biol **217**(2): 278-89.
- Minth, C. D., S. R. Bloom, et al. (1984). "Cloning, characterization, and DNA sequence of a human cDNA encoding neuropeptide tyrosine." Proc Natl Acad Sci U S A **81**(14): 4577-81.
- Miyamoto, N., M. Yoshida, et al. (1997). "Defects of urogenital development in mice lacking Emx2." Development **124**(9): 1653-64.

- Miyazaki, Y., K. Oshima, et al. (2000). "Bone morphogenetic protein 4 regulates the budding site and elongation of the mouse ureter." J Clin Invest **105**(7): 863-73.
- Montesano, R., J. V. Soriano, et al. (1999). "Constitutively active mitogen-activated protein kinase kinase MEK1 disrupts morphogenesis and induces an invasive phenotype in Madin-Darby canine kidney epithelial cells." Cell Growth Differ **10**(5): 317-32.
- Moore, M. W., R. D. Klein, et al. (1996). "Renal and neuronal abnormalities in mice lacking GDNF." Nature **382**(6586): 76-9.
- Moreau, E., J. Vilar, et al. (1998). "Regulation of c-ret expression by retinoic acid in rat metanephros: implication in nephron mass control." Am J Physiol **275**(6 Pt 2): F938-45.
- Muller, U., D. Wang, et al. (1997). "Integrin alpha8beta1 is critically important for epithelial-mesenchymal interactions during kidney morphogenesis." Cell **88**(5): 603-13.
- Mullins, D. E., X. Zhang, et al. (2002). "Activation of extracellular signal regulated protein kinase by neuropeptide Y and pancreatic polypeptide in CHO cells expressing the NPY Y(1), Y(2), Y(4) and Y(5) receptor subtypes." Regul Pept **105**(1): 65-73.
- Nie, M. and L. A. Selbie (1998). "Neuropeptide Y Y1 and Y2 receptor-mediated stimulation of mitogen-activated protein kinase activity." Regul Pept **75-76**: 207-13.
- Nishinakamura, R., Y. Matsumoto, et al. (2001). "Murine homolog of SALL1 is essential for ureteric bud invasion in kidney development." Development **128**(16): 3105-15.
- Nyengaard, J. R. and T. F. Bendtsen (1992). "Glomerular number and size in relation to age, kidney weight, and body surface in normal man." Anat Rec **232**(2): 194-201.
- O'Brien, L. E., M. M. Zegers, et al. (2002). "Opinion: Building epithelial architecture: insights from three-dimensional culture models." Nat Rev Mol Cell Biol **3**(7): 531-7.
- Obara-Ishihara, T., J. Kuhlman, et al. (1999). "The surface ectoderm is essential for nephric duct formation in intermediate mesoderm." Development **126**(6): 1103-8.
- Ohuchi, H., Y. Hori, et al. (2000). "FGF10 acts as a major ligand for FGF receptor 2 IIIb in mouse multi-organ development." Biochem Biophys Res Commun **277**(3): 643-9.
- Pavlidis, P. (2003). "Using ANOVA for gene selection from microarray studies of the nervous system." Methods **31**(4): 282-9.
- Pavlidis, P. and W. S. Noble (2001). "Analysis of strain and regional variation in gene expression in mouse brain." Genome Biol **2**(10): RESEARCH0042.
- Playford, R. J., S. Mehta, et al. (1995). "Effect of peptide YY on human renal function." Am J Physiol **268**(4 Pt 2): F754-9.
- Pohl, M., V. Bhatnagar, et al. (2002). "Toward an etiological classification of developmental disorders of the kidney and upper urinary tract." Kidney Int **61**(1): 10-9.

- Popsueva, A., D. Poteryaev, et al. (2003). "GDNF promotes tubulogenesis of GFRalpha1-expressing MDCK cells by Src-mediated phosphorylation of Met receptor tyrosine kinase." J Cell Biol **161**(1): 119-29.
- Poteryaev, D., A. Titievsky, et al. (1999). "GDNF triggers a novel ret-independent Src kinase family-coupled signaling via a GPI-linked GDNF receptor alpha1." FEBS Lett **463**(1-2): 63-6.
- Qiao, J., K. T. Bush, et al. (2001). "Multiple fibroblast growth factors support growth of the ureteric bud but have different effects on branching morphogenesis." Mech Dev **109**(2): 123-35.
- Qiao, J., H. Sakurai, et al. (1999). "Branching morphogenesis independent of mesenchymal-epithelial contact in the developing kidney." Proc Natl Acad Sci U S A **96**(13): 7330-5.
- Qiao, J., R. Uzzo, et al. (1999). "FGF-7 modulates ureteric bud growth and nephron number in the developing kidney." Development **126**(3): 547-54.
- Quaggin, S. E., L. Schwartz, et al. (1999). "The basic-helix-loop-helix protein pod1 is critically important for kidney and lung organogenesis." Development **126**(24): 5771-83.
- Reich, M., T. Liefeld, et al. (2006). "GenePattern 2.0." Nat Genet **38**(5): 500-1.
- Risau, W. (1998). "Development and differentiation of endothelium." Kidney Int Suppl **67**: S3-6.
- Rosines, E., R. V. Sampogna, et al. (2007). "Staged in vitro reconstitution and implantation of engineered rat kidney tissue." Proc Natl Acad Sci U S A **104**(52): 20938-43.
- Sainio, K., D. Nonclercq, et al. (1994). "Neuronal characteristics in embryonic renal stroma." Int J Dev Biol **38**(1): 77-84.
- Sainio, K., P. Suvanto, et al. (1997). "Glial-cell-line-derived neurotrophic factor is required for bud initiation from ureteric epithelium." Development **124**(20): 4077-87.
- Sakurai, H., E. J. Barros, et al. (1997). "An in vitro tubulogenesis system using cell lines derived from the embryonic kidney shows dependence on multiple soluble growth factors." Proc Natl Acad Sci U S A **94**(12): 6279-84.
- Sakurai, H., K. T. Bush, et al. (2001). "Identification of pleiotrophin as a mesenchymal factor involved in ureteric bud branching morphogenesis." Development **128**(17): 3283-93.
- Saxén, L. (1987). Organogenesis of the kidney. Cambridge [Cambridgeshire]; New York, Cambridge University Press.
- Schmidt-Ott, K. M., T. N. Masckauchan, et al. (2007). "beta-catenin/TCF/Lef controls a differentiation-associated transcriptional program in renal epithelial progenitors." Development **134**(17): 3177-90.
- Schmidt-Ott, K. M., J. Yang, et al. (2005). "Novel regulators of kidney development from the tips of the ureteric bud." J Am Soc Nephrol **16**(7): 1993-2002.

- Schnabel, C. A., R. E. Godin, et al. (2003). "Pbx1 regulates nephrogenesis and ureteric branching in the developing kidney." Dev Biol **254**(2): 262-76.
- Schuchardt, A., V. D'Agati, et al. (1994). "Defects in the kidney and enteric nervous system of mice lacking the tyrosine kinase receptor Ret." Nature **367**(6461): 380-3.
- Schuchardt, A., V. D'Agati, et al. (1996). "Renal agenesis and hypodysplasia in ret-k- mutant mice result from defects in ureteric bud development." Development **122**(6): 1919-29.
- Schwab, K., L. T. Patterson, et al. (2003). "A catalogue of gene expression in the developing kidney." Kidney Int **64**(5): 1588-604.
- Shah, M. M., R. V. Sampogna, et al. (2004). "Branching morphogenesis and kidney disease." Development **131**(7): 1449-62.
- Shawlot, W. and R. R. Behringer (1995). "Requirement for Lim1 in head-organizer function." Nature **374**(6521): 425-30.
- Stark, K., S. Vainio, et al. (1994). "Epithelial transformation of metanephric mesenchyme in the developing kidney regulated by Wnt-4." Nature **372**(6507): 679-83.
- Stuart, R. O., K. T. Bush, et al. (2001). "Changes in global gene expression patterns during development and maturation of the rat kidney." Proc Natl Acad Sci U S A **98**(10): 5649-54.
- Stuart, R. O., K. T. Bush, et al. (2003). "Changes in gene expression patterns in the ureteric bud and metanephric mesenchyme in models of kidney development." Kidney Int **64**(6): 1997-2008.
- Takahashi, M. (2001). "The GDNF/RET signaling pathway and human diseases." Cytokine Growth Factor Rev **12**(4): 361-73.
- Tang, M. J., Y. Cai, et al. (2002). "Ureteric bud outgrowth in response to RET activation is mediated by phosphatidylinositol 3-kinase." Dev Biol **243**(1): 128-36.
- Tatemoto, K. (1982). "Neuropeptide Y: complete amino acid sequence of the brain peptide." Proc Natl Acad Sci U S A **79**(18): 5485-9.
- Tatemoto, K., M. Carlquist, et al. (1982). "Neuropeptide Y--a novel brain peptide with structural similarities to peptide YY and pancreatic polypeptide." Nature **296**(5858): 659-60.
- Tegner, J., M. K. Yeung, et al. (2003). "Reverse engineering gene networks: integrating genetic perturbations with dynamical modeling." Proc Natl Acad Sci U S A **100**(10): 5944-9.
- Torres, M., E. Gomez-Pardo, et al. (1995). "Pax-2 controls multiple steps of urogenital development." Development **121**(12): 4057-65.
- Trupp, M., R. Scott, et al. (1999). "Ret-dependent and -independent mechanisms of glial cell line-derived neurotrophic factor signaling in neuronal cells." J Biol Chem **274**(30): 20885-94.

- Tsigelny, I. F., V. L. Kouznetsova, et al. (2008). "Analysis of metagene portraits reveals distinct transitions during kidney organogenesis." Sci Signal **1**(49): ra16.
- Vandesompele, J., K. De Preter, et al. (2002). "Accurate normalization of real-time quantitative RT-PCR data by geometric averaging of multiple internal control genes." Genome Biol **3**(7): RESEARCH0034.
- Watanabe, T. and F. Costantini (2004). "Real-time analysis of ureteric bud branching morphogenesis in vitro." Dev Biol **271**(1): 98-108.
- Wellik, D. M., P. J. Hawkes, et al. (2002). "Hox11 paralogous genes are essential for metanephric kidney induction." Genes Dev **16**(11): 1423-32.
- Wittmann, W., S. Loacker, et al. (2005). "Y1-receptors regulate the expression of Y2-receptors in distinct mouse forebrain areas." Neuroscience **136**(1): 241-50.
- Xiong, Z. and D. W. Cheung (1995). "ATP-Dependent inhibition of Ca²⁺-activated K⁺ channels in vascular smooth muscle cells by neuropeptide Y." Pflugers Arch **431**(1): 110-6.
- Xu, P. X., J. Adams, et al. (1999). "Eya1-deficient mice lack ears and kidneys and show abnormal apoptosis of organ primordia." Nat Genet **23**(1): 113-7.
- Xu, P. X., W. Zheng, et al. (2003). "Six1 is required for the early organogenesis of mammalian kidney." Development **130**(14): 3085-94.
- Yeung, M. K., J. Tegner, et al. (2002). "Reverse engineering gene networks using singular value decomposition and robust regression." Proc Natl Acad Sci U S A **99**(9): 6163-8.